ARMY RESEARCH LABORATORY

Combustion Mechanisms of Very High Burn Rate (VHBR) Propellant

James T. Barnes
Edward B. Fisher

ARL-CR-242 September 1995

prepared by

Veritay Technology, Inc.
4845 Millersport Highway
P.O. Box 305
East Amherst, NY 14051-0305

under contract

DAAA15-88-C-0046

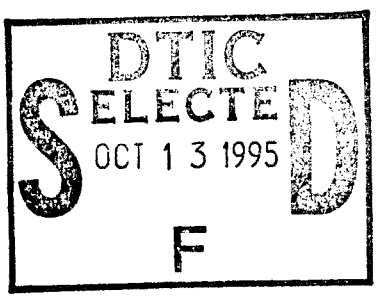

NOTICES

Destroy this report when it is no longer needed. DO NOT return it to the originator.

Additional copies of this report may be obtained from the National Technical Information Service, U.S. Department of Commerce, 5285 Port Royal Road, Springfield, VA 22161.

The findings of this report are not to be construed as an official Department of the Army position, unless so designated by other authorized documents.

The use of trade names or manufacturers' names in this report does not constitute indorsement of any commercial product.

REPORT DOCUMENTATION PAGE

Form Approved
OMB No. 0704-0188

1. AGENCY USE ONLY *(Leave blank)*	2. REPORT DATE	3. REPORT TYPE AND DATES COVERED
	September 1995	Final, July 1988 - July 1990

4. TITLE AND SUBTITLE

Combustion Mechanisms of Very High Burn Rate (VHBR) Propellant

5. FUNDING NUMBERS

C: DAAA15-88-C-0046

6. AUTHOR(S)

James T. Barnes and Edward B. Fisher

7. PERFORMING ORGANIZATION NAME(S) AND ADDRESS(ES)

Veritay Technology, Inc.
4845 Millersport Highway
P.O. Box 305
East Amherst, NY 14051-0305

8. PERFORMING ORGANIZATION REPORT NUMBER

9. SPONSORING/MONITORING AGENCY NAMES(S) AND ADDRESS(ES)

U.S. Army Research Laboratory
ATTN: AMSRL-WT-PA
Aberdeen Proving Ground, MD 21005-5066

10.SPONSORING/MONITORING AGENCY REPORT NUMBER

ARL-CR-242

11. SUPPLEMENTARY NOTES

Point of contact for this report is Dr. Kevin J. White, U.S. Army Research Laboratory, ATTN: AMSRL-WT-PA, Aberdeen Proving Ground, MD 21005-5066.

12a. DISTRIBUTION/AVAILABILITY STATEMENT

Approved for public release; distribution is unlimited.

12b. DISTRIBUTION CODE

13. ABSTRACT ***(Maximum 200 words)***

In this Phase II Small Business Initiated Research (SBIR) program, the various combustion mechanisms of very high burn rate (VHBR) propellant formulations were studied. Toward this end, various diagnostic and specialized instrumentation techniques were developed and evaluated. These techniques included miniature strain gage instrumentation and cine x-ray experimentation. The program resulted in hypotheses regarding combustion mechanisms at work in VHBR propellant formulations.

14. SUBJECT TERMS

VHBR, DDT, PDC, nitramine, boron hydride, combustion mechanics

15. NUMBER OF PAGES

116

16. PRICE CODE

17. SECURITY CLASSIFICATION OF REPORT	18. SECURITY CLASSIFICATION OF THIS PAGE	19. SECURITY CLASSIFICATION OF ABSTRACT	20. LIMITATION OF ABSTRACT
UNCLASSIFIED	UNCLASSIFIED	UNCLASSIFIED	UL

INTENTIONALLY LEFT BLANK.

PREFACE

This report has been prepared by Veritay Technology, Inc. for the U.S. Army Research Laboratory under Contract No. DAAA15-88-C-0046.

INTENTIONALLY LEFT BLANK.

ACKNOWLEDGMENTS

The authors would like to thank technical monitors Dr. Kevin White and Dr. Arpad Juhasz of the U.S. Army Research Laboratory (ARL) for their help and support in performing the work documented in this report. Thanks also go to Dr. Rob Lieb and Mr. Mike Leadore of ARL for their help and the use of their facilities for conducting the Drop Weight Material Properties Tester (DWMPT) work documented in this report. The authors would also like to acknowledge Dr. Kenneth Kuo of the Pennsylvania State University, whose facilities and assistance were instrumental in obtaining the important x-ray data contained in this report. Finally, the authors would like to acknowledge Mr. Henry Ziuko of Veritay, whose skill and attention to detail were invaluable in obtaining the experimental results documented in this report.

INTENTIONALLY LEFT BLANK.

TABLE OF CONTENTS

LIST OF FIGURES

INTENTIONALLY LEFT BLANK.

LIST OF TABLES

INTENTIONALLY LEFT BLANK.

1. INTRODUCTION

1.1 Overview. This report represents the culmination of a 2-yr effort to study the combustion behavior of very high burn rate (VHBR) propellant formulations. The program was funded by the U.S. Army Ballistic Research Laboratory,* contract number DAAA15-88-C-0046, as a Phase II SBIR program. Two earlier programs to investigate this topic have previously been completed by Veritay. These were, specifically, the Phase I SBIR program [1] and a New York State Matching Funds effort [2]. During these two programs, various propellant formulations were studied. However, the efforts were concentrated on a single, relatively slow burning, family of propellants having Hycar (hydroxy-terminated polyacrylate) as their binder. During the present effort, propellant formulations which span the entire range of combustion behavior, from the relatively slow Hycar-based formulations to the Kraton-based (a block copolymer of styrene and ethylene-butylene) propellants which have some slow-burning and some moderately fast-burning formulations, to the PEG-based (polyethylene glycol or Carbowax) family of propellants, all of which exhibit extremely fast combustion behavior, were studied. With this slate of propellants, it was felt that a better overall understanding of the combustion behavior of the propellants which have historically fallen into the VHBR category could be obtained. The overall goals of the present effort include the following: to develop the level of understanding concerning the combustion behavior of VHBR propellant formulations; to determine the controlling factors which cause certain formulations to burn at rates which are orders of magnitude greater than other (similar) formulations; and finally, to incorporate the results of this and other efforts into a combustion model which can explain these large differences in the observed burn rates.

During the course of the current program, it became evident that the overall interest level in VHBR propellants, at least for application to traveling charge gun systems, was declining. With this in mind, the technical monitors of this program requested that this report be written in such a way that it could be utilized as a "jumping off point" should interest in VHBR propellants be revived at some point in the future. As a result, this report contains an especially large literature survey to acknowledge and document as many of the relevant publications concerning these special propellant formulations as possible. In addition, the Veritay work presented here may actually contain some small aspects of work performed

* The U.S. Army Ballistic Research Laboratory (BRL) was deactivated on 30 September 1992 and subsequently became a part of the U.S. Army Research Laboratory (ARL) on 1 October 1992.

during the earlier Veritay experimental programs, in an effort to present as thorough, well-rounded, and cohesive an hypothesis on the nature of the VHBR combustion mechanism as possible.

1.2 Background. VHBR propellants have been defined [3, 4] as those which possess "apparent" burn rates which are in the range of approximately 1 to 1,000 m/s. The bounds of this range were selected so that this burn regime falls intermediately between the standard propellant burn regime (0.1 to 50 cm/s) and the detonation regime (2 to 10 km/s). The VHBR propellants which have historically drawn the most attention are those which contained HIVELITE,* consisting of one of a number of salts of the anion $B_{10}H_{10}^{2-}$. Similar types of propellants have been produced utilizing the $B_{12}H_{12}^{2-}$ anion;** however, a relatively incomplete database is associated with this material.

While different fabrication techniques have been utilized to produce VHBR propellants (e.g., casting, compression in a heated mold, and extrusion), the basic formulation variables are fairly consistent for most members of this propellant family. This generic formulation resembles a low-vulnerability ammunition (LOVA) formulation with high solids loading but with a burn rate enhancer and consists of particulates held in a continuous binder matrix. As stated previously, a common ingredient in most VHBR formulations studied (and all of those studied during this program) is HIVELITE. The two HIVELITE salts contained in the propellants studied during this program are H498 and H466. H498 utilizes potassium as the cation, and H466 utilizes an organic cation (tetramethyl ammonium). Typical HIVELITE concentrations are between 3 and 15 weight-percent and consist of small particles typically 5 μm in diameter. An oxidizer, also in particle form, is present in VHBR formulations. This can be RDX or HMX or a combination of either with TAGN (triaminoguanidinium nitrate). In many cases, the oxidizer particles are present in two size categories to enable a high solids loading density with small binder content. These categories are ground (approximately 5 μm in diameter) and class 5 (approximately 150-μm average diameter). The binder/plasticizer matrix makes up the remainder of a typical propellant formulation. Either the binder or the plasticizer may be energetic; however, systems in which both are inert (nonenergetic) are common.

The mechanism for combustion of VHBR propellants has been the focus of much discussion over the past 10 or more years. A consensus opinion regarding what factors affect the onset of the VHBR

* HIVELITE is a tradename of Teledyne McCormick Selph.

** Available from Callery Chemical Co., Pittsburgh, PA.

observed has yet to be reached. What is agreed upon is that the mechanism differs from that observed with standard propellants, for which a conductive or laminar burn mechanism is well documented. The laminar burn mechanism is characterized by combustion at the surface only, with the rate controlled by the thermal flux from the gases in contact with the propellant surface. However, with VHBR propellants, it has been observed that an in-depth combustion mechanism of some sort is present. While combustion may originate and be sustained at the surface of the propellant grain, the flame front also propagates into the grain. This can lead to volumetric burning, where combustion occurs within a volume of the grain rather than just at the surface. In this instance, the combustion region may act essentially as a packed bed of small burning particles. The associated surface area available for combustion then becomes that of the energetic particulates (oxidizer and boron hydride) in this bed and is, therefore, much greater than for surface burning of the large propellant grain, leading to a much greater energy generation rate.

It is the aforementioned phenomenon which is the source of the term "apparent" burn rate. When conducting burn rate reduction from closed bomb pressure data, it is necessary to assume an applicable form function. Since no form function which can suitably model the volumetric burning phenomenon previously discussed is known, surface burning is assumed and a standard form function used, usually cigarette (end-burning) or cylindrical. Therefore, a burn rate from samples which may be burning in a volumetric mode is reduced to a comparable "apparent" burn rate, as if laminar combustion were occurring.

1.3 Propellant Information. As mentioned earlier, the goal of the present effort was to gain insight into the various factors which contribute to VHBR behavior. With this information in hand, it might, therefore, be possible to tailor an appropriate propellant formulation to an application which requires a specific propellant burn rate.

The various propellant formulations which have been included in the VHBR category do not all exhibit the extremely fast burn rates for which this class is known. In fact, most of the members of the Hycar-based propellant slate have apparent burn rates of less than 50 cm/s (20 inches/s), which would place them at the high end of the standard propellant class. However, since the presence of a boron hydride salt ($B_{10}H_{10}^{2-}$ or $B_{12}H_{12}^{2-}$ anions) is a common feature in the majority of the very rapid burning samples, any propellant containing such a compound, along with a high percentage of granular solid oxidizer, has been labelled a VHBR propellant, regardless of its burn rate. In an effort to remove this misnomer, the authors [5, 1, 2] coined the name "Boron Hydride Enhanced" (BHE) propellants, to reflect

the burn rate enhancement provided by the boron hydride without placing limits on the burn rate range. The propellants that fall into this class have burn rate characteristics which range from those of standard propellants to extremely fast-burning samples having apparent burn rates of well over 100 m/s. The slower burning formulations may be suitable for monolithic charge applications, while the high burn rate propellants appear to be suitable for traveling charge (TC) applications. As mentioned earlier, the very fast-burning propellant formulations of the VHBR category have been shown to exhibit an in-depth combustion mechanism, while the slower-burning formulations tend to exhibit laminar combustion characteristics.

Propellants which exhibit such a wide range of chemical composition and combustion characteristics might not be expected to possess a single combustion mechanism. Indeed, except for the common ingredient (boron hydride salt), differences in the binder/plasticizer material (energetic or inert), factors related to the oxidizer species (RDX, HMX/TAGN), porosity content, and fabrication technique (cast, pressed, or extruded) are typical. Furthermore, several specific boron hydride salts have been used. With all of these variables, one might expect that the mechanical properties of the resulting samples might vary as much as the combustion behavior; and as it turns out, this is the case. Mechanical properties of the samples range from very stiff and brittle to rubbery. In addition, certain formulations show a large degree of nonhomogeneity as a result of the fabrication technique.

The propellants tested during this program possess the various ingredients and properties described previously. These propellants, shown in Table 1, contain either Hycar, Kraton, or Carbowax in the form of an inert binder. These three propellant types were each fabricated using a different technique as discussed in references [6] and [7]. The Kraton samples were made using toluene to form a lacquer. The resulting mixture was spread on trays and dried. The dried propellant was then broken into crumbs and pressed (at 23,000 psi and 240° F) to 90, 95, and 100% of the theoretical maximum density (TMD). The resulting propellant samples exhibit a high degree of nonhomogeneity, with the rather large crumb boundaries still visible. In addition, this slate utilizes an organic salt (tetramethylammonium) of $B_{10}H_{10}^{2-}$, otherwise known as H466.

The PEG slate was produced using the solvent methylene chloride as a processing aid. Any residual solvent was removed, and the mixes were pressed under low vacuum at 70° F and 24,000 psi to 85, 90, and 95% TMD. These samples, although still very stiff and hard, were much more homogeneous than the Kraton slate, since the material was not dried on a tray before pressing.

Table 1. Propellant Formulations Studied

Hycar-Based Samples					
Sample	Hycar	DOA	H498	RDX	% TMD
TC-47	9	1	0	90	95.1
TC-47A	8	2	0	90	96.0
TC-48A	8	2	3	87	96.3
TC-49	9	1	6	84	96.4
TC-49A	8	2	6	84	96.8
TC-50	11	2	3	84	96.7
TC-51	5	2	3	90	93.1
Kraton-Based Samples				(90, 95 & 100% TMD)	
Sample	Kraton	H466	RDX		
TC-14	15	12	73		
TC-15	10	12	78		
TC-16	5	12	83		
PEG-Based Samples				(85, 90 & 95% TMD)		
Sample	PEG	BDNPA/F	HMX	TAGN	H498	Pt/C
TC-40	5	—	50	30	15	—
TC-41	10	—	46.5	28.5	15	—
TC-43	5	5	47	28	15	—
TC-44	5	—	57.5	34.5	2	1
TC-45	5	—	53.75	32.25	8	1
TC-46[a]	6/0.4[a]	2/1.6[a]	46.9	28.1	15	—

[a] The TC-46 formulation actually contains no PEG, but rather a mixture of GAP (6%) and CAB (0.4%), with DOA (2%) as a plasticizer and IPDI (1.6%) as a cross-linking agent. It is included with this slate due to its inherent similarity, both chemically and physically, to the rest of the PEG-based propellants.

NOTE: Hycar - hydroxyterminatedpolyacrylate (Hycar 4051)
Kraton - copolymer of polystyrene and polyethylene-butylene
PEG - [diol-terminated] polyethyleneglycol (Carbowax, C4000)
BDNPA/F - bis-dinitropropylacetal/formal (energetic cross-linking agent)
DOA - dioctyladipate (a plasticizer)
H498 - boron hydride ($K_2B_{10}H_{10}$)
H466 - boron hydride ($[N(CH_3)_4]_2B_{10}H_{10}$)
RDX - cyclotrimethylenetranitramine ($C_3H_6O_6N_6$)
HMX - cyclotetramethylenetetranitramine ($C_3H_8O_8N_8$)
TAGN - triminoguanidinium nitrate
Pt/C - platinum/carbon black (burn rate catalyst)
GAP - glycidyl azide polymer
CAB - cellulose acetate/butyrate
IPDI - isoporone diisocyanate

The Hycar slate was produced via an extrusion process, using ethyl acetate in the form of a solvent. Typical conditions were 120° F and 2,000–4,000 psi in the extruder. The resulting propellants possess very good mechanical properties. In other words, the samples are rubbery and very homogeneous. Both the PEG slate and the Hycar slate utilize H498, the potassium salt of $B_{10}H_{10}^{2-}$. The Kraton slate and the Hycar slate both contain RDX as the oxidizer, while the PEG slate contains HMX and TAGN in the ratio of 5:3. This combination has been credited with a faster burn rate than RDX, primarily due to the TAGN.

1.4 Organization of This Report. This section describes how the remainder of this report is organized. Section 2 contains an extensive literature survey covering topics such as VHBR propellant combustion diagnostics, including both the chemistry and closed bomb burn rate studies which have been undertaken over the years. In addition, papers on the application of certain VHBR formulations to traveling charge gun firings and ballistic modelling of traveling charge systems are reviewed. Also, papers on the subject of DDT (deflagration to detonation transition) and the related topic of PDC (piston driven compaction) are presented due to their apparent relevancy to VHBR propellant combustion. Finally, the topic of catalytic activity in high energy nitramine propellants is briefly addressed.

Section 3 presents an overview of the experimental program conducted and presents descriptions of all of the experimental techniques utilized and the goals of each. Section 4 contains the experimental results from the techniques described in section 3, as well as a discussion of these results. Section 5 contains the conclusions reached as a result of the present program. Section 6 is a summary of the work to date, including this program and some of the work discussed in the literature survey, as well as recommendations for future efforts.

2. LITERATURE SURVEY

2.1 Early VHBR Propellant Studies. VHBR is a name given to a class of propellants with apparent burn rates in the range of approximately 1 to 1,000 m/s. There are a number of potential applications for propellants with burn rates of this magnitude. These applications include such advanced ballistic concepts as the traveling charge and monolithic propellants, as well as rocket propellant and ram jet fuels [3]. While a number of different propellant formulations may exhibit burn rates with magnitudes sufficient to qualify as VHBR propellants [4, 8], the focus of the Veritay programs and most other VHBR studies conducted from the late 1970s until the late 1980s has been on formulations containing HIVELITE ($B_{10}H_{10}^{2-}$) salts. Propellants of this type typically contain three key ingredients: a salt of $B_{10}H_{10}^{2-}$ (with

either an inorganic or organic cation); an oxidizer species, such as RDX, HMX, or TAGN; and a binder/plasticizer matrix, which may be either energetic or nonenergetic in nature.

Since 1981, this class of propellants has been the subject of two Joint Army-Navy-NASA-Air Force (JANNAF) workshops [3, 4]. It is the objective of this section to summarize the large quantity of work which has been aimed at the study of VHBR propellant combustion. In addition, a summary of efforts concentrated in areas potentially related to VHBR combustion, such as the DDT and PDC mechanisms, is presented.

Early VHBR propellant investigations [9, 10, 11] were initiated during the late 1970s and early 1980s to determine the suitability of this family of propellant formulations for traveling charge applications. These investigations included a number of propellant formulations containing boron hydride burn rate modifiers. These formulations exhibited apparent burn rates over the range from 1 to 500 m/s, which meets the burn rate requirement established for traveling charge propellants by interior ballistic calculations. In addition to the high combustion rate, the requirements for this propellant class included such conventional propellant requirements as safety and ease of handling.

During this initial phase of the investigation, the thermochemistry of over 200 different propellant formulations was examined through the use of the BLAKE code [12]. Of these, the eight listed in Table 2 were selected for fabrication and experimental evaluation. The primary energetic constituents selected for these formulations were the granular materials cyclotetramethylenetetranitramine (HMX), ammonium nitrate (AN), and triaminoguanidinium nitrate (TAGN). These materials are also the source of oxygen for the propellants, while the boron hydride element acts as a fuel. The binders used in these formulations included carboxy-terminated polybutadiene (CTPB), nitrocellulose/dinitrotoluene (NC/DNT), and a polyethylene glycol designated carbowax (PEG or C4000). The fuels used in these compositions were HIVELITE formulations denoted by a numerical scheme developed by Teledyne McCormick Selph. The thermochemical properties of these formulations are given in Table 3.

The eight propellant formulations were fabricated into samples of two sizes: one 12.7 mm (0.5 inch) in diameter and 50.8 mm long (2.0 inches), and the other 36.6 mm (1.44 inches) in diameter and 25.4 mm (1.0 inch) long. These samples were compacted to a variety of density values and tested in both confined and unconfined configurations. The confined samples were encased in steel tube sections with walls 1.57 mm (0.062 inch) thick. In addition to confinement, the tubing limited the exposed surface area of

Table 2. Early VHBR Propellant Formulations Studies

Sample Code	BH Fuel	Weight-percent	Oxidizer	Weight-percent	Binder	Weight-percent
1086-ID	498	10.2	HMX	74.8	CTPB	15.0
1086-2C	466	17.1	AN	70.9	CTPB	12.0
1086-3	466	25.7	AN	59.1	NC/DNT	15.2
1086-4B	466	10.6	TAGN	74.2	NC/DNT	15.2
1086-5A	498	8.8	TAGN	76.0	NC/DNT	15.2
1086-6B	466	27.0	AN	67.1	C4000	5.0
1086-7B	466	10.5	TAGN	84.5	C4000	5.0
1086-8A	498	8.6	TAGN	86.4	C4000	5.0

Table 3. Comparison of Selected Thermochemical Properties of VHBR Propellants With M30A1

Propellant	Impetus (J/g)	Temperature (K)	Mol. Wt. of Gas	Co-volume (cm^3/g)	Specific Heat Ratio
M30A1	1064.7	3000	23.430	1.044	1.2406
1086-2C	976.0	2170	14.454	1.246	1.2679
1086-3	1094.6	2538	13.085	1.221	1.2670
1086-4B	1090.4	2402	15.926	1.301	1.2719
1086-5A	1124.7	2647	17.500	1.198	1.2662
1086-6B	1094.1	2488	12.245	1.240	1.2650
1086-7B	1084.4	2329	15.335	1.328	1.2710
1086-8A	1119.1	2539	16.815	1.229	1.2692

the propellant sample to a single end face of the right circular cylinder. In this way, an attempt was made to establish a cigarette-burn form function for closed bomb testing. Combustion rates were derived from the pressure data obtained from a single transducer port location.

The propellant samples were tested in both a conventional closed bomb [10, 11, 13], shown in Figure 1, and a specially designed apparatus which came to be known as the VHBR bomb [14, 15], depicted in Figure 2. The inner diameter of the VHBR bomb was essentially the same as the outer diameter of the VHBR propellant samples; therefore, the bomb provided radial confinement for propellant samples during testing. Instrumentation in the VHBR bomb consisted of pressure ports at the center and both ends of the sample as well as at the center of the bomb itself. As depicted in Figure 2, while one end of the bomb was sealed with a fixed plug and end cap, closure at the opposite end of the bomb was provided by a rod approximately 1 m long that was instrumented with strain gages located adjacent to the end of the bomb. The strain gages were utilized to measure the combined forces of gas and solid phases to allow determination of thrust. This combined force is analogous to the force acting on a projectile.

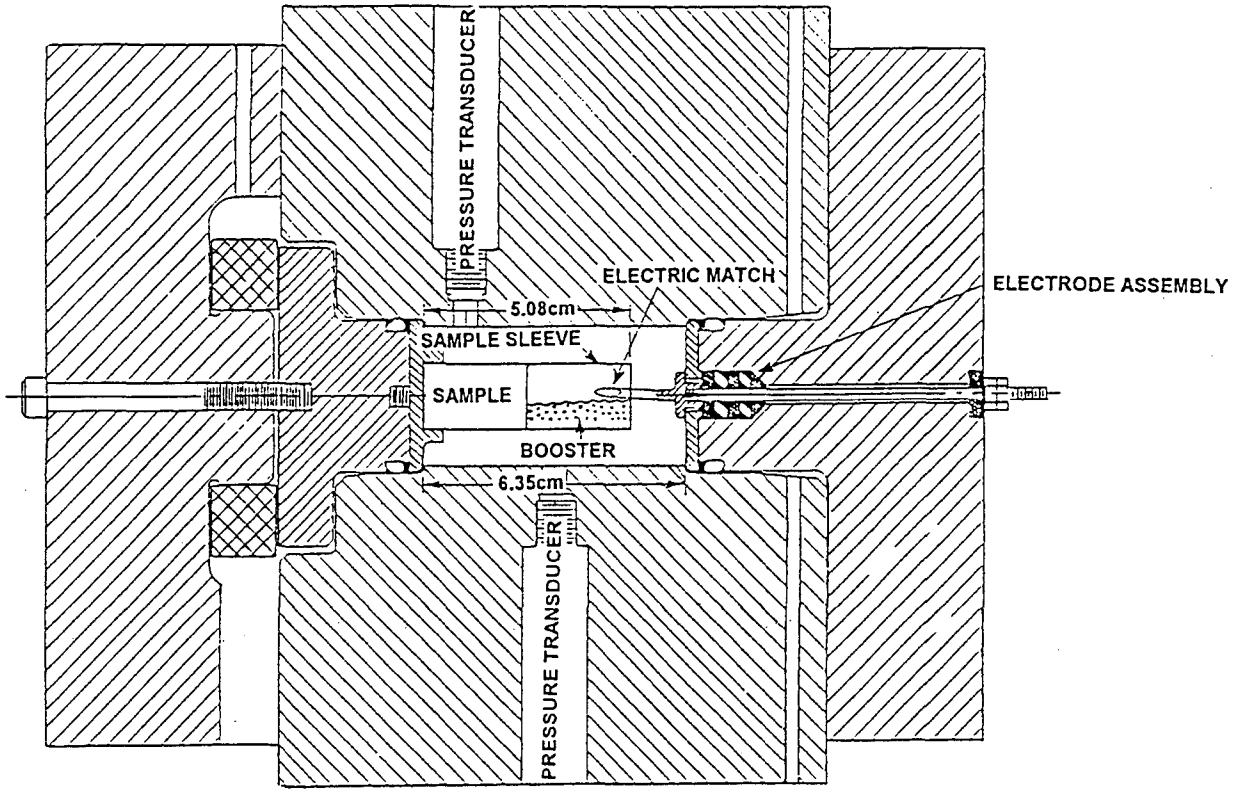

NOTE: This configuration was used for 1-inch samples at the start of Veritay's Phase I program; initially 2-inch samples, which completely filled the tube, had been used. Later, the tube was shortened to coincide with the length of the 1-inch samples. A small sack of black powder was tied to the match to provide a booster.

Figure 1. Conventional closed bomb (approximately 50-cm^3 volume).

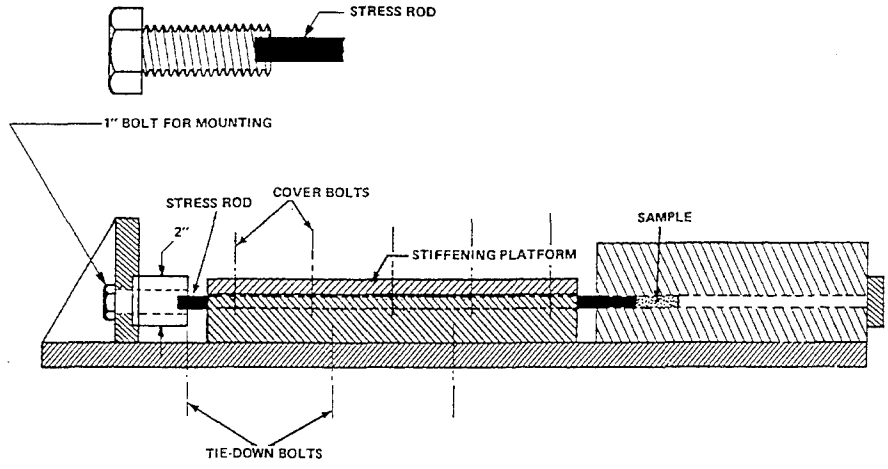

Figure 2. Schematic of Calspan VHBR thrust bomb.

A brief summary of the characteristic apparent burn rate data obtained for these propellants is presented in Table 4. These values were based on the time required for the closed bomb pressure to rise from 10 to 90% of its peak value. It was assumed that this "10–90% burn time" corresponded to the combustion of 80% of the sample length and also that the propellant burned laminarly with a cigarette-burn form function. The test parameters either identified or inferred by the data in this table include propellant formulation identity, sample porosity (%TMD), confinement, and the type of bomb used for testing (conventional or VHBR). Conclusions which may be made from these data include:

(1) The formulations selected for the study did indeed span the required range of apparent burn rates (from 1 to 500 m/s).

(2) Combustion rates for samples with identical composition (denoted by sample identification number) but with different porosity tended to increase with increasing porosity (lower %TMD); however, the effect was much more dramatic with some formulations than with others (NOTE 7B vs. 5A).

(3) The axial retention characteristic of the samples pressed into steel sleeves was a more significant factor than radial confinement as indicated by comparison of tests conducted in the VHBR bomb with tests of confined and unconfined samples in a conventional closed bomb. VHBR bomb samples were free to move to relieve pressure buildup at the base of the sample, while samples pressed into steel sleeves were not. This axial retention may also have contributed to an increased stress level within the propellant sample, leading to fracture.

(4) Combustion results may be greatly influenced by the test technique.

(5) Combustion variability increases with increasing combustion rate, part of which is due to extreme dynamics in the pressure data and deconsolidation processes for fast-burning samples.

(6) The contribution of the boron hydride component is not apparent from these results.

Table 4. Summary of Apparent Burn Rate Measurements

			Average Burn Rate			
			Calspan Tests [Ref. 13]		BRL Tests [Ref. 10, 11]	
Sample 1086-	TMD[a] (%)	VHBR Bomb [Ref. 14, 15]	Bare (m/s)	Confined (m/s)	Bare (m/s)	Confined (m/s)
1D	92	—	—	—	—	1.0
1D	86	0.4	—	—	0.6	—
2C	90	—	—	2.4	—	2.6
2C	86	1.3	—	—	1.5	—
3	91	50	35	—	89	—
3	83	—	—	89	—	104
4B	97	80–100	—	—	82	—
4B	88	—	—	—	—	161
5A	98	—	113	418	238	—
5A	86	—	245	—	357	—
5A	86	—	—	476	—	385
6B	85	22	22	90	24	45
6B	88	21	—	69	16	—
7B	98	2.5	6.1	—	4.5	—
7B	89	180	—	102	—	250
8A	97	21	42	—	32	—
8A	86	—	—	294	—	192

[a] Theoretical Maximum Density.

Other observations resulting from this testing which is not apparent from the data in Table 4 include:

(7) The slower-burning samples exhibit a combustion rate which increases with increasing pressure.

(8) The faster-burning samples exhibit a combustion rate which appears to be regressive with respect to pressure when a laminar form function is used; this is suggestive of an alternative form function that incorporates a convective or volumetric combustion mechanism [13].

(9) Combustion rates are accelerated by increased chamber pressure (effected by increasing loading density in sequential tests) to a greater degree than normally attributed to pressure.

(10) Lubrication of the sample circumference during VHBR bomb tests reduced apparent burn rates significantly.

(11) A data reduction scheme, formulated by Gough [10], incorporating pressure and thrust measurements from the VHBR bomb, indicated that values of interphase stress provided a better correlation to burn rate than did chamber pressure.

(12) Formulations containing HIVELITE with nitrocellulose in the binder were later judged to be unsafe due to an increased sensitivity to friction and static electricity and were subsequently eliminated from consideration in the traveling charge program.

(13) Some samples exhibited a transition from a slow laminar to a high-rate, apparently convective, combustion mechanism after a certain critical chamber pressure was attained.

(14) At times, it was observed during VHBR bomb tests that a rapid pressure rise was first observed at the end of the sample adjacent to the stress rod end closure of the bomb (i.e., the end of the sample opposite the end exposed to the igniter). This is suggestive of a possible stress-induced ignition mechanism or unusual flame propagation sequence.

2.2 Diagnostics for VHBR Propellant Combustion. A number of studies have been dedicated to measurement of apparent burn rates for VHBR propellant formulations. In almost all cases, the apparent burn rates were determined using closed bombs [13, 14, 15, 16, 17]. During early investigations into the combustion mechanism of VHBR propellants, experimental strand burner techniques were utilized. However, uncertainty as to the validity of the measured burn rates obtained via this technique led to a recommendation by the JANNAF community that such techniques not be utilized to study VHBR propellant formulations [4, 8]. Even the validity of standard closed bomb burn rate reduction techniques has been called into question. To perform (apparent) burn rate reduction using the relevant form function, usually end-burning (cigarette-style) or cylindrical, it is necessary to assume that combustion is laminar and limited to the exposed surface region of the propellant. However, as mentioned earlier, evidence exists which indicates that many of the very fast-burning VHBR propellant formulations burn volumetrically. It is suggested that combustion occurs not only at the propellant surface, but also at some depth within the propellant sample, leading to a possible mechanism responsible for the much higher apparent burn rates that have been observed for some samples. Apparent burn rates for a large number of propellant formulations have been measured, allowing a relative comparison to be made of important formulation and experimental variables and their resulting effect on propellant combustion.

An interesting variation of the standard closed bomb technique involved rapid prepressurization by combustion of a relatively large booster charge of conventional propellant [18]. This type of experimental configuration has been utilized to measure burning rates of VHBR propellants under higher pressure conditions, to better simulate combustion in an environment approaching that to which a traveling charge propellant will be exposed. An important result of this study was the fact that formulations which were relatively slow burning at lower pressures showed unexpectedly high burn rates at higher prepressurization levels, rates over and above those expected by extrapolation of the de Saint Robert burn rate relationship.

A number of other diagnostic techniques have been applied in attempts to identify the combustion mechanism of VHBR propellants. As discussed in the previous section, an effort was dedicated to characterizing the thrust generated by a VHBR propellant sample, for application to the traveling charge gun concept. In this study [14], a stress rod was used to measure the total force generated by the burning propellant sample. This measurement could then be related to the thrust generated by the propellant sample by simply subtracting the local gas phase pressure. Some of the propellant samples generated substantial amounts of thrust, although this was by no means true for all of the VHBR formulations tested. Again, at times it was observed that ignition and initial combustion of the propellant sample occurred at the end not exposed to the igniter.

In addition, other diagnostic techniques have been developed or applied to the study of VHBR propellant combustion. Trimble et al. [19] used a flash x-ray technique to investigate VHBR combustion mechanisms. X-ray sequences were used to generate information pertaining to sample regression and density as a function of time to provide increased understanding of the combustion process. For example, Trimble's results showed that the combustion reaction had propagated throughout the entire sample, long before a significant portion of the sample had been consumed. Also, these x-ray diagnostics appeared to show that the transition to a rapid combustion rate was triggered by deconsolidation of the propellant sample. The deconsolidation process also appeared to be related to the means by which the sample was confined. In other words, samples confined with a strong case apparently experienced greater deconsolidation; this led to higher burn rates when compared to experiments performed with samples encased with weaker confinement materials or unconfined.

Another study [17] confirmed these results using high-speed motion pictures of a VHBR sample burning in a transparent fixture. Following ignition of the sample, no regression of the burning sample was evident. However, the combustion reaction did appear to propagate along the length of the sample

until the entire sample contained patches of luminescence. As the combustion process made the transition from slow to fast burning, the entire sample appeared to react (combust) at once, suggesting that volumetric burning had occurred.

Some of the studies mentioned previously employed interesting combinations of instrumentation to investigate the VHBR combustion phenomenon. The thrust bomb study [14], in addition to the instrumented stress rod used to measure thrust, incorporated a total of four pressure transducers to measure pressures at various positions within the bomb. The resulting pressure traces frequently showed unexpected behavior, such as an unusual ignition location of a given sample. In another study [10], photo-diodes were used to detect the presence of lumination, indicative of a combustion reaction within the sample. Once again, on several occasions, the test results indicated the initial presence of light at unexpected locations. For example, at times, the light detector at the rear of the sample registered the presence of light before the detectors near the expected point of ignition (i.e., the exposed surface). This was given as further proof that an in-depth reaction must have occurred while the chamber pressure was still near its initial level.

2.2.1 Safety Aspects of VHBR Propellants. The safety aspects of VHBR propellants have also been explored in several studies [16, 20]. Some VHBR formulations have shown themselves to be sensitive to a variety of stimuli. Therefore, proper safety evaluation of new formulations is essential before routine handling and more thorough research efforts are undertaken. In one such study, the sensitivity of a range of formulations to impact, heat, and electrostatic discharge was measured [16].

Certain combinations of ingredients in the propellant formulation can also increase the sensitivity of a sample. For example, formulations containing a nitrocellulose binder and HIVELITE have been found to contribute to safety problems after aging for a relatively short period of time. Sensitivity to static electricity caused a sample containing nitrocellulose and HIVELITE to ignite when it was being inserted into a fiberglass tube at BRL. Safety concerns led to re-evaluation of VHBR formulations being considered for the traveling charge program at BRL [20]. Another safety-related issue was discovered during open air ignition response tests [13]. While some samples exhibited a slow burn characteristic, others exhibited a high-rate response bordering on a low-rate detonation. These concerns also led to a study of formulations with improved safety characteristics, as well as a more detailed examination of the factors which may contribute to VHBR behavior.

This goal of high combustion rates with improved handling and safety characteristics was, in part, subsequently achieved. However, a somewhat disturbing trend in the results was observed. This trend involved an apparent correlation between the achievement of high combustion rates and an associated increase in propellant sensitivity characteristics.

2.2.2 Analytical Chemistry Diagnostics. Some of the techniques of analytical chemistry have also been applied in an effort to identify the chemical reaction mechanisms at work during VHBR propellant combustion. The thermal decomposition of the common oxidizers contained in VHBR propellants, RDX and HMX, in the presence of boron hydride has been examined using techniques such as differential scanning calorimetry (DSC), thermogravimetric analysis (TGA), gas chromatography-mass spectroscopy (GC-MS) and high-performance liquid chromatography (HPLC). Helmy [21] presented results which indicate that the presence of borohydrides affected the DSC curves of the oxidizers in contact with it. Furthermore, examination of the pyrolysis products generated when HMX and RDX were heated while in contact with HIVELITE showed that the boron hydride modified the decomposition of these oxidizers [22, 23, 24], thereby producing pyrolysis products typically found at much higher temperature levels. In addition, RDX and HMX begin decomposing at lower temperatures when in the presence of HIVELITE salts than when tested alone. These observations imply some sort of catalytic activity on the part of the boron hydride component. These efforts have included examination of the pyrolysis reactions of entire VHBR propellant formulations, including the binder materials.

2.3 Parameters Influencing VHBR Propellant Burn Rates. The closed bomb studies detailed in the previous section have explored the influence of various formulation parameters on the combustion rates of VHBR propellants. In addition, the following propellant and experimental variables have been shown to have an effect on the apparent burn rate of this class of propellants:

(1) Density of the sample (porosity);

(2) Chemical nature and amount of the HIVELITE salt;

(3) Chemical nature and amount of the polymeric binder;

(4) Chemical nature and amount of the oxidizer;

(5) Degree of sample confinement;

(6) Initial pressurization level;

(7) Relative composition of propellant components;

(8) Particle sizes of the fuel and oxidizer.

The discussion following the 1986 JANNAF Workshop [3] provides an excellent overview of the variables influencing combustion rate of VHBR propellants. This section briefly summarizes the results of that discussion.

The sample density can have a significant effect on the burn rate of VHBR propellants, as concluded by a number of studies [13, 14, 17]. However, the amount of burn rate enhancement varied from study to study and is formulation dependent. For example, one study [13] showed only moderate changes (typically around 10 to 25%) in the burn rate with changes in sample density. Another study [17] reported data which showed that a change in density of 12% could change the burn rate by a factor of 20.

Two different HIVELITE salts have been widely used as ingredients for VHBR propellant formulations, each utilizing the $B_{10}H_{10}^{2-}$ anion with different cations. HIVELITE 498 (H498) contains an active metal cation (potassium), while the HIVELITE 466 (H466) compound contains an organic cation (tetramethyl ammonium). Closed bomb testing [17] of propellants containing the two different HIVELITE compounds has indicated that the H498 compound produces higher burn rates than does the H466 compound. The difference between the effect produced by the two HIVELITE species is even more pronounced in formulations containing energetic binders [3]. When compared to other boron hydride salts, the $B_{10}H_{10}^{2-}$ anion appears to be the more effective burn rate enhancer. Salts containing the $B_{12}H_{12}^{2-}$ anion are typically less effective than the $B_{10}H_{10}^{2-}$ anion.

VHBR formulations have also been prepared using both inert and energetic binder systems. Energetic binders contain functional groups which serve to increase the energy of the formulation. Energetic binder additives which have been used in VHBR formulations include GAP (glycidyl azide polymer) and nitrocellulose. VHBR propellant formulations which have utilized inert (nonenergetic) binder systems include, among others, most of the propellant formulations tested during the Veritay experimental program that is the main subject of this report and consists of such things as polyethylene glycol (PEG or Carbowax), hydroxy-terminated polyacrylate (Hycar), hydroxy-terminated polybutadiene, and a mixture of styrene and ethylene-butylene (Kraton). As might be expected, when all else is equal, formulations containing energetic binders tend to burn at faster rates than do those containing nonenergetic binders.

Also, as mentioned earlier, the use of energetic binders may carry the penalty of increased propellant sensitivity. For example, formulations made with nitrocellulose-based binder systems have been shown to be more sensitive to external stimuli than formulations with other binder systems. This may be due to some sort of incompatibility between the nitrocellulose binder and the boron hydride salt [3].

The identity of the oxidizer has also been shown to have an effect on the burn rate of VHBR formulations [3]. The use of TAGN (triaminoguanidinium nitrate), either alone or in combination with HMX or RDX, has been shown to be effective in increasing burn rates. Also, HMX has been shown to produce slightly higher burn rates than RDX, probably due to the higher energy of the HMX molecule.

The degree of confinement and method of sample containment during combustion has been shown to exert a strong influence on the experimental burning rate behavior. In one study [13, 14, 17], side confinement of the sample was necessary to produce high burn rates. Further, the use of thicker metal sleeves, which increased the degree of confinement, led to further increases in the burn rate. Another study [13, 14] showed that confinement yielded burn rates two to three times higher than burn rates from unconfined samples under comparable conditions.

The dependence of the burn rate of some VHBR propellant formulations on pressure is somewhat unusual. Experimental results have shown that some formulations which produce high burn rates under high-pressure conditions burn slowly at ambient pressure conditions [13, 17]. At elevated pressure levels, the effect of pressure on burn rate is not obvious. Closed bomb experiments using a conventional propellant booster charge to attain elevated pressure levels prior to igniting the VHBR sample led to unexpectedly large increases in the burning rate [25]. These increases were found for formulations which did not exhibit VHBR behavior at ambient or moderate pressurization levels [18].

This type of experiment also demonstrated the existence of an interesting paradox [26]. The effect of boron hydride in certain formulations tested under these conditions was not clear cut because certain formulations showed high burn rates in the absence of a boron hydride species. This raised an interesting question pertaining to whether the mechanics of the experiment was responsible for generating the high observed apparent burn rates, or rather the chemistry of the formulation which controlled burn rate behavior.

The relative quantities of the various constituents of VHBR propellants can also influence the burn rate. Increased solid loadings (at the expense of the binder) tend to increase the burn rate. This may be the result of several changes in the propellant simultaneously. Very high solids loading can lead to a weakening of the mechanical properties of a propellant grain and a corresponding increase in its porosity. As the proportion of solid particles within a formulation increases, the corresponding increase in particle surface area may exceed the area that the available binder can successfully coat. In addition, when the amount of binder material in the propellant is very small, there may exist no truly continuous phase. This tends to weaken the mechanical properties of a given heterogeneous propellant sample. Also, increased concentrations of fuel and oxidizer particles in the propellant sample (resulting from reduced binder content) might logically be expected to produce increased combustion rates as a result of increased chemical reactivity.

The particle size distribution of the granular solid components also has an effect on VHBR propellant burn rates [3]. An increase in the average particle size of HMX or RDX granules tends to increase the overall propellant burn rate. For TAGN particles, the opposite is true. That is, a *decrease* in the size of TAGN particles tends to increase the overall propellant burn rate. The effect of particle size on combustion rate is strongly influenced by the decomposition mechanism of the oxidizer species [3]. A decrease in the particle size of boron hydride granules tends to increase the propellant burn rate.

It is important to realize that changes in propellant formulation variables can also produce changes in the physical properties of the propellant. For example, changes in the chemical nature of the polymeric binder can affect the mechanical strength and character of the sample. Other variables, such as porosity, solids loading, and particle sizes of the respective species can similarly affect the sample strength. Thus, some of the trends reported in the cited literature must be counter-balanced by the knowledge that changes in the burn rate may be due to subtle combinations of a number of compositional variables.

2.4 Combustion Mechanisms of VHBR Propellants.

2.4.1 An Early Combustion Theory. Based on the observations and results of the early diagnostic testing of VHBR propellants, a combustion mechanism was proposed [3] in which the ignition phase involved decomposition of the oxidizer, possibly catalyzed by the presence of the boron hydride. During the initial stages of combustion, it was felt that the boron hydride might act as a source of hydrogen in the form of a free radical. This could then be followed by rapid oxidation-reduction reactions, which

could be at least partially responsible for the rapid deflagration observed. During the later stages of the mechanism, the boron hydride could act as a fuel, to be oxidized by either the nitrogen or oxygen species present.

Propellant formulation variables that influence physical properties of the propellant (for example, the diameter of the solid particulates) may affect propagation of in-depth reactions. Any initial porosity in the sample tends to increase the reaction propagation due to increased surface area available for combustion and a potentially weakened propellant matrix, although this does not appear to be a prerequisite for fast-burning formulations. Variables which aid in the breakup of the sample, such as heavy confinement or poor physical properties, tend to also increase the burning rate of the sample. Therefore, the effects of physical properties must also be considered when formulating in-depth reaction mechanisms to explain the differences between slow and fast burning VHBR propellant formulations [3].

2.4.2 Other Potential Combustion Mechanisms. The observed combustion characteristics exhibited by the eight VHBR propellant formulations discussed earlier and shown in Tables 3 and 4 were suggestive of combustion mechanism(s) substantially different from that of conventional propellants [10–16]. Understanding this mechanism(s) sufficiently enough to lead to the development of a working hypothesis of the combustion of these propellants is an evolutionary process. Because most VHBR formulations contain at least some porosity, it was believed that a convective combustion zone, propagated by infiltration of hot combustion products through pores in the sample ahead of the flame front [4, 8], was responsible for the in-depth combustion phenomena. An early one-dimensional traveling charge code [27] prepared by Gough assumed the existence of a thin flame zone. Baer [28], however, discovered that closed bomb combustion results could not be correlated with that code.

To eliminate these deficiencies, Kooker [29] formulated a code using the assumption that the deflagration of a confined end-burning column of high-density, compacted-granular, energetic material does not accelerate from a surface burning mode by convective combustion through a rigid, stationary, porous matrix. Instead, it was proposed that porous material upstream of the burning interface collapses to form a plug of higher-density material. Proper confinement then leads to an increase in the stress field beyond the allowable rate of shear, which then is responsible for local ignition in shear bands and fracture of the collapsed plug. The fragments are entrained into the flame zone, creating a two-phase flow combustion process which is capable of supporting rapid increases in pressure. Subsequent studies have

not supported the entrained particulate, two-phase flow aspect of this combustion model. However, the in-depth ignition of the propellant may occur via Kooker's hypothesis.

Another combustion mechanism was proposed following experiments conducted by White [3, 17] in which a transition to in-depth burning and sample deconsolidation was clearly demonstrated. Samples tested during this work were at or near the theoretical maximum density, with little or no expected gas permeability. During this effort, high-density VHBR materials, which exhibited low burning rates under low pressure closed bomb conditions, were found to burn rapidly when prepressurized to higher pressures by relatively large conventional propellant booster charges. This observation appears to be analogous to the burn rate enhancement effect of increased loading density [14] on VHBR burn rate noted previously in which burn rate increases in excess of levels attributed to pressure alone were measured. Thus, a new pressure-driven in-depth or porous burn mechanism is suggested as a basis for at least some observed VHBR behavior.

The chemical contribution of boron hydride is believed to be related to catalysis of the thermal decomposition of the nitramine [30] or other oxidizer. The boron hydride $B_{10}H_{10}^{2-}$ and $B_{12}H_{12}^{2-}$ salts appear to be stable, even in an oxidative atmosphere, at temperatures below 300° C. DSC curves of uncatalyzed RDX exhibit a melting endotherm at 205° C and a broad intense decomposition exotherm over the range from 225 to 250° C. When catalyzed by a boron hydride salt, these characteristics are replaced by a sharp exothermic spike that appears to occur at 205° C, precisely the temperature that uncatalyzed RDX melts. These observations seem consistent with a catalysis mechanism involving attack of the B-H bonds of the catalyst on the nitramine. This mechanism involves direct reaction of the nitramine with the catalyst. However, it is possible, but thus far not demonstrated, that the catalysis of the decomposition reactions may occur at a later stage in the combustion process, such as with reactions involving the initial decomposition by-products (e.g., such as H_2CO, NO_2, N_2O, HCN, etc.). Heat release from these accelerated reactions could then act to accelerate the initial decomposition reaction steps. Thus, it appears that the presence of boron hydride species may increase the chemical reactivity and reaction rates of nitramines, potentially leading to greatly increased local combustion rates.

2.4.3 Mechanical Contribution to Combustion Mechanism. As touched on previously, the very fast burning characteristics of certain VHBR propellant formulations has suggested to investigators that the propagation mode of the reaction may be a stress-induced phenomenon. In the model of Kooker and Anderson [31], the combustion mechanism was tied to fracture and compaction of the solid propellant,

leading to formation of small grains at the free surface. These grains were then entrained into the flame zone, creating a two-phase flow combustion process, with the particles burning as they left the propellant interface. It is the rate at which such a compressive wave can travel in addition to the rapid combustion rate of these relatively small propellant grains which would lead to the very high apparent burn rates observed.

However, little experimental evidence has been reported to support this model. In fact, strong evidence has been reported, revealing that in some instances very little surface regression of the propellant has occurred when the sample has been ignited and burned almost to completion. Flash x-ray data [19] have been reported which shows VHBR propellants deconsolidating (as was found using the ciné x-ray technique during the present effort). However, these results indicate that the propellant breaks into rather large particles, and the small fragments hypothesized by the Kooker model are not observed. It should be noted that this x-ray technique may not have sufficient resolution to observe these small particles were they to exist.

2.4.4 The DDT and PDC Mechanisms. Propellants are known to burn via a stress-induced mechanism when the correct physical environment and combustion conditions are present. The mechanism which controls this type of combustion is known as the DDT. A good overview of this phenomenon is presented by Kooker [32]. The typical configuration for DDT experiments consists of a bed of granular propellant confined within a cylinder with thick walls. The bed of propellant is ignited by a booster charge and begins to burn quite rapidly due to the very high loading density of the cylinder (usually about 1 g/cm^3). This rapid deflagration then transitions to a detonation if the various factors which influence this transition are satisfied. These include a sufficiently strong confinement, the appropriate propellant particle size, low propellant bed permeability, high sensitivity to mechanical shock, adequate energy release rate from combustion, and adequate length of propellant bed.

Two modes of DDT behavior have been outlined by Bernecker [33, 34]. In each of these modes, it appears that the response of the granular bed to compressive stress waves plays a dominant role. The following discussion is taken from Kooker's report [32]. In the first mode, convective combustion of the propellant near the igniter end of the confined bed creates a rapidly increasing pressure field, which then propagates into the unburned material as a system of compressive waves. This stress wave system can compact the propellant bed, thus altering the propagation rate of the convective flame in a manner analogous to Kooker's VHBR model [29]. However, if the pressurization rate from the propellant

combustion is sufficiently strong to drive the compaction waves to shock wave strength, unburned propellant may be ignited ahead of the flame front by mechanical compression, providing a pathway for detonation. In the second mode, combustion leads only to a mild pressurization rate of the bed, although compaction may still be extensive. Then suddenly, at some point within the propellant bed, a violent reaction drives a rapid pressure buildup (which may propagate in both directions). This leads to shock wave formation and provides a pathway to detonation.

Although the aforementioned discussion centers on a transition to detonation which begins with an initial convective flow from an igniter system or a deflagration, this is not a prerequisite. Studies have shown that high strain rate compression or impact of a quiescent granular propellant bed can also lead to a transition to detonation. This phenomenon has been investigated in studies in which pistons were used to compact the propellant bed to initiate the event. These experiments, termed PDC, along with the DDT and shock to detonation experiments, all suggest that the transition to detonation can be initiated in different ways, including by booster combustion products (thermal) or by an impact (mechanical). The transition to detonation mechanism is essentially the same for both events, with the pressure generated by the convective combustion acting in the same way as a piston driving a system of compressive waves into the unburned propellant bed. Kooker's hypothesis, then, is that the successful transition to detonation appears to require the formation and maintenance of a strong compressive wave which ignites material in its path, before a full detonation wave has been established. Some data presented in Kooker's [32] report indicate that the compaction wave speed increases directly with the theoretical maximum density of the propellant bed. Values for the compaction wave speed from PDC experiments performed by Sandusky and Glancy [35], show a compaction wave speed of about 600 m/s in a bed of 65% TMD melamine and a compaction wave speed of about 1,250 m/s in a bed of 85% TMD melamine, when each is impacted with a projectile moving at about 200 m/s. Melamine is an inert material, used here to help define the response of a bed of material with substantial porosity to compressive waves.

Bernecker [36] gives propagation rates of various wave fronts in a double-base spherical powder. These range from 260 m/s for a weak compaction wave driven by the igniter, to 620 m/s for a strong compaction wave driven by the combustion of the ignited propellant, to 2,150 m/s for the reactive shock wave and 5,190 m/s for the detonation velocity.

While the aforementioned DDT discussion applies to granular propellants, Campbell [37] cites cases of reactive shock waves in cast propellants (DINA and pentolite). These waves are said to be plastic and actually propagate at speeds less than the local sound velocity. That paper also describes experiments with pressed PETN (97% TMD) in which detonation waves at velocities as low as 1,300 m/s were achieved when initiated by a flame. Stable detonation velocities both below and above that of sound were observed depending on the degree of confinement; greater confinement led to higher-order (faster) detonations.

The various stages of the DDT mechanism may be summarized as follows [38]:

(1) Preignition and compaction

(2) Ignition/conductive burning

(3) Convective burning, if sufficient porosity remains

(4) Compressive ("Hot Spot") burning from the coalescence of compressive waves driven by conductive/convective burning

(5) Shock formation

(6) Compressive burning behind shock

(7) Detonation.

Stages 5 through 7 constitute the shock-to-detonation transition (SDT), while the mechanism at work in PDC experiments, in which the compressive burning is initiated by a piston, may be described by stages 4 through 7.

Fifer [4] also recorded DDT experimental data for the VHBR formulations which they studied [39]. The samples tested were about 33 mm in diameter and 25.4 mm in length. The propellant was confined in a cylinder with an ID roughly equivalent to the OD of the propellant samples, with an ullage space at the ignition end from 12.7 mm to 63.5 mm long. The samples tested were denoted 4, 5A, 6, 7B, and 8A. The resulting data indicated that samples 6 and 7B did not detonate, even with 355 mm of propellant and either 12.7 or 38 mm of ullage. Sample 4 was found to detonate at a propellant bed length close to 190 mm, while samples 5A and 8A were found to detonate at propellant bed lengths between 114 and 190 mm. The study indicates that VHBR propellants can be made to detonate and an approximate inverse relationship was correlated between the length to detonation and the apparent burn rates from closed bomb

tests. In addition, the amount of ullage present did not seem to affect the results in any way, possibly suggesting that radial confinement and axial retention are more important than the ullage which serves to modify initial ignition strength and early-time pressure rise rates.

3. EXPERIMENTAL PROGRAM

3.1 Overview. To gain important insight into the combustion mechanisms of the VHBR propellant formulations, various experimental and diagnostic test techniques were utilized during the present program. These include traditional techniques such as closed bomb burn rate reduction, as well as new and innovative techniques devised or adapted for use during this program. An example of the latter is the strain gage measurement technique developed during this program to evaluate the rate at which the combustion zone propagates into VHBR propellant samples. Also, a new technique was developed as a result of a collaborative effort between Veritay and Dr. Kenneth Kuo of the Pennsylvania State University which allows extremely short exposure video images of the combustion region of very fast-burning propellant samples to be obtained using an x-ray source. These techniques and others are included in this summary of the various experimental techniques utilized during the Veritay experimental programs.

3.2 Closed Bomb Tests. The basic experimental technique utilized during the present program was closed bomb testing. In fact, a closed bomb in one form or another was used in virtually all of the combustion experimentation conducted during the program, which includes the ciné x-ray work at Penn State and diagnostic testing at Veritay. Each specific application of the closed bomb testing is addressed in the following sections.

3.2.1 Apparent Burn Rate Measurement. Experimental determination of apparent burn rates from closed bomb tests was the basic means for evaluating and comparing the combustion characteristics of the different VHBR propellant samples available for this program. Historically, evidence has indicated that some VHBR propellants do not burn by the normal surface combustion mechanism, but rather by some complex in-depth volumetric combustion mechanism for which no form function exists. Consequently, the term "linear burn rate" is no longer meaningful for VHBR propellants that exhibit a volumetric combustion mechanism. Instead, apparent burn rates are determined by assuming and applying a traditional form function to the combustion event, quantified by a closed bomb pressure history, as if laminar surface combustion were occurring. As a result, extremely high *apparent* burn rate values can result for propellants which deviate significantly from this assumed form function (i.e., those which have

a large volume of propellant burning at a time). The experimental closed bomb technique utilized during the current program resembled approaches used in previous VHBR experimental efforts. Specifically, the technique consisted of combustion of a propellant sample within the 50-cm^3 closed bomb that was approximately 12.5 mm (0.5 inch) in diameter, 25.4 mm (1 inch) in length, and 5 g in mass. This produced a closed bomb loading density of approximately 0.1 g/cm^3.

For the closed bomb testing, the sample was typically confined within a stainless steel tube, held in place using epoxy. This sleeve configuration has been used commonly to simulate the configuration of a traveling charge propellant as it is confined in the aft section of the projectile. In this way, only the surface of one end of the cylindrical propellant sample was exposed to igniter gases during a typical closed bomb test. In this configuration, a cigarette-burning form function is assumed for reduction of burn rate data. By encasing most of the propellant surface area with steel, any variations due to flamespreading during ignition were reduced substantially. In addition, strong confinement of the VHBR propellant has been shown to have a significant effect on the resulting combustion, tending to increase the combustion rate of some VHBR propellant formulations.

In the standard closed bomb experimental configuration used during the current program, the booster was contained in a bag formed from cigarette paper and ignited with an electrical resistor. A 1-g mass of BULLSEYE* powder was the standard booster charge used for this closed bomb testing. However, a small portion of this program was dedicated to the investigation of the effect of variations in booster chemistry on ignition of the Hycar-based propellant slate, as discussed in a succeeding section of this report.

A high-pressure closed bomb was constructed during the course of the program to evaluate the effect of higher booster pressure levels on combustion of slower-burning VHBR propellant samples. This bomb may be operated at volumes of 50 and 100 cm^3 by addition or removal of a steel insert. In this bomb, the propellant sample is actually mounted within the removable endcap assembly. This allows longer samples (up to 51 mm (2 inches) in length) to be tested and provides sample confinement with an extremely high degree of mechanical strength.

* BULLSEYE is a double base propellant produced by HERCULES, Inc.

To reduce the closed bomb pressure-time data into the standard form of linear (apparent) burn rate vs. pressure, the VU-POINT* software package was first utilized to convert the pressure data into an appropriate data file format. To do so, a pressure range was selected, starting at a pressure level higher than that produced by the booster charge and ending at approximately 90% of the peak chamber pressure. For the standard 1-g BULLSEYE booster, the pressure generated was about 21.4 MPa (3,100 psi). The pressure range which has become a de facto standard for closed bomb burn rate reduction is 10–90% of peak pressure. However, this range was not adequate when the 1-g booster of BULLSEYE powder was used in conjunction with most members of the Hycar propellant slate. This is due to a combination of the relatively low peak pressures and relatively high booster pressure produced. In other words, the value of 10% of peak pressure was actually lower than the pressure level developed by the booster charge. Consequently, pressure ranges of 20–90% or 25–90% of peak pressure were used in instances where this was situation existed.

The resulting pressure data were then smoothed using a combination of smoothing functions and skipping data points, and the resulting data were then input to a closed bomb burn rate reduction code. During the present program, a PC-based derivative of CBRED, known as the MINICB** [40] burn rate reduction code, was utilized. The apparent linear burn rate data generated from this code were then plotted as a function of closed bomb chamber pressure on log-log coordinates.

3.2.2 Closed Bomb Testing With Diagnostic Instrumentation. In addition to the standard closed bomb tests that involve burn rate reduction analysis, some innovative test techniques were utilized to further study the combustion phenomena of various VHBR formulations during the three Veritay experimental programs. These techniques included embedded fine wire thermocouples to measure the thermal environment as the flame front approaches; embedded fiber optic probes to measure light output at specific locations within the propellant sample; and miniature strain gages mounted on the exterior of the sample confinement sleeve to measure the propagation rate of strong stress waves that were indicative of the presence of combustion within the propellant sample.

The strain gage technique proved to be most useful for the study and quantification of combustion zone propagation into the sample for some of the very fast-burning members of the VHBR class of

---

* VU-POINT is a product of S-CUBED, a division of Maxwell Laboratories, Inc.

** Supplied by BRL.

propellants. The fine wire thermocouples proved to have only limited utility in this study, being too fragile to withstand the rigorous stresses within the slower-burning samples for which they were utilized. The optical fibers were also susceptible to these stress fields. In addition, any analysis of light data, beyond merely using it as an indicator for the arrival of the combustion region, must be interpreted with a knowledge of the frequency range over which the detector is useful. Also, the fiber itself may tend to filter certain frequency ranges, depending on the material, and quality of construction of the fibers. Consequently, light energy frequencies outside of the ranges detectable by this method were not observed. Ultimately, to get the most from this approach, it would be desirable to resolve the spectrum of frequencies emitted by the light energy resulting from combustion of the propellant. This might then be used to provide valuable information concerning the chemical reaction mechanisms at work. However, this type of analysis was outside the scope of this program.

As mentioned previously, the main objective of each of the types of special diagnostic instrumentation was to study the rate of propagation of the in-depth combustion zone in VHBR propellants. Of the three types of instrumentation described previously, the most useful and informative data were obtained using the strain gage technique developed during this program. This approach is noninvasive to the propellant sample and is relatively robust (unaffected by combustion of the sample). The strain gage technique has some similarities to a technique utilized in the field of DDT/PDC experiments. The main objective of this strain gage approach was to measure the rate of propagation of the strong stress waves within samples of the very fast-burning members of the VHBR family of propellants. This was accomplished by measurement of the strain on the sidewall of the confinement tube imposed by the passing stress waves.

The strain gages utilized during this program were quite small in size, having a width of 0.5 mm (0.020 inch). In most experiments, four gages were typically used, centered at 5-mm (0.2 inch) spacings along the length of the sample. These miniature strain gage elements were fastened onto the propellant confinement tube with an epoxy adhesive. For testing in the standard closed bomb, the confinement tube to which the gages were fastened was made from 304 stainless steel. However, when these gages were utilized in conjunction with the ciné x-ray experiments, a confinement tube made from epoxy-impregnated, wound Kevlar fibers was used. Instrumentation wires were then run along the length of the confinement tube, covered with epoxy, and fed through a sealed port in one of the bomb endcaps. With this configuration, strain measurements were made at several axial locations along the confinement tube as a function of time.

3.2.3 Quenched Combustion Studies. During the early stages of Veritay's VHBR investigations, which include Phase I SBIR, New York State Matching Fund, and Phase II SBIR programs, quenched combustion studies were conducted on samples of several Hycar-based VHBR propellant formulations. These samples were recovered and analyzed, qualitatively and quantitatively, following rapid depressurization of the bomb to quench combustion. Depressurization was achieved using a vented bomb configuration, consisting of a specially designed endcap equipped with a rupture disk. Quantitative chemical analysis of the quenched combustion surface was achieved using the ESCA (electron spectroscopy for chemical analysis) technique. ESCA was used to ascertain the identity of the condensed phase reaction products involving boron species that were contained in the residue on the surface of the quenched propellant sample.

Results of these early tests indicated that for the Hycar propellant slate it was not possible to quench samples which contained more than 3% boron hydride. In addition, it was also found to be impossible to quench a sample (TC-51) with a low boron hydride content but a high level of porosity. The current Phase II program concentrated more on the very fast-burning VHBR propellant formulations. Often, these formulations had a boron hydride content substantially greater than the 3% level identified as potentially significant in the earlier study. In addition, many samples of these formulations had substantially higher porosity levels than the members of the Hycar slate, suggesting a further potential difficulty in quenching the samples. This, combined with the fact that the mechanical contributions to the combustion mechanism of VHBR propellants received more emphasis during the present effort, led to the quenching technique not being utilized during the Phase II program.

3.2.4 Elevated Pressure Combustion Rate Characterization. As mentioned earlier, in order to obtain apparent burn rate data on the Hycar slate of VHBR propellants at higher pressure levels, a high-pressure closed bomb was fabricated which had a selectable volume of 50 or 100 cm^3. With this bomb, much higher pressure levels could be generated by larger booster charge masses and larger VHBR propellant samples (approaching 10 g). In addition, variable loading densities were attainable by varying the propellant mass and bomb volume. With the resulting high pressure burn rate information, obtained at pressure levels closer to those which exist in the barrel of a gun, these propellant formulations could be evaluated for use as traveling charge propellants. In addition, any unexpected increases in burn rate over that predicted by the burn rate exponent and coefficient determined at the lower pressure regime could be evaluated. This type of behavior had been observed for some of the slower-burning formulations in previous studies. For most of the current testing, the bomb was configured with a 100-cm^3 chamber. The

propellant sample was epoxied within the robust endcap, which provided extremely strong sample confinement. Using this endcap, samples up to 51 mm (2 inches) in length could be tested.

3.2.5 Effect of Booster Chemistry. It was felt early in the current program that evaluation of the effect of booster chemistry on the ignition and burn rate reproducibility of members of the Hycar slate might help shed some light on the VHBR combustion mechanism. During the Phase I program, when the Hycar slate of propellants was studied extensively, it became apparent that there was a clear relationship between the ignition delay experienced by a given formulation and the resulting apparent burn rate of these propellants. Specifically, it was found that the longer the ignition delay, the lower the resulting burn rate of the propellant sample.

It was felt that if the ignition of the various propellant formulations could be made more reproducible, then it would be likely that the resulting apparent burn rate values would become more reproducible. This would make correlations between formulation variables and burn rate characteristics more discernable. The different boosters tested during this task were designed to produce a variety of output characteristics including the temperature of product constituents; the fraction of condensed phase material produced; and the chemistry of the gaseous product species.

3.3 Ciné X-Ray Testing. A series of experimental tests was conducted at the Pennsylvania State University Laboratories of Dr. Kenneth Kuo to help evaluate the combustion mechanism(s) of some of the faster-burning VHBR propellant formulations. The equipment utilized during this effort consisted of a Phillips Constant Real-Time X-ray source of 320 kV and 10 mA; a Precise Optics Image Intensifier [Model PI 2400 ATF] which has a 735-ns response time and a 9-inch-diameter viewing area; either a Spin Physics 2000 Video Camera, with a maximum framing rate of 12,000 pps or a Xybian CCD Camera with a multiple exposure (gating) capability and the ability to take video images of extremely short duration (down to 25 ns); an advanced digital image processing system [Quantex model 9210], to perform various image processing and enhancement functions; and a variety of data acquisition equipment.

The data which resulted from these tests consisted of video image(s) recorded from the screen of the image intensifier, in the form of either a cinematic sequence if the Spin Physics camera was used or a single video field (half a frame) if the Xybian camera was used; the pressure data from the closed chamber; and data from any specialized instrumentation used, such as the strain gages utilized during the present program.

X-ray photography is an extremely valuable diagnostic tool for investigation of the combustion mechanism of VHBR propellant samples. This is due to the inherent nature of the technique, which allows density variations along the length of a sample to be evaluated while it is burning, both qualitatively (visually) as well as quantitatively, using the Quantex system. The Quantex was used to produce isophote (constant luminosity) images, which were representative of the density at various positions within the propellant sample. In this way, the state of the propellant sample at the exposed (unconfined) surface as well as at points within the sample could be ascertained in a nonintrusive manner.

The x-ray technique allows a burning propellant sample to be analyzed while confined in a manner similar to that used in the standard closed bomb. This confinement must be provided by a suitable, nonmetallic material to avoid significant degradation of the quality of the x-ray transmission. During this program, the confinement material used was an epoxy-impregnated, Kevlar fiber-wound tubing. Strength of confinement has been shown to be an important parameter affecting VHBR combustion. Therefore, utilizing a tube material which approximated the strength of the stainless steel tubing used in the standard closed bomb test configuration was critical in order to be able to make meaningful correlations between the two test configurations.

3.4 Thermochemical Calculations. To compare the energy contents of different VHBR propellant formulations, the NASA-LEWIS and BLAKE thermochemical computer codes were utilized. Aside from being used to make general comparisons, the output from these codes was also required as input data for the MINICB computer code and used to determine propellant burn rate from closed bomb pressure data. The thermochemical codes allow the effect of relatively small changes in propellant composition on various thermochemical properties, such as impetus and flame temperature, to be evaluated.

3.5 Miscellaneous Testing. Since the mechanical contribution to the combustion mechanism of the very fast-burning members of the VHBR family of propellants became of primary interest during the current program, it became critical to somehow quantify the relationship between various physical properties and the resulting combustion behavior of these propellants. This section documents the use of some specialized testing techniques aimed at this goal.

3.5.1 Physical Property Testing. Early in the program, attempts were made to evaluate what were felt to be the physical properties of most importance to VHBR propellant combustion. These were the compressive and bulk moduli of the propellant samples, as well as the speed of sound within the

propellant sample. After a preliminary effort aimed at this, which included the fabrication of testing hardware and limited experimentation, it was determined that to properly accomplish these goals would require a level of effort and funding greater than that available under the scope of this program. As a result, another means was pursued to accomplish the goals of this task.

To evaluate the physical properties of the VHBR propellants, an arrangement was made to utilize the Drop Weight Material Properties Tester (DWMPT) at BRL.* This device consists of a weight cage, dropped onto an unconfined propellant sample; an optical displacement follower, utilized to quantify the sample strain; and a force transducer, utilized to quantify the compressive stress. The resulting data were used to determine the compressive modulus and ultimate stress values, as well as the stress, strain, and strain rate values at failure. The tests were conducted on propellant samples which were approximately 12.7 mm (0.5 inch) in diameter and 12.7 mm in length. During the testing, a 2-kg weight was dropped 20 cm (8 inches) onto each propellant sample. All testing was conducted at an ambient temperature of 25° C. The resulting data were then utilized to compare the mechanical properties of various propellant formulations. These comparisons could then be used to ascertain any potential relationship to observed combustion behavior.

4. EXPERIMENTAL RESULTS AND DISCUSSION

4.1 Propellant Formulations. The relative compositions of the various VHBR propellant formulations studied during the three Veritay programs have been presented in Table 1. For convenience, Table 1 is repeated on the following page. As the table shows, the general formulation of the VHBR family of propellants consists of a high content of granular nitramines and a relatively small quantity of granular boron hydride (in the form of a burn rate enhancer), all held in a continuous binder matrix. The VHBR propellants which have historically attracted the most attention are those containing HIVELITE, one of a number of salts of the anion $B_{10}H_{10}^{2-}$. Similar formulations containing the $B_{12}H_{12}^{2-}$ anion have also been investigated; however, a less complete database is available for propellants made with this material. The two HIVELITE salts most commonly used to date in VHBR propellants are proprietary formulations of Teledyne-McCormick-Selph (TMS), designated H498 and H466. In H498, a potassium cation is utilized, while in H466, an organic cation (tetramethyl ammonium) is utilized.

* The authors would like to thank Rob Lieb and Mike Leadore of BRL for their help in performing these tests and for the use of their facilities.

Table 1. Propellant Formulations Studied

Hycar-Based Samples					
Sample	Hycar	DOA	H498	RDX	% TMD
TC-47	9	1	0	90	95.1
TC-47A	8	2	0	90	96.0
TC-48A	8	2	3	87	96.3
TC-49	9	1	6	84	96.4
TC-49A	8	2	6	84	96.8
TC-50	11	2	3	84	96.7
TC-51	5	2	3	90	93.1

Kraton-Based Samples				(90, 95 & 100% TMD)
Sample	Kraton	H466	RDX	
TC-14	15	12	73	
TC-15	10	12	78	
TC-16	5	12	83	

PEG-Based Samples				(85, 90 & 95% TMD)		
Sample	PEG	BDNPA/F	HMX	TAGN	H498	Pt/C
TC-40	5	—	50	30	15	—
TC-41	10	—	46.5	28.5	15	—
TC-43	5	5	47	28	15	—
TC-44	5	—	57.5	34.5	2	1
TC-45	5	—	53.75	32.25	8	1
TC-46[a]	6/0.4[a]	2/1.6[a]	46.9	28.1	15	—

[a] The TC-46 formulation actually contains no PEG, but rather a mixture of GAP (6%) and CAB (0.4%), with DOA (2%) as a plasticizer and IPDI (1.6%) as a cross-linking agent. It is included with this slate due to its inherent similarity, both chemically and physically, to the rest of the PEG-based propellants.

NOTE: Hycar - hydroxyterminatedpolyacrylate (Hycar 4051)
Kraton - copolymer of polystyrene and polyethylene-butylene
PEG - [diol-terminated] polyethyleneglycol (Carbowax, C4000)
BDNPA/F - bis-dinitropropylacetal/formal (energetic cross-linking agent)
DOA - dioctyladipate (a plasticizer)
H498 - boron hydride ($K_2B_{10}H_{10}$)
H466 - boron hydride ($[N(CH_3)_4]_2B_{10}H_{10}$)
RDX - cyclotrimethylenetranitramine ($C_3H_6O_6N_6$)
HMX - cyclotetramethylenetetranitramine ($C_3H_8O_8N_8$)
TAGN - triminoguanidinium nitrate
Pt/C - platinum/carbon black (burn rate catalyst)
GAP - glycidyl azide polymer
CAB - cellulose acetate/butyrate
IPDI - isoporone diisocyanate

In typical VHBR propellants, HIVELITE concentrations range between 3 and 15 weight-percent and are in the form of small particles (typically on the order of 5 μm). The granular nitramine, or oxidizer, might be RDX, HMX, or either combined with another energetic, such as TAGN. In most cases, the nitramine particles are present in a bimodal particle size distribution in order to enable a high solids loading density with good surface wetting of the relatively low binder content. The particle size classifications most often used are ground (approximately 5-μm in diameter) and class 5 (approximately 150-μm average diameter). The combination of the binder with a plasticizer and/or cross-linking agent constitute the remainder of a typical propellant formulation. The latter combination may be either energetic or nonenergetic in nature; however, systems in which these materials are nonenergetic (inert) are the most common.

As stated in the Introduction, the goal of the present effort was to gain insight into the various factors which contribute to VHBR behavior. In so doing, it was hoped that this would result in the ability to tailor a specific propellant formulation to an application (i.e., burn rate performance). The propellants tested possess a range of ingredients and properties (both thermochemical and physical) as is documented later in this report. Each of the major propellant families tested utilized an inert binder system. As Table 1 shows, these binders were either Hycar, Kraton, or Carbowax. It should be noted that one member of the PEG slate (TC-46) actually possessed an energetic binder system based on glycidyl azide polymer (GAP). However, this formulation was included in the PEG-based propellant slate due to its inherent similarity, both physically and chemically, to the remainder of the PEG-based propellants.

The three families of VHBR propellants tested were produced, each using a different manufacturing process, at the Naval Surface Weapons Center, Indian Head Division [6, 7] (formerly Naval Ordnance Station, Indian Head). Some of the following discussion concerning the propellant manufacturing steps is summarized from references [6] and [7]. The Kraton-based propellant samples were made using toluene to form a lacquer. The resulting mixture was spread onto trays and dried. The dried propellant was then broken into crumbs and compressed (at 21.8 MPa [23,000 psi] and 116° C) to 90, 95, and 100% of the theoretical maximum density (TMD). The resulting propellant samples exhibit a high degree of nonhomogeneity, with the rather large crumb boundaries still visible. In addition, this slate differs from the other two by the fact that it utilizes H466, the organic salt (tetramethylammonium) of $B_{10}H_{10}^{2-}$.

The PEG slate was produced using methylene chloride as a processing aid (solvent). Any residual solvent was removed, and the mixes were pressed under low vacuum at 21° C and 165 MPa (24,000 psi) to 85, 90, and 95% TMD. These samples, although still very stiff and hard, were much more

homogeneous than the Kraton slate, since the material was not formed into dried crumbs before pressing. These samples also differed from the other two propellant slates in their composition. The energetic species utilized in the PEG slate were a combination of HMX and TAGN, in the ratio of 5:3. This combination has been credited with a faster burn rate than RDX, which was utilized in the other two propellant slates. In addition, two of the members of the PEG slate utilized 1% of a 50/50 mixture of platinum and carbon (graphite) as an additional burn rate enhancer.

The Hycar slate was produced via an extrusion process, using ethyl acetate as the solvent. Typical extruder conditions were 49° C and a pressure range of 13.8–27.6 MPa (2,000–4,000 psi). The resulting propellant samples were rubbery and very homogeneous, possessing very good mechanical properties. As in the PEG slate, the Hycar slate utilized H498, the potassium salt of $B_{10}H_{10}^{2-}$. As in the Kraton slate, the Hycar slate utilized RDX as the oxidizer.

4.2 VHBR Propellant Closed Bomb Combustion Behavior. In addition to the distinct differences between the physical appearance, physical properties, and manufacturing processes used for each of the three families of VHBR propellants studied during the Veritay programs (namely the Hycar, Kraton, and PEG slates), members of these three propellant slates appear to represent three distinct combustion regimes. For the purposes of this report, we define "true VHBR" combustion behavior to be the extremely fast combustion rate behavior exhibited by virtually all of the PEG slate and some members of the Kraton slate. The Hycar slate, on the other hand, appears to burn in a laminar fashion with the exception of one member (TC-51), which burns at a somewhat faster rate. For the rest of this slate, the magnitudes of the rate are consistent with the high energy content of the formulations. In addition, rate enhancement was observed with the addition of the boron hydride species. However, no true VHBR behavior was observed for this propellant slate.

Members of the Kraton slate appear to exhibit intermediate combustion behavior, with certain propellant formulations and densities combining to produce high burn rate behavior, while others exhibit a combustion behavior which more closely resembles the laminar-type combustion of the majority of the Hycar slate. On the other hand, all members of the PEG propellant slate appear to demonstrate true VHBR propellant combustion behavior. The latter is signified by extremely fast, violent combustion, which tends to destroy the steel sleeve used to confine the propellant samples. However, the high burn rate behavior associated with the Kraton slate will not be classified here as true VHBR behavior. There is clearly a difference between the relative violence of the combustion events observed for the Kraton

slate, in which the confinement sleeve is only slightly deformed, and that observed for the PEG slate. A more thorough discussion of the combustion characteristics of the respective propellant formulations is contained in the following sections.

4.2.1 The Hycar Propellant Slate. The Hycar propellant formulations may be characterized as being extremely homogeneous and exhibiting excellent mechanical properties (high elasticity and nonfrangibility). For the most part, these propellants, with a substantial energy content resulting from the high concentration of RDX (84–90 weight-percent) in these formulations, burned at relatively slow rates in comparison to the other propellant slates that were investigated. Figure 3 illustrates typical closed bomb pressure histories for the Hycar propellant formulations. Figure 4 contains the apparent burn rate data, reduced using the MINICB burn rate reduction code, for the closed bomb tests shown in Figure 3. Additional burn rate data for the Hycar slate are characterized in Table 5.

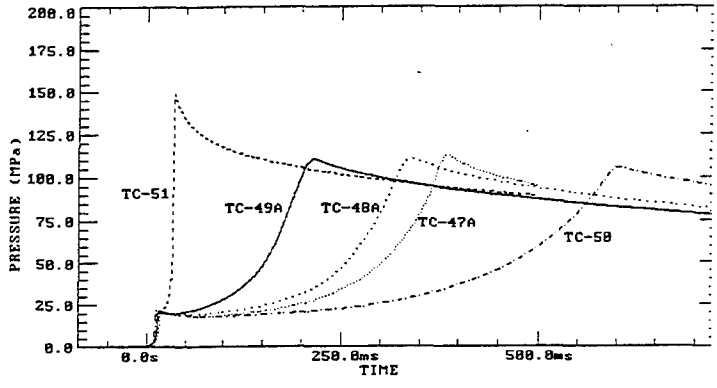

Figure 3. Closed bomb pressure histories for Hycar-based propellant slate.

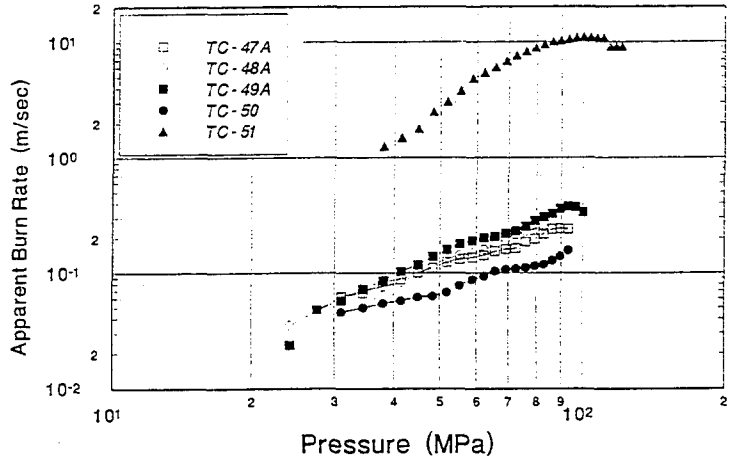

Figure 4. Apparent burn rate vs. pressure for Hycar slate.

Table 5. Results of Closed Bomb Tests With Hycar Propellants

Sample	Formulation[a] (weight-percent)	Total Burn (ms)	Burn Time 20–90% (ms)	Avg. Burn Rate (m/s)
TC-47	9/1/0/90	297.4 (22.0)	70.6 (15.6)	.324
TC-49	9/1/6/84	208.2 (17.2)	40.2 (8.6)	.569
TC-47A	8/2/0/90	434.3 (33.6)	158.8 (12.5)	.144
TC-48A	8/2/3/87	344.1 (8.3)	164.4 (9.1)	.139
TC-49A	8/2/6/84	313.0 (50.1)	162.0 (16.7)	.141
TC-50	11/2/3/84	688.9 (7.9)	236.7 (33.9)	.097
TC-51	5/2/3/90	90.8 (29.7)	5.33 (0.78)	4.29

[a] HYCAR/DOA/H498/RDX.
NOTE: Numbers in parentheses represent sigma values.

The reduced burn rate data are referred to as apparent burn rates due to the uncertainty caused by assuming a geometrical form function for VHBR propellant combustion. In other words, the in-depth mechanism which apparently governs the behavior of certain members of the VHBR propellant class cannot be described by any geometrical form function normally associated with conventional gun propellant. Nevertheless, the geometrical form function that would normally apply to cigarette burning in conventional propellant was used to determine effective or apparent burn rates for the VHBR propellant formulations. Thus, it may be said that a VHBR propellant sample is consumed at an apparent rate which is commensurate with the rate at which a conventional propellant would be consumed via laminar cigarette-type combustion, even though mechanistically this might not be an accurate representation of the combustion.

As Figure 4 and Table 5 indicate, only slight differences in burn rate exist among most of the Hycar propellant formulations. The only exception to this is the TC-51 formulation, which has a significantly greater porosity, as indicated by a lower %TMD value in Table 5. This higher degree of porosity can contribute to increased combustion rates by allowing a greater surface area to be exposed for combustion, and by reducing the mechanical strength of the sample, possibly leading to deconsolidation and even more exposed surface area. The TC-51 sample will be discussed further in the section on the ciné x-ray results.

In Table 5, the 20–90% burn time values are defined as the time required, after the sample is ignited, for the pressure to change from 20% to 90% of P_{max}, the maximum pressure achieved during a constant volume closed bomb test. The closed bomb pressure histories, such as those shown in Figure 3, consist of an initial pressure rise resulting from combustion of the booster charge, a subsequent slight pressure decrease due to heat transfer losses to the bomb and, finally, the pressure rise corresponding to ignition and combustion the propellant sample. The 20% of peak pressure time must occur during this period of pressure rise after ignition is assured. The total burn time is the time from the booster peak to the time at which P_{max} occurs and includes the sample ignition delay. Table 5 gives average values for total burn time, 20–90% burn time and burn rate. In addition, sigma values are included to give a representation of the reproducibility of the specific parameters for each formulation of the Hycar slate listed. The average burn rate values are obtained by dividing the length of propellant sample burned by the time interval over which it is burned—in this case, the 20–90% burn time. At the start of this time interval, the sample is assumed to be just ignited, since the pressure generated by the booster produces approximately 20% of peak pressure. From this time to the time when 90% of peak pressure is reached, approximately 90% of the propellant sample is consumed. Therefore, the average burn rate values listed in Table 5 assume 22.9 mm (0.9 inch) of propellant is consumed during the 20–90% burn time.

As Table 5 suggests, samples with lower plasticizer (DOA) concentrations show significantly shorter burn times than do corresponding samples with higher plasticizer concentrations, as symbolized by the DOA concentrations and burn times for TC-47 and TC-49 vs. TC-47A and TC-49A, for 0 and 6% HIVELITE, respectively. The effect of a plasticizer is to cause a polymeric material to become more elastic or rubbery and less brittle. In addition, it may allow the binder material to more thoroughly wet the particulates (oxidizer and fuel), possibly increasing the binding strength of the sample even though the amount of binder itself is decreased. Therefore, the decreased burn rate of more plasticized samples may be due to a reduced tendency for the sample to deconsolidate during combustion. Due to difficulties encountered by NOSIH personnel in successfully producing the low plasticizer content formulations repeatably, these samples were investigated in a cursory manner, at the suggestion of NOSIH and BRL representatives.

The addition of HIVELITE is seen to produce a significant decrease in the total burn times, as illustrated in Figure 3. Here it may be seen that the addition of 3 and 6% HIVELITE (TC-48A and TC-49A, respectively) at the expense of RDX, while keeping the binder and plasticizer content constant (thereby keeping the granular solids content constant), produces respective 12.5 and 44.4% decreases in

the total burn time, when compared with the HIVELITE-free sample, TC-47A. The 20–90% burn times in Table 5 are approximately the same for the three formulations, within reasonable experimental variation. The reduced apparent burn rate vs. pressure curves in Figure 4 show that a slight increase in burn rate accompanies this decrease in total burn time. It is apparent that the major effect attributable to the addition of boron hydride to the propellant formulations was the significant reduction in ignition delay observed in Figure 3. As is seen in the section on thermochemical properties, the substitution of boron hydride for RDX actually decreases the total energy of the propellant. Therefore, for these samples to be more easily ignited and to actually burn slightly faster, some type of kinetic effect triggered by the presence of the boron hydride must be occurring.

It has been shown in previous studies that the degree of solids loading [14, 21] of VHBR propellants can strongly influence the resulting burn rate. While it is not possible to vary solids loading without also affecting the propellant chemistry, this trend is clearly evident in the results obtained for the Hycar propellant family. Looking carefully at Figure 4, it may be seen that the three formulations having 90% solids—namely, TC-47A (0% HIVELITE), TC-48A (3% HIVELITE), and TC-49A (6% HIVELITE)—all have relatively similar burn rate profiles. In addition, at 87% solids content, TC-50 (3% HIVELITE) has a somewhat lower burn rate than the group at 90% solids. Also, at 93% solids loading, the TC-51 formulation has a substantially (approximately a factor of 30) higher burn rate than the other formulations. These trends are mirrored in the data contained in Table 5.

As has already been pointed out, higher burn rates are also observed for the two formulations which contain less plasticizer, TC-47 and TC-49, in Table 5. It would appear that the effect of less plasticizer is related, in a way, to the effect of higher solids loading described in the preceding paragraph. In other words, both effects tend to weaken the degree to which solid particulates are held in the binder matrix, either through a reduction in the amount of binder itself or through a reduction in the ability of the binder to wet the surface of the particulates. What is clear is that this mechanical effect dominates the relatively slight chemical effect observed by the addition of boron hydride at the expense of RDX.

Increased burn rate may also be related to propellant density (or %TMD in Table 1). The TC-51 sample was produced at 93.1% TMD, while the values for the remainder of the Hycar slate are in the range of 95 to 96% TMD. The relatively low sample density for TC-51 is almost certainly a result of the low binder content (only 7%). This, combined with the fact that the majority of the RDX has a fairly large particle size (average diameter is 150 μm) may combine to limit the final sample density due to

packing considerations. In other words, the relatively low binder content is unable to fully fill all of the void volume.

Reduced density can also be interpreted as increased porosity or void volume. The combination of reduced density and reduced binder is suggestive of weakened mechanical strength, which favors deconsolidation; and increased permeability to gas flow, which favors gas penetration and convective burning within the sample. All of the aforementioned characteristics—increased energy, weaker mechanical properties, and greater porosity—tend to promote higher burn rates.

- High-Pressure Closed Bomb Testing. As mentioned in section 3 of this report, a specially designed bomb was constructed during this program to test VHBR samples at higher pressure levels, approaching those to which the propellants would be exposed as travelling charge propellants in a gun. This testing was conducted for the members of the Hycar slate of propellants using larger booster masses to generate the higher initial pressure levels. In this way, it could be determined whether a transition in combustion behavior occurs for propellants which do not exhibit VHBR behavior under normal closed bomb conditions. Also, other investigators [3] have reported combustion behavior which does not obey the same burn rate relationship, with respect to pressure, that was established at the lower pressure levels.

The reduced apparent burn rate vs. pressure data for the tests of the Hycar slate conducted in the high pressure bomb are presented in Figure 5; the low and high pressure burn rate curves contained in Figures 4 and 5, respectively, are presented together in Figure 6. As indicated in Figure 6, the relative order of the magnitudes of the burn rate data for the respective formulations is the same at low- and high-pressure conditions. In addition, it does not appear that a dramatic change in the combustion rate dependence on pressure exists for any member of the Hycar slate with the possible exception of a slope break beginning at 70–80 MPa and extending into the higher pressure regime. When comparing the apparent burn rates at the two pressure regimes, the regions of dynamic combustion that pertain to the ignition and burn-out portions of the curves, where samples may be burning nonuniformly, should be ignored. If these regions are ignored, then a fairly continuous burn rate vs. pressure relationship is observed from the data in Figure 6. In fact, the only propellant sample which displayed a somewhat unusual (regressive) burn rate curve at elevated pressures was TC-50, a formulation which contained a great deal of binder material. Although no evidence exists to corroborate this, the unusual combustion profile of TC-50 may suggest some sort of deconsolidation process, which only occurs at elevated pressure levels.

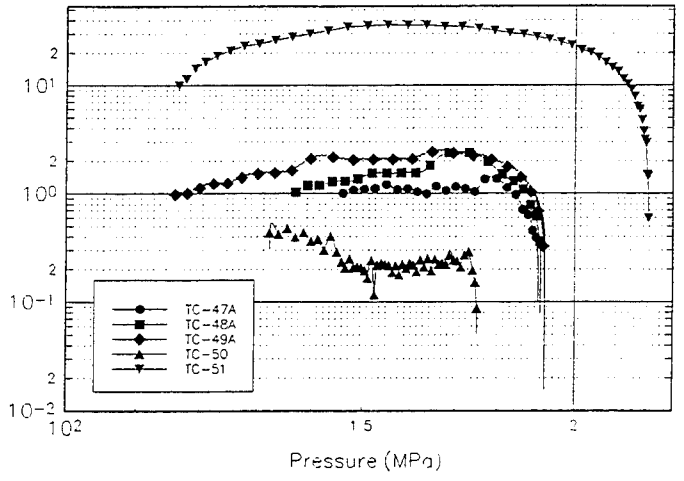

Figure 5. Results from high-pressure bomb testing of Hycar slate.

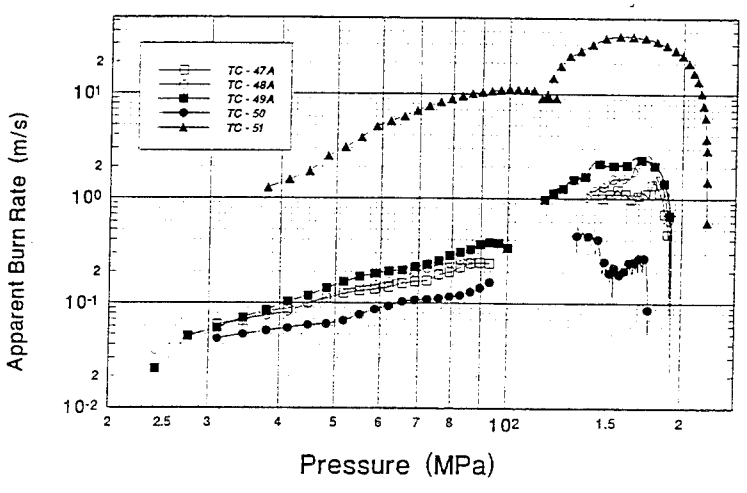

Figure 6. Combined apparent burn rate results for Hycar slate at high and low pressures.

The observations made by other investigators [18] concerning unexpected increases in combustion rate at elevated pressure levels was not corroborated during the current effort for the Hycar slate of propellants. As mentioned earlier, this family of propellants exhibits excellent mechanical properties, and its members show a high degree of homogeneity. These properties undoubtedly play some role in the well-behaved combustion observed at elevated pressure levels.

• Igniter Chemistry Evaluation Testing. A number of closed bomb tests were also conducted early in the Phase II program to improve the closed bomb combustion reproducibility of a specific VHBR

propellant formulation. This formulation, TC-49A, a member of the Hycar slate, had shown a relatively high degree of ignition and combustion variability during earlier testing using what had become the standard ignition system for the testing conducted at Veritay, 1 g of BULLSEYE powder. The igniter improvement effort was conducted through the use of various igniter materials in an attempt to investigate a variety of output properties, including heat, chemistry, and condensed phase products.

The results for these tests demonstrated improved ignition by varying the booster composition to create more favorable combustion product chemistry of the booster. The average burn time for the TC-49A tests using the standard BULLSEYE igniter (1 g) was 302.1 ms, with a standard deviation of 56.8 ms (18.8%). However, when 1 g of FFFFg black powder was substituted, the booster gas pressure dropped from 21.3 MPa (3,100 psi) to about 6.89 MPa (1,000 psi), and the average propellant burn time increased over threefold, to 1002.3 ms. Conversely, the variability in the burn time was actually decreased to a standard deviation of only 23.2 ms (2.33%) using the black powder booster, which is indicative of an improved ignition. The long delay before ignition is attributable to the significantly lower flame temperature of, and lower gas pressure generated by, the black powder. The better reproducibility is most likely a result of the relatively large quantity of condensed phase products produced by the black powder. Hot condensed phase products can improve ignition reproducibility, especially at cold temperature conditions, by conductive heat transfer to the propellant sample.

Based on these results, a test series which utilized both materials in an equipart mixture of 0.75 g each was conducted. This mixed booster produced a gas pressure roughly equivalent to that of the standard BULLSEYE booster. The average burn time obtained with this hybrid booster was 255.0 ms with a standard deviation of 38.4 ms (15.1%). While the results of this test series indicated a slight improvement over the standard booster, in light of the large database already accumulated which utilized the standard booster configuration, it was felt that the improvement was not significantly better to justify a change to a new booster material. These results demonstrate that some of the slower burning VHBR propellants, which resemble high-energy LOVA formulations, may experience some of the same ignition problems which plague LOVA propellants. Moreover, as with LOVA propellants, ignition of these VHBR propellants may be improved by modifying the booster chemistry.

4.2.2 The Kraton Propellant Slate. As stated earlier, the members of the Kraton propellant slate exhibit combustion behavior which appears to be in a transitional region between the relatively slow-burning Hycar slate and the very fast-burning PEG slate. In fact, in some instances, members of the

Kraton slate have been observed to exhibit combustion behavior which transitions from a slow-burning mode to a fast-burning mode during a closed bomb test. This transition is characterized by a sudden and drastic increase in the slope of the pressure-time history and by a correspondingly large and discontinuous jump in burn rate.

Figures 7, 8, and 9 contain representative closed bomb pressure traces for each of the members of the Kraton slate, TC-14, TC-15, and TC-16, respectively, in each of the densities at which the respective formulations were available. As the data in these three figures suggest, a wide range of combustion behavior was experienced during the testing of this propellant slate. A trend in the data is also apparent from these closed bomb tests. The total burn time, the 20–90% burn time, and the apparent burn rate of these propellants are strong functions of the percent of theoretical maximum density (%TMD) of the sample tested. At 100% TMD, the combustion rates signified by the pressure-time histories were relatively low and well behaved, in most instances. However, at densities lower than 100% TMD, the combustion rates increased dramatically. This type of phenomenon was observed in an earlier study of these and other VHBR propellant formulations [17]. A certain increase in burn rate is expected when the density of the propellant is decreased, as a result of an increase in the porosity of the sample and an associated increase in available burn surface. However, the dramatic changes in burn rate associated with the VHBR propellants have long been felt to be indicative of a different combustion mechanism.

As can be seen in both Figures 8 and 9, the combination of higher propellant energy level and low sample density, lead to very fast combustion rates, with virtually no recognizable ignition period. It was these observations which first suggested the potential connection between VHBR behavior and the mechanical properties of the respective propellant formulations.

The data in Figure 9 for the TC-16 formulation at 100% TMD show the type of transitional combustion behavior described previously. As the figure indicates, the pressure was rising gently after ignition, in a manner not unlike that observed for most of the Hycar slate. However, at a pressure level of approximately 55 MPa (8,000 psi), a sharp break occurred in the pressurization curve. This was followed by a much greater pressurization rate, which is indicative of a higher burn rate.

The reduced apparent burn rate data that correspond to the pressure traces given in Figures 7–9, for the Kraton family of propellant formulations, are presented in Figure 10. As the figure clearly shows, this propellant family exhibits a much broader range of combustion behavior than for the Hycar slate (see

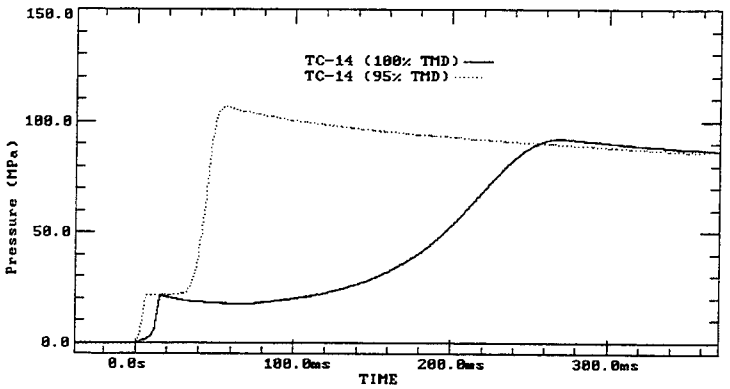

Figure 7. Closed bomb pressure histories for TC-14 at different densities.

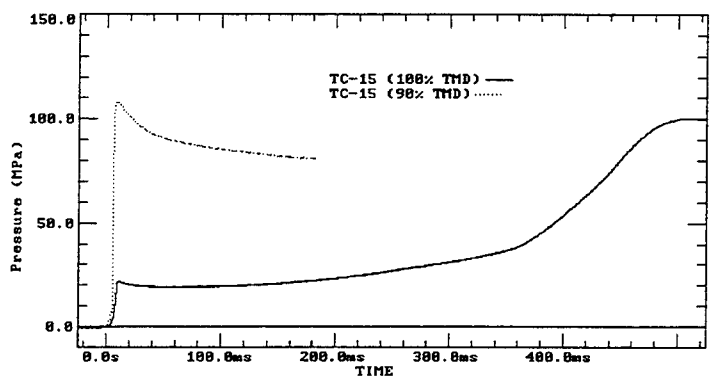

Figure 8. Closed bomb pressure histories for TC-15 at different densities.

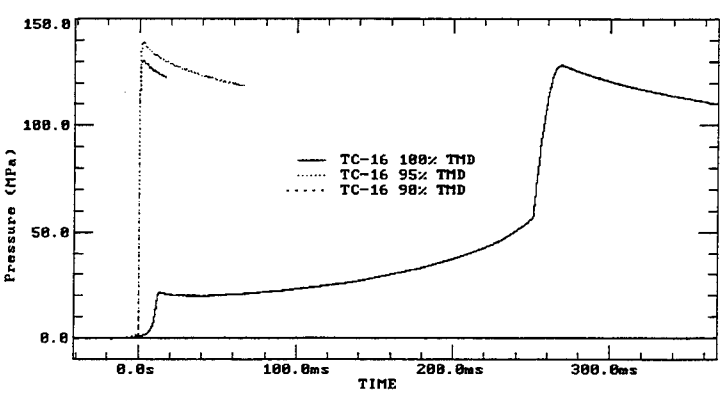

Figure 9. Closed bomb pressure histories for TC-16 at different densities.

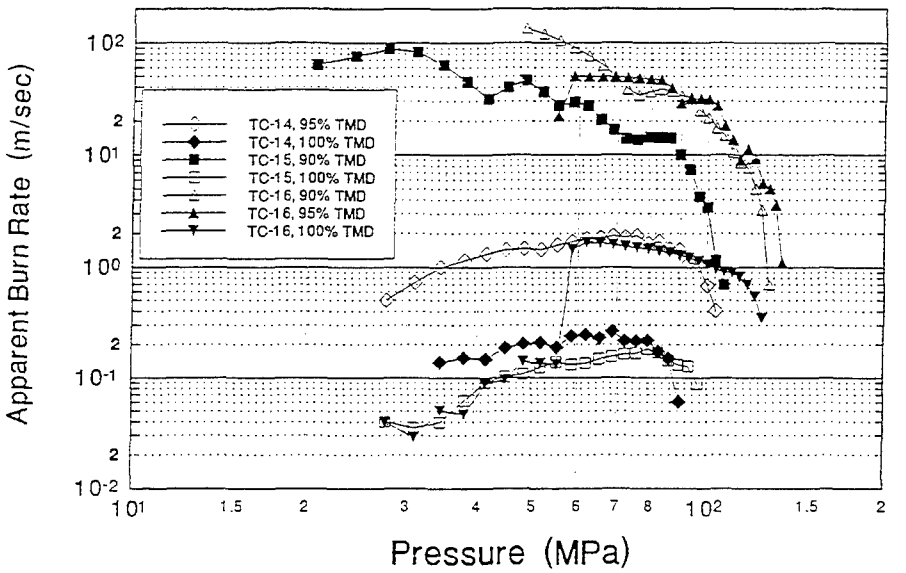

Figure 10. Apparent burn rate vs. pressure for Kraton slate.

Figure 4), with burn rates ranging from 0.1 m/s to 100 m/s. In addition, the burn rate data corresponding to the sharp slope change break in the closed bomb pressurization curve for the TC-16, 100% TMD, propellant formulation is seen to show a rapid jump to a burn rate almost an order of magnitude higher at the pressure slope discontinuity. As mentioned previously, this type of phenomenon has been observed in the past [17], and has historically been attributed to a transition from normal laminar combustion to an in-depth (possibly convective) combustion mechanism.

The closed bomb pressure histories for the Kraton samples shown in Figures 7–9 are presented again in Figures 11–13; this time the data in the plots are grouped according to the percent of TMD (% TMD) and the main parameter in each figure is the RDX-binder content. As Figure 11 suggests, the RDX content does not consistently correlate the resultant closed bomb data. For this propellant slate, the energy level of the respective formulations is directly proportional to the RDX content, since the boron hydride composition is the same for each. Because the density of each material in Figure 11 is at its maximum, it would be expected that the most energetic material (TC-16) would have the highest burn rate and fastest burn times of the three, followed in order by TC-15 and then TC-14. However, from Figure 11, it can be seen that the data for the TC-14 formulation is out of sequence with this expectation. Furthermore, when looking at the burn rate data for these tests in Figure 10, it can be seen that the TC-14 sample has a higher burn rate than both TC-15 and TC-16 at low pressures. After the burn rate transition, however, the TC-16 formulation burns at a rate which far surpasses the other two formulations. In addition, the low

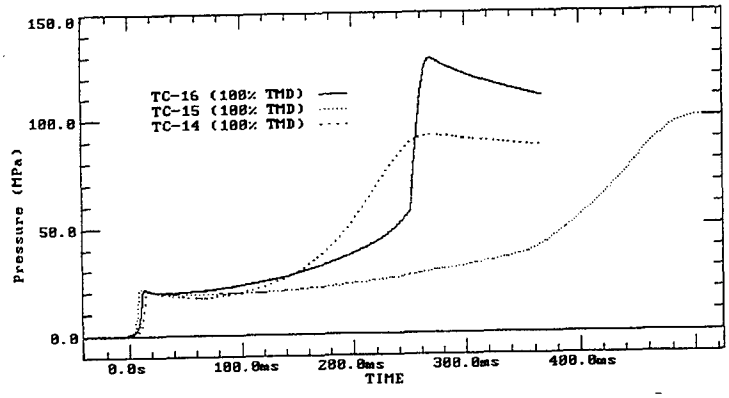

Figure 11. Closed bomb pressure histories for Kraton slate at 100% TMD.

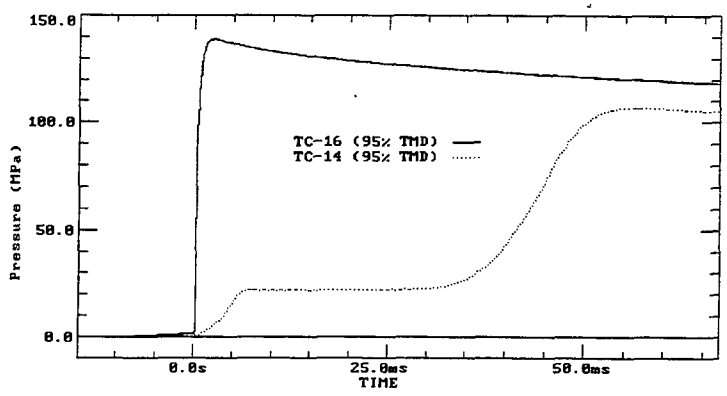

Figure 12. Closed bomb pressure histories for Kraton slate at 95% TMD.

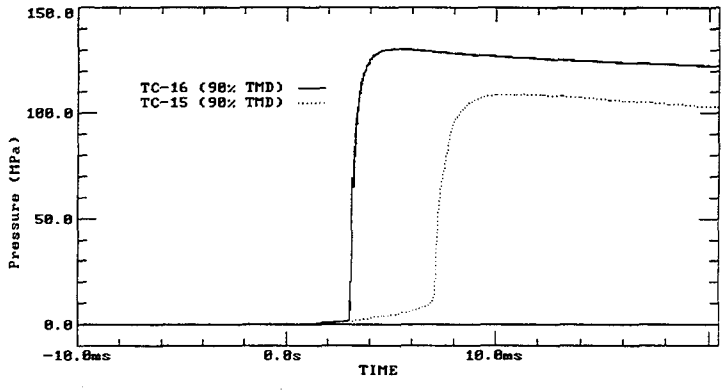

Figure 13. Closed bomb pressure histories for Kraton slate at 90% TMD.

pressure burn rate data for the TC-15 and TC-16 formulations is virtually indistinguishable until the transition point for TC-16.

Figure 12 compares closed bomb data for the members of the Kraton slate which were produced at 95% TMD. These data, along with the corresponding burn rate data in Figure 10, show a dramatic increase in burn rate for these lower density samples when compared to the 100% TMD versions. The reduced density of these samples results in higher porosity and weaker mechanical strength properties. As might be expected, the result obtained for the more energetic formulation (TC-16) had a much shorter burn time and a significantly higher burn rate than did the sample of the less energetic formulation (TC-14). In fact, as Figure 12 indicates, there is very little buildup of pressure from combustion of the igniter before vigorous combustion of the TC-16 propellant sample is observed.

Figure 13 contains the data for members of the Kraton slate at 90% TMD. As is apparent from this plot, the more porous, mechanically weaker propellant samples burn extremely quickly. Neither of the two samples at this density level required complete igniter combustion before becoming ignited and quickly burning to completion. Also, the effect of propellant impetus can clearly be seen in this plot. The more energetic TC-16 ignites quicker and reaches a higher pressure level than does the TC-15 sample.

Table 6 contains data for the 20–90% burn times for the Kraton slate. As the table shows, these results agree quite well with the observations made throughout this section. Although there appears to be a deviation of the data for TC-16 at the lower densities (90 and 95% TMD) from the trend of reduced burn times with decreased %TMD, the presence of superimposed pressure waves at these fast pressurization (combustion) rate conditions, can contribute uncertainty to these measurements. In addition, there is some uncertainty associated with the burn time for the TC-14, 100% TMD sample in Table 6. For this sample, as with many of the slower burning propellant samples, the 20% of peak pressure value actually falls below the igniter pressure. This is not usually a problem, since the igniter pressure usually drops slightly, to a level just below the 20% mark, due to cooling of the hot combustion gases. However, for this sample, as can be seen in Figure 7, the pressure does not drop after the igniter peak but continues rising at a very slow rate. This is indicative of combustion of the VHBR propellant sample itself. As a result, the value for the 20% of peak pressure point was somewhat arbitrary for this sample and was chosen at a point just after the peak igniter pressure (and at a level above the actual 20% mark).

Table 6. 20–90% Burn Times for Kraton Propellant Slate

TMD (%)	TC-14 (ms)	TC-15 (ms)	TC-16 (ms)
100	164.0	381.3	140.2
95	39.9	—	0.590
90	—	1.02	0.619

Another factor which contributes to peak pressure differences among the samples is the theoretical maximum density for the three members of this slate. The TC-16 has the highest theoretical maximum density (1.53 g/cm^3), followed by TC-15 (1.45 g/cm^3) and TC-14 (1.41 g/cm^3). These density variations are related to the differences in propellant composition, with the less dense samples having a greater concentration of binder material than the more dense samples.

4.2.3 The PEG Propellant Slate. As mentioned previously, the third slate of propellant formulations studied utilized a Carbowax or polyethyleneglycol (C4000 or PEG) binder and exhibited extremely fast burn rates for all of the formulations and densities tested. As with other fast burning samples, the short burn times associated with these extremely fast-burning samples prohibit obtaining reliable apparent burn rates using the MINICB burn rate reduction code. That is, the chamber of the closed bomb is pressurized so rapidly upon initiation of these propellant samples that it is only possible to obtain a limited number of data points during the pressure rise. Furthermore, the pressure history is not characterized by a quasi-steady rise but by a dynamic profile with a high degree of superimposed pressure waves. The combination of pressure dynamics and limited number of data points makes it extremely difficult to obtain accurate or reliable burn rate values, since the MINICB code determines burn rate from the slope or derivative of the pressure data. As a result, the 20–90% burn time parameter was again utilized to quantify the combustion rates of these extremely fast-burning samples. These data are contained in Table 7 for each propellant sample in the PEG slate at the density (%TMD) values for which it was supplied.

Data for the closed bomb tests conducted to characterize the members of the PEG slate (TC-40, 41, 43–46 at various %TMD values) are contained in Figures 14–19. As before, the compositions of the respective formulations are given in Table 1. It should be noted that, as with the Kraton slate, all of the PEG samples were much more frangible than the Hycar slate. However, members of the PEG slate

Table 7. 20–90% Burn Times for PEG Propellant Slate

TMD (%)	TC-40 (ms)	TC-41 (ms)	TC-43 (ms)	TC-44 (ms)	TC-45 (ms)	TC-46 (ms)
97	—	—	—	—	—	0.290
95	—	0.222	0.179	0.217	0.164	0.218
90	—	0.210	0.244	0.218	0.170	0.267
85	0.271	0.229	0.235	0.189	0.164	—

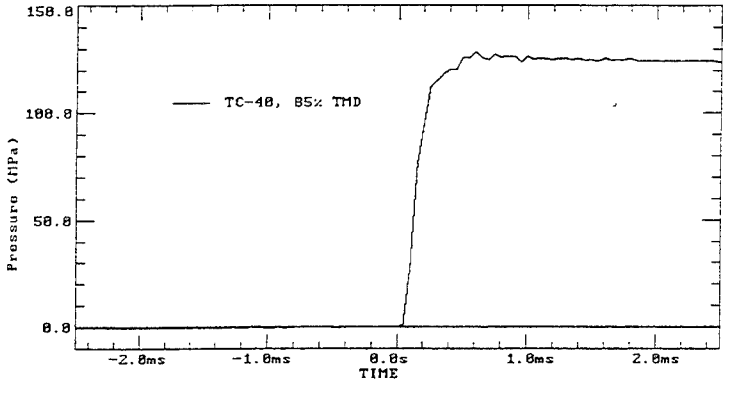

Figure 14. Closed bomb data for sample TC-40 at 85% TMD.

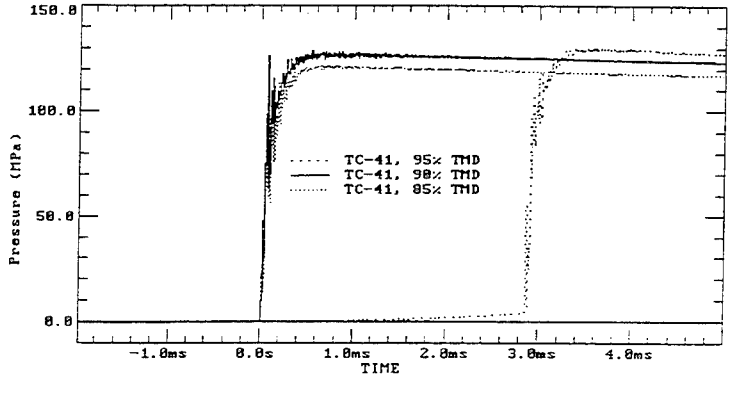

Figure 15. Closed bomb data for TC-41 at various TMDs.

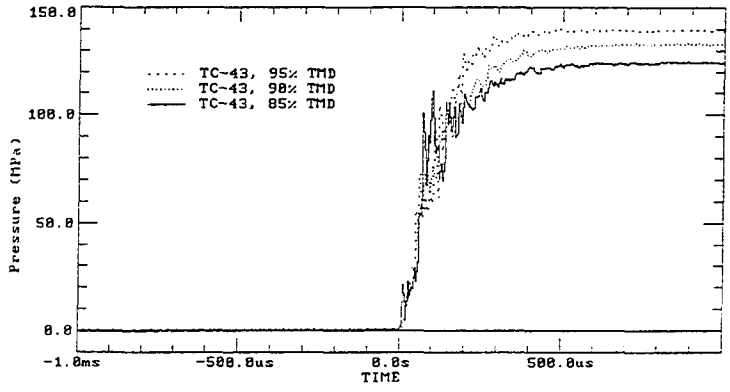

Figure 16. Closed bomb data for TC-43 at various TMDs.

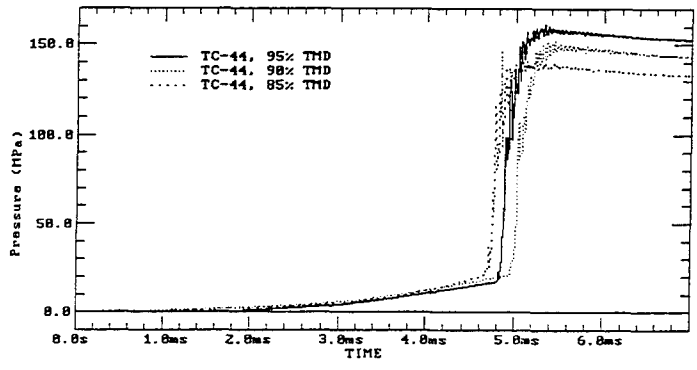

Figure 17. Closed bomb data for TC-44 at various TMDs.

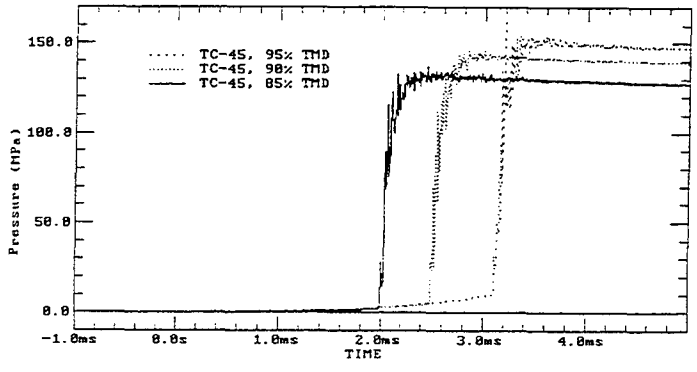

Figure 18. Closed bomb data for TC-45 at various TMDs.

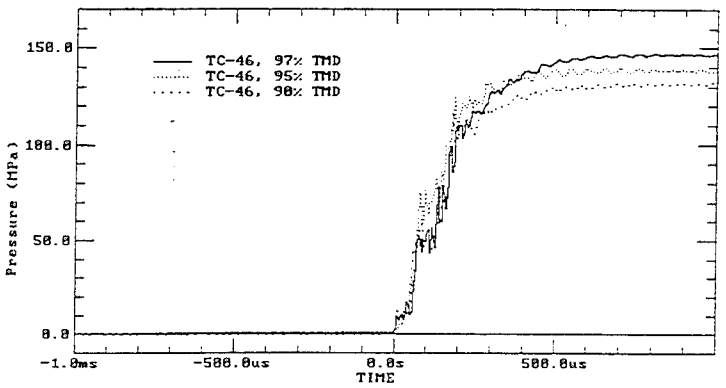

Figure 19. Closed bomb data for sample TC-46 at various TMDs.

showed a much greater degree of homogeneity a result of a preferred manufacturing technique, than did members of the Kraton slate. The PEG samples were compression molded using a homogeneous mixture of the ingredients. This differed from the crumb formation, breakup, and reconsolidation in a compression mold process that was performed for the Kraton propellant slate.

Some general observations may be made regarding the data contained in Figures 14–19, for the PEG slate of propellants. As the figures suggest, all of the samples in this slate burned extremely rapidly. From Table 7 it can be seen that the 20–90% burn times ranged from 0.16 to 0.29 ms over the entire range of compositions and densities. As the table shows, the density values tested for each of the formulations were nominally 85%, 90%, and 95% TMD, with the exception that the TC-46 sample was provided with a sample compressed to 97% TMD in place of 85% TMD. In addition, sample TC-40 was available only in the 85% TMD form.

A comparison of the burn times in Table 7 with those in Table 6 for the Kraton, and Table 5 for the Hycar slate, indicate that all of the members of the PEG slate burned faster than even the fastest members of the Kraton slate and that the Hycar slate was orders of magnitude slower. For the PEG propellant slate, the very fast combustion characteristics were observed at all density values and with all compositions. The only significant behavioral difference observed among the various density samples was that, for certain formulations at the higher density levels, a longer ignition period was apparent before the combustion process made a transition to the rapid burning mode. For a given formulation, the ultimate pressure level attained in the closed bomb was directly proportional to the sample's density; higher density

(%TMD) samples generated greater pressure levels in response to the corresponding increase in propellant mass (i.e., more total energy).

Figure 14 contains the closed bomb results for a sample of TC-40 (85% TMD). As is readily apparent from the trace, the peak pressure is reached in under 0.5 ms. Since this was the first member of the PEG slate to be tested, the data sampling rate was less than optimum, resulting in a loss of resolution for this data when compared to later tests in this series. Many of these tests were characterized by large amplitude pressure waves and spikes superimposed on the measured pressure data. In any event, as with some members of the Kraton slate, it is clear that the pressure generated by combustion of the propellant sample rose sharply, before any apparent pressure contribution from the combustion of the igniter powder.

Figure 15 contains the closed bomb pressure histories for sample TC-41 for nominal density values of 85%, 90%, and 95%. As intimated previously, the only perceptible difference among these samples is the roughly 3-ms ignition delay experienced by the sample with the greatest density. Higher density propellants also contain lower porosity, and are mechanically stronger than lower density samples.

Figure 16 contains the closed bomb results for samples of TC-43. This formulation contains virtually identical quantities of the oxidizers, HMX and TAGN, and boron hydride found in sample TC-41; however, approximately half of the nonenergetic binder, PEG, has been replaced with an energetic plasticizer, BDNPA/F (refer to Table 1). This change in binder chemistry seems to have reduced the differences in combustion behavior that were previously observed for the TC-41 formulation and attributed to the density of the samples. Once again, the ultimate pressure level attained during each test is proportional to the propellant density (or mass). All of the TC-43 propellant samples reach their peak pressure levels within 0.2 ms without any significant ignition delay period as was observed for one value of density for formulation TC-41.

The next two propellant formulations tested, TC-44 and TC-45, are chemically quite similar, as can be seen from Table 1. Both formulations contain high solids loading (only 5% binder), and a relatively small boron hydride content (only 2% and 8%, respectively) when compared to the other members of the slate. However, as Figures 17 and 18 suggest, even with this lower BH content, the burn rates of these samples remain very high. This may be attributable to the addition of 1% of a Pt/C catalyst (a 50/50 mixture of platinum and graphite fine powders), commonly referred to as "pixie dust." This additive has been shown [41] to promote high burn rates at reduced boron hydride contents.

The pixie dust-containing formulations appear to show a greater propensity for ignition delay than did other members of this slate. This delay may come, at least in part, as a result of the reduced level of boron hydride; however, it could also be related to other factors such as differences in energy or mechanical strength. In any event, the delays are of relatively short duration (no more than 5 ms), and the propellant burn rates when ignition does occur are quite large. The magnitude of the delay appears to increase with increasing density (as happened with TC-41) for both TC-44 and TC-45.

The final propellant formulation which has been included in the PEG slate for the purposes of this study is TC-46, which utilized an energetic binder system rather than PEG. From Table 1, it may be seen that 6% GAP makes up the energetic binder component, with various quantities of nonenergetic binder (CAB), plasticizer (DOA) and cross-linking agent (IPDI) also present. This formulation was included in the PEG slate because, other than the binder system, its composition is similar to the remainder of the PEG slate; the similarity pertains specifically to the fuel (boron hydride) and oxidizer (HMX/TAGN) components. Also, this formulation is extremely similar to the TC-43 propellant formulation, which has 5% BDNPA/F in the form of an energetic plasticizer. In addition, the closed bomb data for this formulation are also quite similar to the data obtained for the TC-43 formulation. As with the data in Figure 16 for TC-43, the data for TC-46 contained in Figure 19 shows no appreciable differences between the various densities, save for the ultimate pressure level.

4.3 Thermochemical Calculations for VHBR Propellants. In order to obtain a means for comparison of the chemical energy content of the various formulations of the respective VHBR propellant families studied, equilibrium thermochemical calculations were conducted using the NASA-Lewis (CET86 version) and BLAKE codes. Calculations using both codes were conducted on an IBM-PC compatible computer platform based on the 80386 microprocessor. The NASA-Lewis calculations were utilized to obtain better component information for use in reject statements in the BLAKE input file, since BLAKE can sometimes have trouble achieving convergence of its calculations for complex chemical formulations. BLAKE produces more accurate pressure predictions than does NASA-Lewis because it uses nonideal gas equations of state and accounts for the volume exclusion produced by condensed species. This should not affect the prediction of major component species but will affect minor components. As far as the rest of the thermochemical output, there is not a great deal of difference between the predictions of the two codes (with the possible exception of the specific heat ratio, γ); however, for ballistic calculations, BLAKE has become the de facto standard. All of the thermodynamic properties presented in this section are results of BLAKE calculations.

Table 8 contains the results of these thermochemical calculations for each of the three propellant families studied. The calculations were made at a loading density of 0.1 g/cm^3, the same as that utilized in the closed bomb experiments. The flame temperature reported in Table 8 is the isochoric (constant volume, T_v) flame temperature often utilized in ballistic calculations. As the table shows, the propellant family which exhibited the slowest overall combustion rates, the Hycar slate, actually has some of the highest overall energy content or impetus values. The magnitude of the impetus is related to the energetic material content of the propellant. For VHBR propellants of interest, the primary energetic materials are RDX or a mixture of HMX and TAGN (Table 1).

Table 8. Thermochemical Properties of VHBR Propellants

Propellant Formulation	Impetus (J/g)	Flame Temp. (K)	Molecular Weight of gas	Co-Volume (in^3/lbm)	Frozen Gamma
Kraton Propellant Slate					
TC-14	1039.	2412	16.43	1.254	1.269
TC-15	1119.	2575	17.24	1.247	1.272
TC-16	1205.	2851	17.96	1.287	1.268
PEG Propellant Slate					
TC-40	1152.	2990	19.35	1.161	1.252
TC-41	1116.	2849	18.52	1.175	1.257
TC-43	1142.	2967	19.26	1.160	1.253
TC-44	1238.	3089	20.74	1.191	1.249
TC-45	1204.	3002	19.98	1.199	1.253
TC-46	1135.	2924	19.15	1.170	1.255
Hycar Propellant Slate					
TC-47A	1260.	3286	21.68	1.179	1.251
TC-48A	1231.	3181	21.49	1.188	1.252
TC-49A	1194.	3059	21.30	1.195	1.252
TC-50	1171.	2938	20.85	1.219	1.259
TC-51	1283.	3417	22.15	1.158	1.245

NOTE: Calculated at closed bomb conditions of 0.1-g/cm^3 loading density.

The relationships between the impetus and flame temperature of the various VHBR propellants and the energetic materials and boron hydride contents are contained in Figures 20 and 21 for the Hycar and Kraton propellant slates and in Figures 22 and 23 for the PEG propellant slate. These figures show that there is a strong dependence of the energy or impetus of a VHBR propellant sample on the amount of energetic material (or oxidizer) present in the sample. As Figures 20 and 22 show, both impetus and the isochoric flame temperature are linear with energetic material content. For the data in Figure 22, quite similar-looking plots can be produced for either of the energetic constituents, HMX or TAGN, individually which show the same sort of linear trend. The data in Figures 20 and 22 were not plotted together because formulation variables for the PEG slate caused the functional dependency to differ from that exhibited by the Hycar and Kraton slates. That is, while the data in Figure 22 definitely show a linear trend, the slopes are greatly reduced when compared to the correlation in Figure 20.

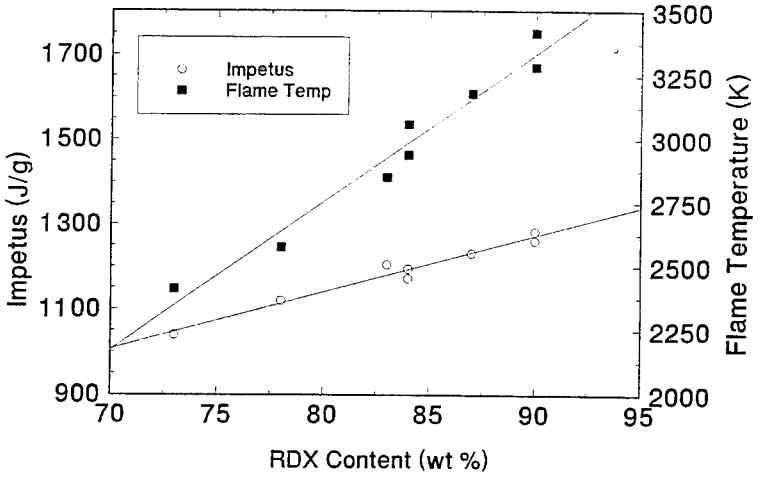

Figure 20. Impetus and flame temperature vs. RDX content for Hycar and Kraton slates.

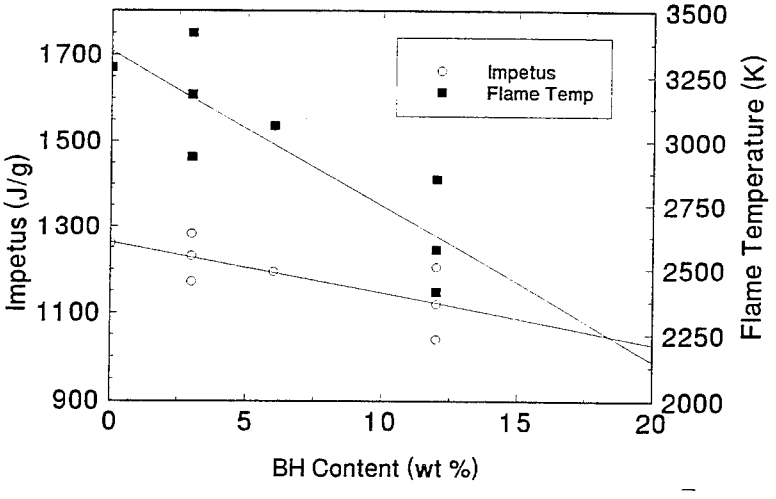

Figure 21. Impetus and flame temperature vs. boron hydride content for Hycar and Kraton slates.

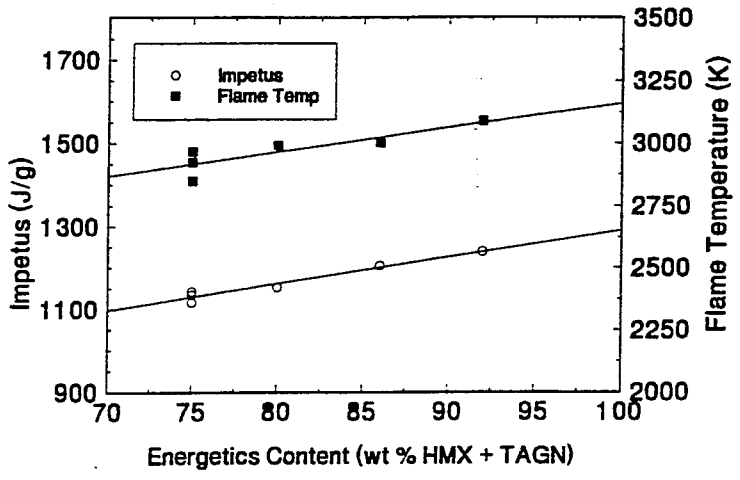

Figure 22. Impetus and flame temperature vs. energetic content for PEG slate.

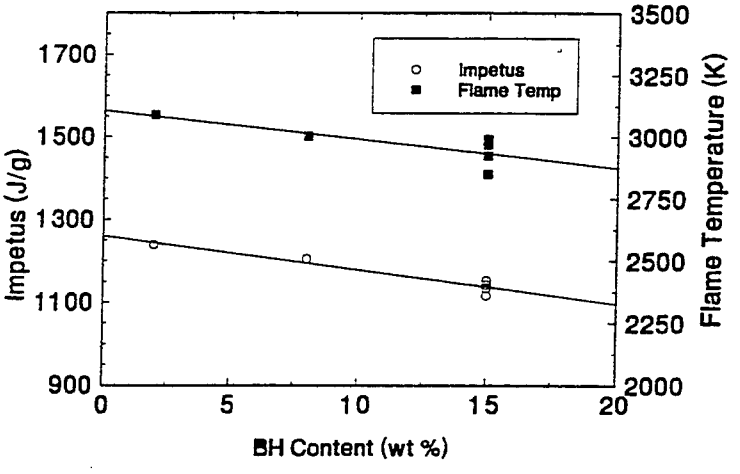

Figure 23. Impetus and flame temperature vs. boron hydride content for PEG slate.

Figures 21 and 23 contain comparable thermochemical data for the two groups plotted as functions of the boron hydride content of the formulations. As the two figures and other information in Tables 1 and 7 indicate, there is a net downward trend in both energy and flame temperature if the boron hydride content is increased at the expense of the primary energetic material in each of the three propellant slates. Therefore, the addition of the boron hydride in all instances actually tended to *decrease* the overall energy content of the propellant formulation. Now, it should be noted that these calculations reflect equilibrium conditions and do not represent any kinetic events which may be present in the VHBR combustion mechanism. This is especially apparent in the cases of the very fast-burning formulations.

In Figure 21, there is a fair amount of scatter in the information contained in the plots. While it is true that this figure contains a composite of data for two different propellant families, the data break down along family lines, with the entire Kraton slate located at the 12% boron hydride position and the Hycar slate at the 0–6% BH concentrations. The reason for the scatter is most likely a result of differences in binder content among the formulations. The binder used in each of the formulations, whether in the Hycar or Kraton slates, is energetically inert. Therefore, variations in the binder content and, by inference, the energetic content of the propellant will produce various energy levels for a given boron hydride content.

The point should be made here that the boron hydride species used in the Kraton slate (H466) differs from that used for either the Hycar or PEG slates (H498). The H466 species has a heavier organic (tetramethyl ammonium) cation than the H498 species which has potassium as the cation. This has the effect of exaggerating the weight-percent of the boron hydride $B_{10}H_{10}^{2-}$ cage in propellants containing H466 compared to those containing H498. However, when a comparable plot is made of impetus and flame temperature vs. the $B_{10}H_{10}^{2-}$ content, the result (not shown here) looks markedly similar to Figure 21.

4.4 The Mechanical Combustion Mechanism. As discussed in an earlier part of this section, the three propellant slates studied during this program exhibited markedly different closed bomb combustion behaviors. Characteristic closed bomb combustion data for the Hycar slate were given in Figure 3. These samples clearly experienced an ignition delay period, during which the booster combustion gases initiated propellant combustion. This ignition delay was inversely proportional to the relative apparent rate of combustion for the slate. In other words, the samples with higher burn rates had shorter ignition delays, likely due to the faster energy release and combustion gas generation rates present during ignition.

A representative sample of the closed bomb combustion behavior of the Kraton slate was given in Figures 7–13. As these figures suggest, the lower density or higher porosity samples exhibited virtually instantaneous ignition and combustion—what has come to be recognized as VHBR behavior, while the higher density (100% TMD) samples experienced an ignition delay period similar to that seen with the Hycar slate. Finally, the closed bomb data for the PEG slate, representative samples of which were given in Figures 14–19, showed virtually no ignition delay in comparison with the other two slates. Certain of the formulations show a slight delay, no longer (and usually much shorter) than would be required for the booster charge to reach its full combustion pressure.

These observations regarding the different ignition and combustion characteristics of the various propellants studied, along with other observations related to the mechanical properties of the propellants themselves, eventually led to the development of the strain gage experimental approach. That is, the three families of propellants exhibited dramatic differences in combustion behavior, with the Hycar slate showing no signs of VHBR behavior, the PEG slate showing only VHBR behavior, and the Kraton slate showing both VHBR and non-VHBR behavior. To go along with this, the propellants exhibited significant qualitative differences in their physical properties: the Hycar slate of propellants seemingly possessed a high degree of elasticity; the Kraton slate was much harder and had an outwardly nonhomogeneous appearance; and the PEG slate was also much harder than the Hycar slate but had a much more homogeneous appearance. The differences between the manufacturing processes used for each of the propellant families are documented earlier in this report.

These observations led to the hypothesis that for the very fast burning propellant samples, the fast combustion rates may be related to the response of the propellant to mechanical stimuli. That is, the extremely fast ignition of these samples, in some cases even before the pressure from combustion of the booster could be sensed by the pressure transducer, might be explained by compressive ignition of the sample. It was felt that if normal thermal ignition of the propellant were occurring, this would take on the order of milliseconds to occur. In some instances, for the identical propellant chemistry, different ignition mechanisms were apparent, as signified by the results obtained for the various densities of TC-16 in the Kraton slate. Therefore, if the slower mechanism governing ignition of the 100% TMD sample is considered to represent thermal ignition, then some much faster mechanism must be present in the ignition and combustion of the lower density samples of this formulation where the booster pressure traces were not apparent.

Furthermore, in the cases where this unique ignition mechanism was present, it was felt that the resulting very fast combustion rates might also be explained by some sort of mechanical combustion model. That is, the sample might be ignited throughout (in-depth) by one of two possible scenarios: (1) either by friction at the interface between fractured propellant fragments, which ignites the surface of these macroscopic fragments; or (2) by the propagation of a strong mechanical compression wave through the sample, which ignites virtually the entire sample volume through ignition on the microscopic level. The applied stress could conceivably be from the same impulse which ignited the sample, or could be a result of compression of the sample by vigorous combustion at the free surface. In these scenarios, the rate at which combustion proceeds through the sample is governed by (1) the degree to which the sample

is fractured and the resulting size of the fragments or (2) the propagation rate of the stress wave through the sample.

In order to investigate the compressive ignition hypothesis, a sample of TC-16 (90% TMD) was mounted as usual in a stainless steel confinement tube, with the free surface inhibited with a thin layer of silicone grease approximately 0.8 mm (0.03 inch) thick. The inhibitor was applied to prevent ignition of the sample by hot combustion products, gases and condensed matter, generated by the booster. When tested in the closed bomb, the results (Figure 24) indicate that ignition and combustion of the sample were still achieved, although delayed by about 5 ms when compared to combustion of a similar uninhibited sample. Also contained in Figure 24 is the result obtained when a charge of booster powder (1 g of BULLSEYE) was combusted using an inert propellant sample (plastic). As the figure shows, the early time portion of the combustion trace for the inhibited sample follows very closely that for the booster alone, with the exception of low amplitude superimposed pressure oscillations. Although the nature and cause of these pressure pulses is not absolutely known, they seem to be consistent with pressure waves that might be generated by combustion of the propellant sample at regions beneath the silicone coating.

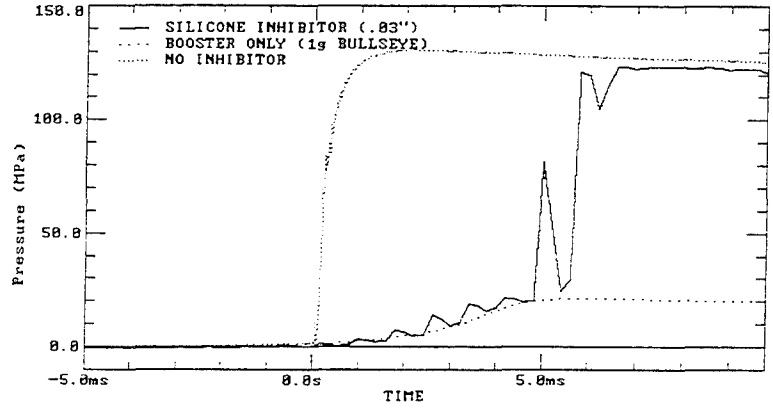

Figure 24. Closed bomb tests of sample TC-16 (90% TMD) with and without silicone inhibitor.

It also should be noted that another similar test was conducted that utilized a thicker coating of silicone grease (approximately 2.5 mm [0.10 inch] thick) and which resulted in no sample ignition. Therefore, since it was apparent that addition of the silicone had the effect of delaying or preventing ignition of the sample, it would seem as though the silicone had the effect of insulating the surface of the

propellant from the heat of the combustion gas, if thermal ignition is assumed, or from the force of the rapidly expanding gas cloud, if a compressive ignition mechanism is assumed. Ordinarily, the silicone grease is considered incompressible when utilized to insulate pressure transducers. However, under those circumstances, the grease is typically confined within the transducer port. When utilized on the propellant samples during the current effort, no confinement of the grease coating was present. With the thicker silicone coating, then, it is possible that the pressure pulse generated by combustion of the booster charge may have yielded some degree of radial flow in the grease, resulting in absorption of a quantity of the mechanical energy of the gas.

In any event, the speed with which combustion occurred once ignition was achieved suggested to the authors that some sort of mechanical combustion mechanism may have been present. To further investigate this phenomenon, two additional tests were conducted. One of these tests utilized an inert (plastic) sample coated with a layer of silicone grease of approximately the same thickness (0.8 mm) as that which allowed ignition of the TC-16 sample. This inert sample was then placed in the closed bomb and exposed to a booster charge. The pressure data resulting from this test is shown as the "booster only" curve in Figure 24. Following this test, the silicone grease was found to be still intact and showed virtually no sign of combustion, which would have been signified by a powdery white ash. This result was obtained following exposure for more than a minute to the hot booster combustion gases. The only significant change in appearance of the grease was a carbon-like deposit on the exterior surface of the grease.

The other test in this study utilized a sample of TC-49A, also deterred in the aforementioned manner. The results of the test showed a dramatic increase in the burn time of the sample, ordinarily in the range of 200–300 ms (Figure 3), to about 700 ms. This delay is surely due to the thermal barrier presented by the grease. In other words, ignition was delayed until sufficient heat was transferred from the booster combustion gases to raise the temperature of the inhibited propellant surface above that required for ignition. Following ignition, sample combustion proceeded in a fairly normal, laminar-burn fashion.

Although not conclusive, when this evidence is taken together, the observations are consistent with a mechanical combustion mechanism, in mode observed for the TC-16, 90% TMD sample. The result of the test with the inert sample suggests that the silicone grease should not have been burned by the booster gases prior to ignition of the propellant sample. In addition, although the compositions are different, the ignition temperatures of the TC-49A and TC-16 formulations are not expected to differ

dramatically. This is deduced from a comparison of closed bomb pressure histories where thermal ignition is almost surely the mechanism at work (see Figure 3, the TC-49A sample, and Figure 9, the TC-16 sample). These two propellants have comparable ignition delays before sample combustion is evident. Therefore, if thermal ignition were to have occurred with the inhibited TC-16, 90% TMD sample, the ignition portion of the curve might be expected to more closely resemble that of the 100% TMD sample in Figure 9. Therefore, the test which utilized the inhibited TC-49A sample gives further evidence that a thermal ignition most likely did not occur within the 5-ms delay period before ignition of the inhibited TC-16 sample.

4.4.1 The DDT Mechanism. At approximately the same point in time as the experimental study of the connection between VHBR combustion and a compressive mechanical combustion mechanism was being investigated, a discussion took place between the authors of this report and Dr. Douglas Kooker of BRL concerning the DDT mechanism. Kooker had been actively involved in modelling both the DDT and PDC mechanisms [42–45]. The PDC mechanism is often used as a simplified experimental configuration to model DDT and consists of ignition of a bed of propellant by purely mechanical compaction of the propellant by an impinging piston. Following the discussion with Kooker, some interesting similarities between the hypothesis of the VHBR compressive ignition mechanism and the DDT/PDC combustion mechanism presented in the literature became apparent.

The various stages [38] of the DDT mechanism are summarized as follows. Stages 5–7 constitute what has been referred to as the shock to detonation transition (SDT).

(1) Preignition and compaction

(2) Ignition/conductive burning

(3) Convective burning, if sufficient porosity remains

(4) Compressive ("Hot Spot") burning from the coalescence of compressive waves driven by conductive/convective burning

(5) Shock formation

(6) Compressive burning behind shock

(7) Detonation.

An in-depth discussion of the DDT mechanism was given in section 2 of this report. It is mentioned here in order to stress the similarities between this mechanism and the observed characteristics of the VHBR combustion mechanism. Typical DDT experiments are conducted with granular propellant beds confined in either plastic or steel tubes with substantial porosity (50–60% TMD). The transition to detonation has been found to depend on such things as: strength of confinement, bed permeability (porosity), compressibility (bulk modulus) of the compacted aggregate, shock sensitivity, and the energy release rate during combustion. Sandusky [46] presents a discussion of two different but related mechanisms which seem to pertain to the observations regarding the TC-16, 90% TMD VHBR formulation discussed in the preceding section. Specifically, Sandusky points out that the sensitivity of energetic materials to compressive ignition is considerably increased by the introduction of porosity to the sample, corresponding to a lowering of the %TMD. Furthermore, the ensuing reaction may quickly generate a shock wave of sufficient strength to allow the shock-to-detonation transition (SDT) to proceed. The latter is essentially the mechanism active in the PDC experiments (stages 4–7 mentioned previously).

In each of the two modes of DDT behavior outlined by Bernecker, it appears that the response of the granular bed to compressive stress waves plays a dominant role. The following is a summary of the discussion of these two DDT modes in Kooker's [32] report. In the first mode, convective combustion of the propellant near the igniter end of the confined bed creates a rapidly increasing pressure field, which then propagates into the unburned material as a system of compressive waves. This stress wave system can compact the propellant bed, thus altering the propagation rate of the convective flame. If the pressurization rate from the propellant combustion is sufficiently strong to drive the compaction waves to shock wave strength, unburned propellant may be ignited ahead of the flame front by mechanical compression, providing a pathway for detonation. In the second mode, combustion leads only to a mild pressurization rate of the bed, although compaction may still be extensive. Then suddenly, at some point within the propellant bed, a violent reaction drives a rapid pressure buildup (which may propagate in both directions). This leads to shock wave formation and provides a pathway to detonation.

As stated previously, evidence for the support of these mechanisms in VHBR propellant combustion may be seen with the TC-16 data in Figure 9. The two lower density samples appear to be initiated immediately, possibly by a compressive ignition mechanism as discussed earlier, with virtually no way of distinguishing between the onset of the booster pressure and the pressure generated by the transition to VHBR behavior. On the other hand, the higher density (100% TMD) sample experiences an ignition period followed by a low-rate combustion period before transitioning to VHBR behavior. This transition

to a more rapid burn rate could be interpreted as a transition to a stress-induced combustion mechanism, triggered by the increased stress level produced by the laminar surface combustion early in the test. It was felt that, in light of the newfound information regarding the possible connection between the DDT and VHBR combustion mechanisms, an experimental approach which could lend supporting experimental evidence to the investigation must be developed.

An experimental technique which employs strain gages mounted on the confinement vessel containing the energetic material being tested has been utilized in the study of both DDT and PDC combustion mechanism experiments. The results of these experiments provide the stress history in the bed of energetic material as a function of time. An approach similar to this, utilizing miniature strain gages mounted on the exterior of the sample confinement tube during closed bomb testing, was developed for use in studying the VHBR combustion mechanism.

4.4.2 Strain Gage Experiments. As mentioned in the previous section, an important experimental technique was developed during this Phase II program which utilized miniature strain gages mounted externally along the length of the confinement tube during closed bomb testing, as depicted in Figure 25. The objective of the strain gage experiments was to measure the stress field at each gage location as a function of time. In this way, insight into the propagation rate of the in-depth combustion mechanism, deduced from the arrival time of a stress wave at each gage location, and potentially any connection to the DDT mechanism could be ascertained.

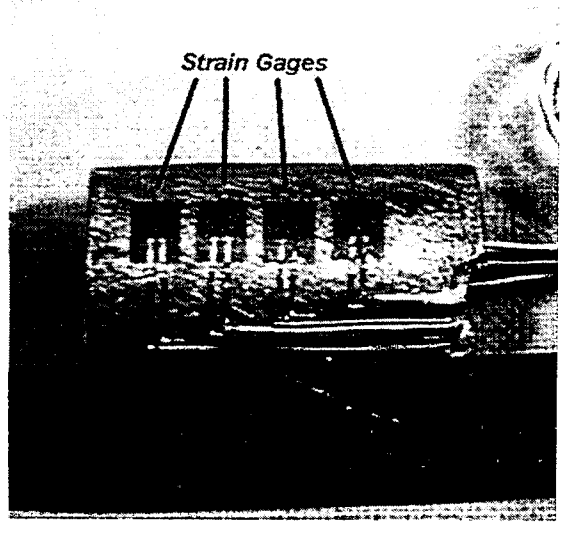

Figure 25. Experimental strain gage configuration.

Using a specially designed endcap for the closed bomb pictured in Figure 1, which allows instrumentation lines to be easily passed to the outside without leakage of combustion gases, first two, and later four miniature strain gages were mounted on the stainless steel propellant sample sleeve. The dimensions of the active regions of the strain gages used were 1.0 mm (0.039 inch) wide and 0.6 mm (0.024 inch) in the direction of strain.

In these experiments, the gages are used to measure the hoop strain of the sleeve caused by the compressive waves in the solid propellant material. The strain data may be left as is or converted to pressure via an appropriate quasi-static relationship, given in equation 1.

$$P_i = \frac{(b^2 - a^2)}{2a^2} E_y \varepsilon_t , \qquad (1)$$

where:

P_i = Internal tube pressure
b = Tube outer radius
a = Tube inner radius
E_y = Young's modulus
ε_t = Tangential (hoop) strain.

The propellant samples tested were nominally 25 mm (1 inch) in length. In the two-gage tests, the first strain gage was centered 9.5 mm (0.375 inch) from the leading edge of the sample sleeve. The second gage was then placed an equal distance from the centerline of the first gage (19.1 mm or 0.75 inch from the leading edge). The first test was conducted with strain gages mounted on the inside circumference of the sample sleeve; however, one of the gages apparently failed in this configuration. All subsequent experiments utilized strain gages mounted externally on the sample sleeve.

Strain gage data for one test were converted to pressure within the steel confinement sleeve using equation (1) and are shown in Figures 26–28. This test utilized a sample of TC-41 at 85% TMD, the composition of which is given in Table 1, with a typical standard closed bomb combustion trace shown in Figure 15. This sample was selected as the first to undergo strain gage testing because, during earlier closed bomb testing, it exhibited violent combustion characteristics which resulted in a "mushrooming"

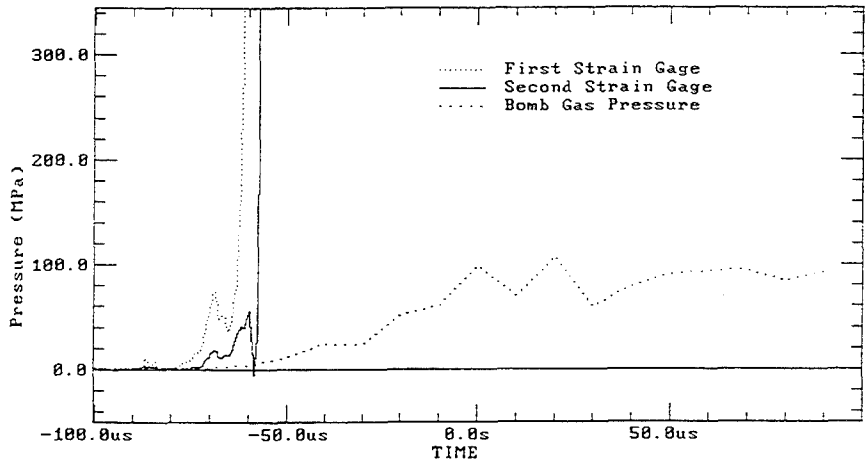

Figure 26. Closed bomb test of TC-41 (85% TMD) showing strain gage data and chamber (gas) pressure.

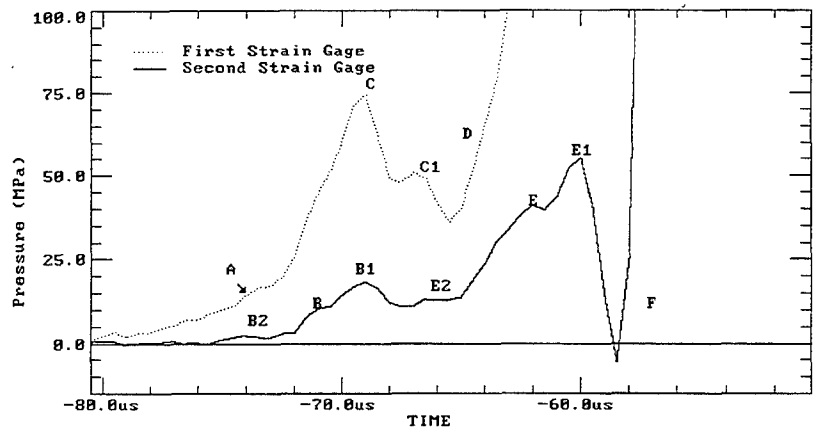

Figure 27. Expanded view of low-pressure strain gage data for TC-41 (85% TMD).

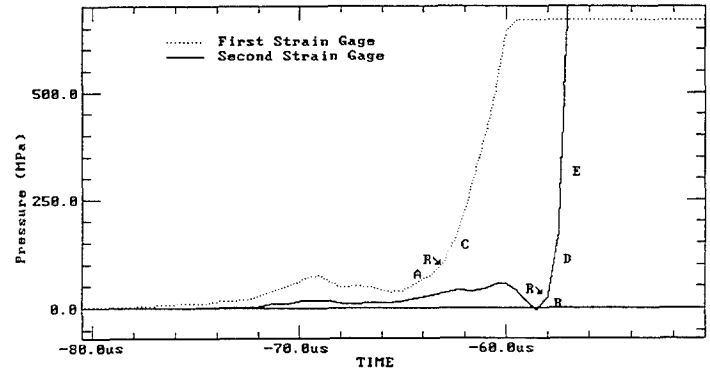

Figure 28. Expanded view of high-pressure strain gage data for TC-41 (85% TMD).

of the steel sample sleeve from the rapid pressure generation. This mushrooming of the steel sleeve was also observed for many, if not all, members of the PEG slate. It was felt that if a stress-related combustion mechanism resembling DDT were to exist for the VHBR class of propellants, this formulation would be a good candidate to exhibit this mechanism.

The magnitude and dynamic characteristics of the strain-inferred pressure within the steel confinement tubing are indicative of combustion wave phenomena. As shown in Figure 26, the sharp pressure signals appear sequentially at each gage and rise to more than 300 MPa (44,000 psi). In actuality, the amplitude of these strain gage pulses was clipped to increase the resolution of the lower amplitude signals. In each case, the amplitude of the raw strain gage data approached 700 MPa (102,000 psi) before the gages failed (see Figure 28).

If the data are analyzed in terms of DDT/PDC terminology, then this strong pressure wave could be termed the reactive front, or possibly a reactive shock wave. In any event, from the data in Figure 26, it is clear that this pulse had passed each strain gage location before significant gas pressure was sensed by the closed bomb pressure transducer. This gives strong evidence in support of a compressive mechanism for ignition and combustion of the TC-41, 85% TMD sample, in this test configuration. It should be noted that the gas pressure data were sampled at a much slower acquisition rate, 10 μs/point, than the strain gage data, which were sampled at 0.5 μs/point. This slower acquisition rate had the effect of eliminating any potential high-frequency signals ("ringing") which might have existed in the bomb chamber and is also responsible for the "saw-tooth" variations in pressure level observed in Figure 26. Also visible in the strain gage data in Figure 26 are low amplitude compressive wave fronts traveling through either the sample itself or the steel confinement sleeve, which appear to be generated by the igniter combustion gases.

An expanded view of the early-time portion of the strain data for the closed bomb test of TC-41 at 85% TMD is pictured in Figure 27. The strain gage data depict a complex set of dynamic strain measurements which begin with a relatively mild pulse, probably from the igniter, and end with the onset of a strong pressure wave, probably generated by the local ignition and combustion of the propellant sample. This entire event occurs extremely quickly, over a period of only about 25 μs and before the measured gas pressure in the closed bomb has risen appreciably.

The set of dual peaks in Figure 27, labelled C, C1 at the front gage location and E, E1 at the rear, would seem to possibly represent the propagation of the igniter pressure pulse within the propellant sample, since this would be expected to be the first stress-generating event the propellant would sense. However, if these pulses are used to calculate a propagation velocity, the result is 1,360 m/s, much lower than the speed of sound expected for the propellant. The velocity of sound for similar propellant formulations, as determined by Costantino [47] range from 3,100 to 3,700 m/s for pressures ranging from 50 MPa (7,250 psi) to 200 MPa (29,000 psi). Furthermore, it should be remembered that the strain gages were mounted on the exterior of a steel tube, which also would be expected to contribute to the measured stress field.

Figure 28 shows the high amplitude strain gage component information data for this same test, expanded with respect to time. Visible in the figure, and denoted as regions A and B, is what appears to be a compaction front generated by the combustion of the sample ahead of the gage locations, prior to the arrival of the reactive wave front. The arrival of the reactive front could then be considered the region labelled R for each gage. This pulse travels at a rate of about 1,900 m/s. The magnitude of the propagation rate for the reactive shock wave is quite similar to that reported by Bernecker [36] for a spherical double-base propellant (2,150 m/s). This might indicate that the reactive front is propagating through fractured or deconsolidated propellant, since this propagation rate is substantially lower than the velocity of sound attributable to the original propellant matrix (on the order of 3,800 m/s).

Also evident from Figure 28 is the fact that the reactive wave front appears to have strengthened during the time it took to travel between the front and rear strain gage locations; this is suggested by the steeper slope of region D as compared to that of region C. In addition, the slope of the reactive front measured by the rear strain gage again increases at about the 172 MPa (25 ksi) mark (region E), possibly suggesting even more rapid combustion downstream of this gage. The fact that the reactive front seems to have strengthened could also indicate that it accelerated while traveling between the front and rear gage locations. This adds some uncertainty to the value of the propagation rate reported previously (1,900 m/s). As a result, additional strain gages were utilized in later testing for better time and distance resolution of the developing reactive front.

Figure 29 contains data from two strain gages from a closed bomb test of a Kraton slate TC-15 sample at 90% TMD. An earlier closed bomb test with another sample of this propellant, shown in Figure 8, had yielded a combustion trace similar to those for the PEG slate described previously, which were suggestive

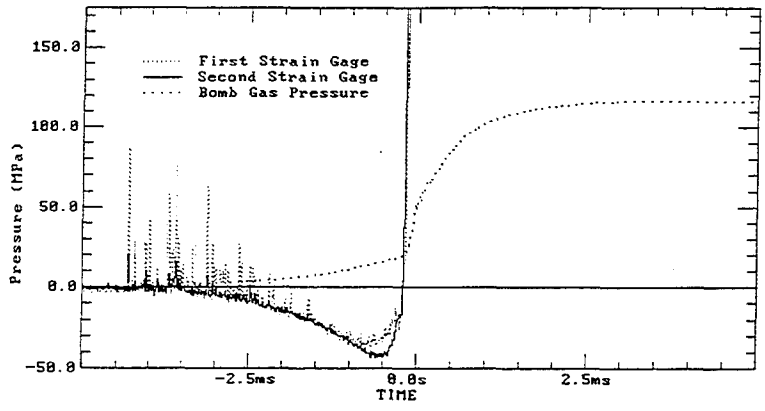

Figure 29. Strain gage data for sample TC-15 (90% TMD).

of compressive ignition. However, as the data in Figure 29 indicate, an ignition delay was experienced during the strain gage test. This suggests that, initially, compressive ignition may not have occurred during this particular test; however, rapid propagation of the combustion zone in-depth was still obtained once ignition did occur. The negative magnitude of the strain gage data prior to the arrival of the reaction front is a result of radial compression of the sample by the pressure from the booster combustion gas. During this initial period, the rise in external booster gas pressure exceeded that of the internal sample pressure.

Figure 30 shows the strain gage data for this test expanded with respect to time. In the figure, the region of the curve labelled A may be seen to be characterized by a generally increasing internal stress level. If the data are expanded further, both vertically and with respect to time, additional dynamic wave activity is apparent in region A. The propagation speed between the two gage locations of this compressive wave was determined to be roughly 1,730 m/s. The front gage experienced a reduction in the pressure level at label B, instead of the arrival of the reactive front as might have been expected from previous test data. However, the rear gage does show the arrival of a reaction wave front and a general stress profile similar to that previously observed in the earlier TC-41 data. The reasons for the behavior of the front gage are not obvious. Possible explanations for this behavior include hot spot ignition occurring within or at the base of the propellant sample, or ignition along fault lines within a sample due to friction. Examples of this type of phenomenon, in which ignition appears to occur at the rear of the sample either before, or soon after, ignition at the free surface, have been observed for VHBR propellants in other studies [13, 14]. Also, as described earlier, the nonhomogeneous, crumb-like nature of the Kraton propellant granulations may allow ignition in-depth via friction of these macroscopic crumbs. The

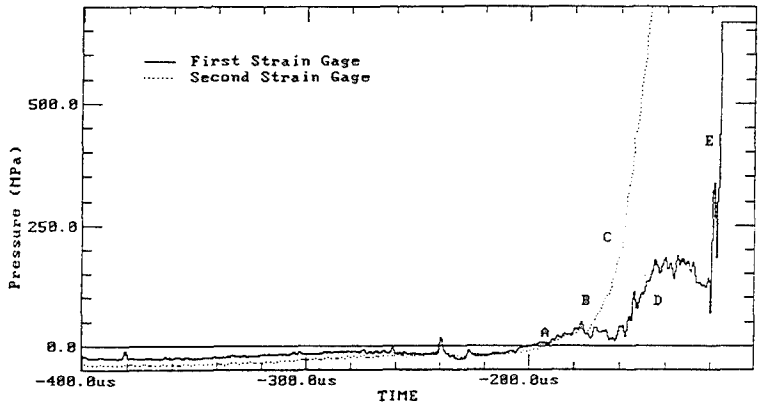

Figure 30. Expanded view of strain gage data for TC-15 (90% TMD).

occurrence of either of these situations could then lead to propagation of a pressure wave from the rear of the sample confinement sleeve to the front, the reverse of that expected. In addition, the high internal pressure developed could force the propellant sample from the tube, to burn at a high rate due to the sudden increase in available surface area.

It should be noted that following the TC-15, 90% TMD test, the stainless steel sample sleeve remained intact with both of the strain gages still securely bound to the sleeve. Only a slight deformation of the sleeve was observed, with the diameter increasing from 15.85 mm (0.624 inch) to 15.93 mm (0.627 inch) at the front gage location and to 16.12 mm (0.637 inch) at the rear gage location. Obviously, a far less violent combustion event occurred during the testing of this sample than with the PEG sample.

As mentioned earlier, the strain gage technique was refined during later testing to utilize additional gages in an effort to increase the resolution of the developing reactive front in very fast-burning VHBR propellant formulations. In addition, this also allowed the in-depth propagation characteristics of the reaction front to be better defined. Figure 25 shows what came to be the standard strain gage configuration, four gages separated by 5 mm (0.2 inch), beginning 5 mm from the leading edge of the sample. In addition, the gages utilized in the four strain gage configuration were smaller by about half than those previously used, having a width of 0.51 mm (0.020 inch). These smaller units not only allowed four gages to fit along the length of the sample sleeve, but provide sharper signals of the onset of stress waves due to the narrower width of the strain-measuring region.

Figure 31 shows the results of another test of sample TC-41 at 85% TMD using four strain gages. In this test, the sample was confined in a stainless steel sleeve in the usual manner. The data in this figure show low amplitude pulses similar to those seen previously, labelled as C and E in Figure 27. These pulses had been attributed to the propagation of pressure pulses generated by the booster combustion gases through either the propellant sample itself or the steel confinement sleeve on which the gages were mounted.

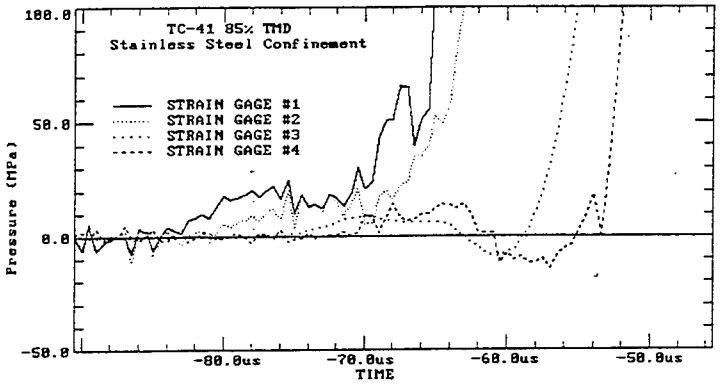

Figure 31. Strain gage data for a sample of TC-41, 85% TMD, with stainless steel confinement.

However, strain data obtained with samples confined in Kevlar sleeves suggest that these oscillations were most likely due to the propagation of stress waves, initiated by the booster pressure pulse, through the stainless steel confinement sleeve. This conclusion was drawn from the data in Figure 32 and other similar tests, which show strain gage data from a sample of TC-41 at 90% TMD that was epoxied in a polymeric confinement tube. This tube consisted of wound Kevlar fibers impregnated with epoxy, and had a tensile strength equal to or greater than that of stainless steel.

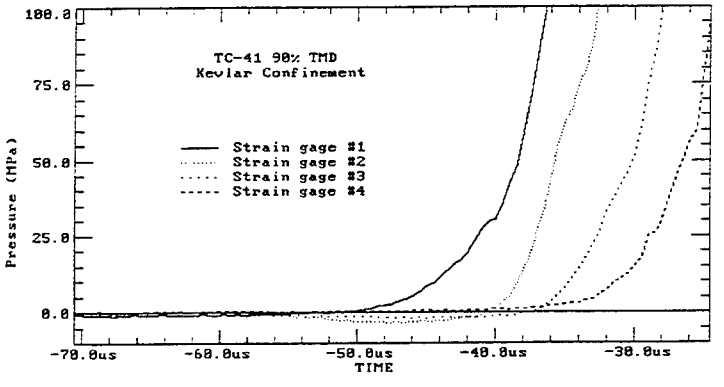

Figure 32. Strain gage data for a sample of TC-41, 90% TMD, with Kevlar confinement.

The Kevlar tubing was utilized for this testing to ensure that it would give suitable confinement for closed bomb VHBR combustion and that meaningful strain gage data could be obtained using gages mounted to this material. The Kevlar tubing was intended for use in the ciné x-ray studies at Dr. Ken Kuo's laboratory at the Pennsylvania State University, for which a strong tubing comparable to the strength of stainless steel was needed, but which would transmit x-ray signals suitably.

The resulting data showed that the change in confinement material had no ill effects on the combustion of the sample. From Figure 33, it can be seen that essentially no difference in chamber pressure is observed, other than what might be expected naturally due to the difference in density between the two propellant samples, when data using both Kevlar and stainless confinement, respectively, are compared. In addition, the use of the Kevlar tubing provides a far clearer view of the stress environment during the ignition and combustion of this propellant type, without the presence of confusing low amplitude pulses such as those present in Figure 31. In Figure 32, the stress within the propellant is gradually seen to increase, before transitioning into a strong stress wave, at about the 25-MPa level, which propagates quickly through the propellant sample at a rate of approximately 1,300 m/s. The relative magnitude of the internal pressure developed within the confinement tubing in each of these tests is suggestive of propellant sample ignition.

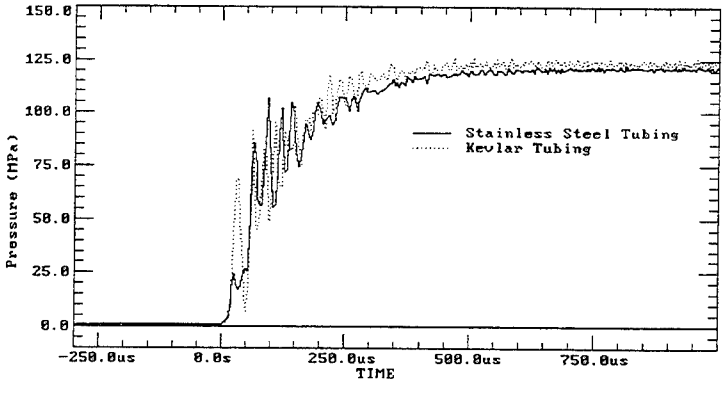

Figure 33. Comparison of closed bomb pressure data for samples of TC-41 at 90% TMD with Kevlar, and at 85% TMD with stainless steel confinement.

The previous discussion suggests strongly that a stress-induced combustion mechanism, similar to the DDT/PDC mechanism, plays a role in the combustion of the very fast-burning members of the VHBR propellant slate. Under the heading of stress-induced combustion mechanisms, two possible and related

combustion scenarios are apparent. In each, ignition may occur either by compression or by normal thermal means followed by in-depth ignition within the unburned propellant when the combustion-induced local pressure gradients at the free surface become strong enough to compress the propellant matrix. In the first scenario, the most common method of ignition is compression, caused by the onset of booster combustion which serves as a sort of piston acting on the free surface of the propellant grain to ignite the sample virtually instantaneously. The ignition of the sample may then be propagated in-depth at an extremely fast rate by either the same ignition pulse or by a system of strong stress waves generated by vigorous combustion at the surface of the propellant itself. These stress waves disrupt the propellant matrix on a microscopic level and cause ignition via friction of the minute fractured particles. In the second scenario, the propellant bed is not ignited volumetrically to the same degree as before but rather along the edges of macroscopic grain fractures caused by the compression of the sample. The resulting combustion rates are quite fast due to the rapid increase in available surface area for combustion and high degree of confinement. The high local combustion rates could then have the effect of causing the remaining propellant to be expelled from the confinement sleeve, leading to an even more dramatic increase in surface area available for combustion.

4.4.3 DWMPT. In an effort to derive some relationship between propellant mechanical properties and combustion rate, a majority of the propellant samples studied during the experimental program were evaluated using a DWMPT at BRL. Because the combustion characteristics of all propellant formulations and densities that comprise the PEG slate were so similar, only a representative sampling of this propellant family was exposed to DWMPT analysis.

The DWMPT device consists of a weight cage which is dropped onto an unconfined propellant sample, an optical displacement follower to quantify the sample deformation (strain) and a force transducer to quantify the load transmitted by the sample (stress). Before testing, the drop weight device was carefully balanced to allow free fall of the weight cage without contact with the guide rails. The propellant samples were carefully prepared for the DWMPT by using a precision circular saw having diamond-edge cutting blades to produce square ends on each propellant grain sample. Propellant samples tested in this way were prepared to have a length-to-diameter ratio of approximately 1:1 to reduce the tendency that longer samples might have to topple or to develop nonsymmetric deformations. The VHBR propellant samples tested had nominal dimensions of 12.7 mm (0.5 inch) in diameter and 12.7 mm (0.5 inch) in length. For the testing, a 2-kg weight was dropped from a height of 20 cm (8 inches) at an ambient temperature of 25° C.

The data resulting from this testing, summarized in Table 9, were used to determine various mechanical properties of the propellant samples, including the compressive modulus, ultimate stress, and the stress, strain, and strain rate at failure. These results represent average values for multiple (five tests) drop weight tests for each sample, with the exception of TC-43 at 85% TMD, for which only one sample was available. The data were intended to allow comparison of the mechanical properties of the various propellant formulations in order to ascertain whether any discernible relationship existed between these properties and the observed combustion behavior of the propellant samples, with the understanding that the chemistry of the respective samples also varies substantially.

As Table 9 shows, the members of the Kraton and PEG slates have higher compressive moduli than do the members of the Hycar slate. The compressive modulus can be described as a measure of the stiffness of an object, with stiff materials having higher modulus values than more elastic materials. These data, then, tend to quantify the observations made earlier in this report that the Hycar propellants were quite elastic or rubbery, with the possible exception of TC-51, which was somewhat stiffer. Also, the maximum stress values of the Kraton and PEG samples, calculated as the maximum measured force transmitted through a propellant sample divided by the original sample area, were substantially higher than those of the Hycar samples. The exceptions to this observation were the low-density members of the Kraton and PEG groups which had only slightly higher maximum stress values than did the Hycar samples. In fact, the value for the 85% TMD sample of TC-43 was actually much lower than the Hycar slate, due to its extremely weak propellant matrix.

It should be noted that the data for the Hycar propellants showed a high degree of reproducibility, while the data obtained for both the Kraton and PEG slates varied significantly, even when utilizing samples cut from a single grain of propellant. This suggests a possible superiority of the manufacturing technique utilized for the Hycar propellants (extrusion) over that utilized for both the Kraton and PEG slates (a compression molding technique). It is more difficult to draw conclusions from the data for the Kraton and PEG slates. However, as stated previously, it is clear that all of these propellants were stiffer than the Hycar slate, with the exception of TC-14 at 95% TMD, which had a compressive modulus much closer to that found for the Hycar propellants.

Table 9. DWMPT Results

Sample Name	TMD (%)	σ_{max} (MPa)	ε_{max}	σ_F (MPa)	ε_F	$(d\varepsilon/dt)_F$ (s^{-1})	$(d\varepsilon/dt)_{max}$ (s^{-1})	E_c (GPa)	Failure Mode
TC-14	100	20.92	0.0365	11.53	0.0136	164.9	167.2	1.015	P
TC-14	95	16.14	0.0442	8.336	0.0143	172.1	174.0	0.665	P/F
TC-15	100	25.10	0.0307	14.93	0.0138	156.5	163.2	1.276	P/F
TC-15	90	14.38	0.0416	8.328	0.0138	168.4	170.4	0.696	P/S
TC-16	100	38.02	0.0206	24.61	0.0105	153.6	157.8	3.515	P/F
TC-16	95	25.44	0.0207	18.93	0.0123	155.1	161.8	2.084	P/S
TC-16	90	14.94	0.0194	9.63	0.0086	158.06	160.03	1.257	P/S
TC-41	95	34.27	0.0205	26.33	0.0147	149.8	161.8	2.858	B/D
TC-41	90	37.78	0.0171	27.24	0.0116	153.2	159.9	3.362	B/D
TC-41	85	12.04	0.0208	9.03	0.0132	158.8	164.5	0.809	B/D
TC-43	95	18.44	0.0206	14.31	0.0134	154.6	157.9	1.359	B/S
TC-43	90	14.02	0.0158	9.74	0.00928	153.7	159.0	1.435	B/S
TC-43	85	5.53	0.0136	4.64	0.0077	159.7	175.6	0.824	B/S
TC-47A	96.0	11.72	0.0568	2.839	0.0062	148.0	173.8	0.531	P/F
TC-48A	96.3	11.62	0.0579	2.271	0.0046	133.8	173.7	0.580	P
TC-49A	96.8	11.11	0.0587	2.037	0.0045	132.8	173.5	0.554	P
TC-50	96.7	10.23	0.0691	1.691	0.0056	145.2	175.0	0.371	P
TC-51	93.1	10.09	0.0569	2.703	0.0049	138.5	172.1	0.638	P/F

NOTES: σ_{max} - Maximum stress
ε_{max} - Strain @ maximum stress
σ_F - Stress @ failure
ε_F - Strain @ failure
$(d\varepsilon/dt)_F$ - Strain rate @ failure
$(d\varepsilon/dt)_{max}$ - Maximum strain rate
E_c - Compressive modulus
Failure modes: P - plastic, B - brittle, F - fractured, S - shattered, D - disintegrated.

Apart from the stiffness and strength differences exhibited by the propellants, it also appears that the mode of failure which a propellant sample undergoes during compression may play a role in classifying the effect of mechanical properties on combustion rate. Table 9 shows an entry which contains a description of the mode in which each sample failed. As the table indicates, each member of the Hycar slate failed in a plastic mode, with TC-48A, TC-49A, and TC-50 showing no visible flaws and TC-47A and TC-51 displaying some cracks along the length of the outer circumference. The TC-14 samples, the members of the Kraton slate with a high binder content, also appear to fail in this manner. The 100% TMD samples of TC-14 showed no flaws, and the 95% TMD samples showed only minor flaking from the outer circumference after compression. The TC-15 samples, which had an intermediate binder content, show more severe cracking than did the TC-14 samples. The 100% TMD samples exhibited minor cracks along the length of the outer circumference and the 90% TMD samples exhibited fracture within the sample, causing some fragmentation of the sample to occur. The TC-16 propellants, which had the lowest binder content of the Kraton slate, showed much more severe fracturing than either of the other Kraton formulations when compared on the basis of equivalent %TMD. Both the 90 and 95% TMD samples of TC-16 fragmented severely, or shattered when impacted by the weight cage. The 100% TMD sample showed signs of severe cracking along the outer circumference, more severe than those observed for TC-15; however, the samples did not deconsolidate. In summary, the Kraton slate experiences plastic failure modes for each of its members which may transition into brittle failure for the members of the slate with low binder content and sample density (%TMD).

For each member of the PEG slate of VHBR propellants tested, the fracture mode exhibited was brittle failure. However, two brittle failure modes which appear to differ slightly were observed. When each of the TC-41 propellant samples were tested, the samples were completely pulverized into very small fragments (dust). However, when the TC-43 propellant samples were tested, the samples shattered into substantially larger fragments or chunks. The TC-43 samples resembled a hard clay-like substance, while the TC-41 was more like a hard chalky substance. This difference in the formulations is most likely attributable to the 5% BDNPA/F (energetic plasticizer/cross-linking agent) contained in the TC-43 formulation. However, this relatively large plasticizer content in formulation TC-43 was apparently not sufficient to prevent brittle failure that may have been caused by the small binder content of the sample. It is suggested that a larger binder/plasticizer ratio would have improved the mechanical properties of the formulation; however, this might also have compromised the burn rates achieved by changing the combustion mechanism of the formulation to one more like that exhibited by the Hycar propellant slate.

4.4.4 Ciné X-ray Experimental Program. In an effort to correlate the results obtained using the strain gage technique with information about the nature of the in-depth combustion reaction, a series of ciné x-ray experiments was conducted at the laboratory of Dr. Kenneth Kuo at the Pennsylvania State University. In an effort to obtain a "snapshot" of the in-depth combustion event using x-ray emissions, these experiments were conducted using a special Xybian CCD video camera which had the capability of obtaining images with exposure times as short as 25 ns in duration. However, this camera could only produce successive images at a framing rate on the order of seconds. At this rate, only one image could be taken during a typical closed chamber combustion event. A special circuit board was constructed by Dr. Wen Hsieh of Dr. Kuo's lab, which could produce multiple, superimposed exposures on a single video field by repeatedly gating the camera.

However, initial tests indicated that the fast-burning propellant samples did not burn with a laminar, end-burning form function. As a result, the video fields obtained with the multiple exposure technique were composed of multiple superimposed images in various stages of volumetric burning and were often not clear enough to discern any useful information. Consequently, this approach was discontinued after several attempts, and only single exposure images were obtained for the majority of the Penn State x-ray testing.

The strain gage data given earlier in Figures 26 and 32 indicate that a combustion-driven stress wave propagates through the sample at extremely high rates; therefore, a very short exposure time was required to capture the essence of the combustion process. The tests completed during this phase of the program utilized an exposure time on the order of microseconds for the x-ray images in an effort to resolve the nature of the interior of propellant sample during the time when these stress waves were being measured by the strain gages. As a consequence of the speed of the event, the short exposure time required, and the fact that the stress fields of interest within the propellant sample occurred before any significant pressure was developed within the closed vessel, the camera was triggered by the signal generated by the first strain gage, which was nearest the end of the sample to be ignited. Some of the resulting video images produced during these x-ray experiments are contained in succeeding pages. In each instance, the free surface of the sample exposed to the ignition gases is positioned to the right in the image.

It should be stressed that it is not strictly possible to compare the degree of combustion in the x-ray images for two different tests. These images result from a computer analysis using an advanced digital image processing system, the Quantex 9210. In some instances, as in Figure 34, colors were assigned to

Figure 34. X-ray video image for a sample of TC-41 at 90% TMD.

the different light intensities of the resulting analysis of the light energy (isophote analysis) of the image. These color images, or "pseudo-color" images, then, are indicative of the density values of the different regions of the image. Some of the x-ray images contained in this report are gray-scale representations of color images which have been retouched using image editing software to provide an enhanced contrast between the various shades of gray. In other figures, the isophote analyzed image was used directly, as in Figure 35. The objective here was to obtain the best possible image for the report which would show the *relative* combustion features for each test. In all cases, the darker regions of these images represent greater densities of the propellant sample, and lighter regions lower densities. However, making absolute comparisons between different test images should be discouraged.

Figure 35. Dual exposure x-ray image of TC-41, 90% TMD.

Several samples of the PEG-based TC-41 formulation were tested during the Penn State experimental program. The single-exposure x-ray image for a 90% TMD sample of this formulation is shown in Figure 34. Due to a shortage of strain gages, a single strain gage was used for this and many other tests conducted at Penn State. The single strain gage for these tests was located in exactly the same position as the first strain gage in the tests which utilized four gages. For all tests utilizing strain gages at Penn State, the signal from this gage was utilized to trigger the data acquisition equipment and to gate (expose) the CCD camera. The x-ray images, like that pictured in Figure 34, are produced using an image intensifier to translate the image, produced when x-rays are passed through the side of a propellant sample, to the CCD (or ciné) video camera. The images produced in this way give an indication of the propellant density variations in two dimensions, the axial position and as a function of sample width (variations with depth of the sample are not apparent but figure into the x-ray intensity values measured). These images can be considered as portraits of the in-depth combustion phenomena interrupted after a certain amount of the sample had been consumed.

Figure 36 contains the strain gage, chamber pressure and camera gate data for the x-ray image shown in Figure 34. As the figure shows, the x-ray image was obtained 36 μs after the onset of measured strain and well before (about 60 μs) any significant pressure was sensed by the transducer. There is a small (5 MPa) and gradually increasing pressure level apparent in Figure 36 before the pressure increases dramatically which was not present in the testing conducted at Veritay. This is most likely attributable to the fact that electric matches, which contain a small but finite quantity of combustible material, were utilized in the Penn State experimental configuration. On the other hand, the Veritay closed bomb work utilized ceramic electrical resistors which contribute only heat to ignite a booster charge and therefore do not significantly affect the initial pressure level in the bomb.

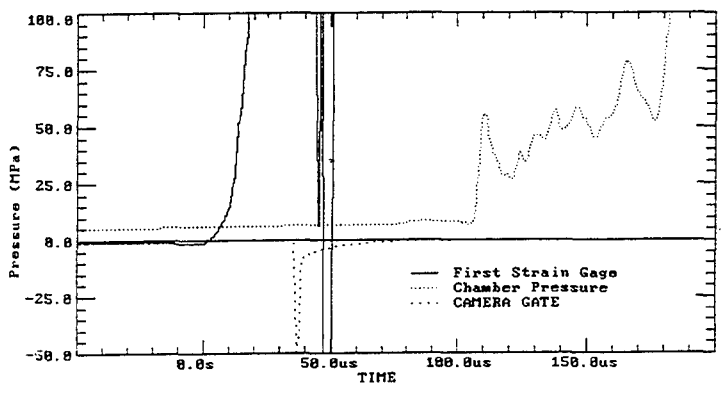

Figure 36. Data for x-ray image shown in Figure 34 for TC-41, 90% TMD.

From the density information available in the image shown in Figure 34, it appears that the sample has been ignited and is burning throughout. In addition, there appears to be a strong region of combustion concentrated toward the bottom and right-hand portion of the image. A possible explanation for this nonsymmetric combustion region might be that the propellant underwent a stress-related grain fracture following a nonsymmetric pattern or fault in the shape depicted in the x-ray image. Weak or otherwise nonhomogeneous regions within the propellant matrix may have existed and helped to promote the fracture.

The data for another test which utilized an 85% TMD sample of TC-41 is contained in Figure 37. As the camera gate data indicate, the corresponding x-ray image (not shown) for this test was obtained at a later point in time than for the previous test, 125 μs after the onset of strain at the first strain gage and just after the onset of pressure in the chamber. The corresponding image showed that the sample had been completely consumed, essentially before any pressure was sensed in the chamber. Also, four strain gages were utilized in the test. However, due to the erratic nature of this data and for the sake of clarity, only data for the first gage are shown in the figure. However, the data did show that the time between the onset of the strong stress wave at the first and fourth gage locations was only 20 μs for this test. Therefore, referring to Figure 37, the stress wave had propagated fully into the sample by the 30-μs mark, a full 85 μs before any pressure was recorded by the transducer and about 90 μs before the x-ray image was obtained, at which time the propellant was seen to be completely consumed.

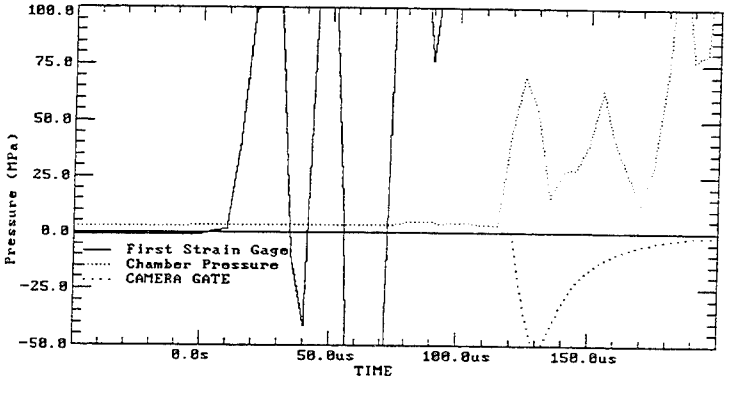

Figure 37. Data for a sample of TC-41, 85% TMD (no corresponding x-ray image shown).

If we draw an analogy between the data in Figures 36 and 37, ignoring the difference in density, additional insight may be gained. The time from the onset of strain at the first gage position to the onset of chamber pressure is quite similar for these two tests. Therefore, if we also assume that the time for

propagation of the stress wave between the first and fourth gage locations (had four been used for the test in Figure 36), then the x-ray image shown in Figure 34 would have been taken just a few microseconds after this stress wave had propagated past the fourth gage position. As the figure shows, in-depth combustion, although not symmetric, is clearly evident at this early time. These observations give the strongest evidence yet, aside from the magnitude of the stress waves themselves, that the measured stress waves are indicative of propellant ignition and combustion and not merely a result of mechanical activity within the propellant sample.

A third test of the TC-41 formulation, also with 90% TMD, was conducted early in the Penn State program and produced an x-ray image consisting of two superimposed images. The resulting image is shown in Figure 35. From the image, it can be seen that in-depth combustion was again apparent in this image. However, due to the superposition of the two images, it is not possible to resolve the degree of in-depth combustion as a function of time. It can be observed that a much greater degree of combustion has occurred on the right hand side of the sample as expected, since this region has burned for a longer period of time than the rest of the sample.

Figure 38 contains the strain gage, chamber pressure, and camera gate data for the dual exposure image shown in Figure 35. As Figure 38 shows, the two superimposed images were obtained at approximately 20 and 65 μs, respectively, after the onset of strain at the first strain gage position. The timing of the strain data in relation to the chamber pressure data is consistent with the previous two sets of data for TC-41. The stress wave quickly propagates through the sample, igniting it as evidenced by the body of x-ray data presented, and the sample is virtually consumed before any pressure is sensed by the chamber transducer.

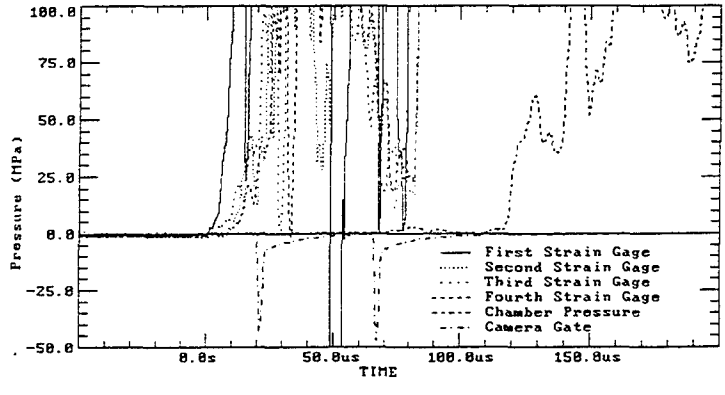

Figure 38. Data for x-ray image shown in Figure 35 for TC-41, 90% TMD.

Two additional tests were conducted with samples of TC-43, both at 90% TMD. An x-ray image taken approximately 53 μs after the onset of strain at the first gage is shown in Figure 39. This image shows a much more symmetric pattern of propellant density, with respect to apparent in-depth combustion, than does a comparable image for the TC-41 formulation, shown in Figure 34. However, this image does show a greater similarity to the double-exposure image of TC-41, shown in Figure 35. This may be a result of the fact that the second exposure in Figure 35 is taken at a relative point in time closer to that in which Figure 39 was taken, and that the first exposure in Figure 35 may not contribute substantially to the resulting image due to the early time at which the exposure was made (not much combustion expected).

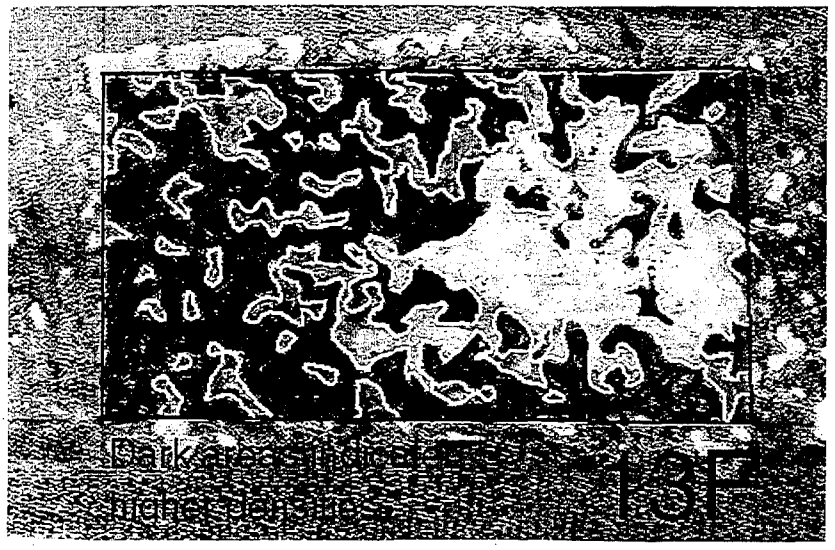

Figure 39. X-ray video image for a sample of TC-43 at 90% TMD.

The strain, pressure, and video gate timing data for the image in Figure 39 are shown in Figure 40. The image in Figure 39 appears to show the sample to be ignited and burning at various points throughout its volume; however, as stated previously, the combustion appears to be concentrated in a region which is radially symmetric. It should be remembered that this image is a two-dimensional representation of a three-dimensional event; a view of this sample from a different angle might show a more asymmetric combustion pattern. The image in Figure 39 is a pseudo-color image, as was Figure 34, which favors the possibility of comparing combustion characteristics between the two test images. Such a comparison tends to suggest that the combustion of the TC-41 sample had proceeded further after 36 μs (Figure 34) than had the combustion of the TC-43 sample after 52 μs (Figure 39). However, as stated earlier, these kinds of conclusion are only tentative because the pseudo-color images are produced by assigning colors to different density levels for each image on a relative basis. In addition, the resulting gray-scale images have been retouched by Veritay personnel to enhance and highlight the different shades of gray for

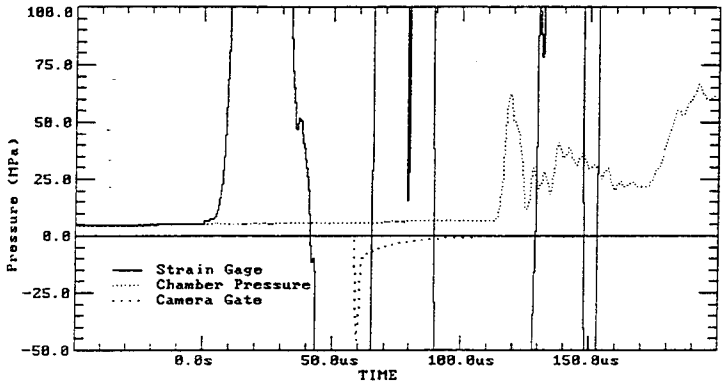

Figure 40. Data for x-ray image shown in Figure 39 for TC-43, 90% TMD.

presentation purposes. Therefore, it is not known, at least to Veritay, how readily these density assignations may be compared between images.

The other test utilizing TC-43 at 90% TMD was taken at a later point in time, about 120 μs after the onset of strain at gage one. The associated strain gage, pressure, and camera gate data are shown in Figure 41. As the figure shows, the x-ray image was taken at a point in time, just after the onset of chamber pressurization, comparable to that shown previously for the TC-41 test, shown in Figure 37, in which the sample was already consumed. As in that test, the x-ray image (which is not shown here) showed this sample to be completely consumed at the time the x-ray image was taken.

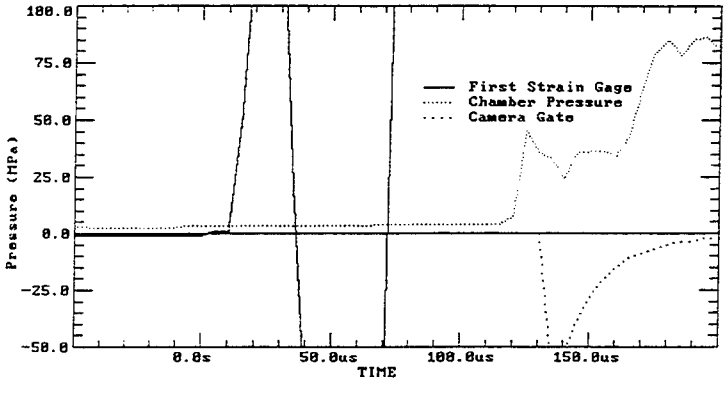

Figure 41. Data for TC-43, 90% TMD (no x-ray image shown).

Therefore, although some relatively minor differences between the data for the TC-41 and TC-43 samples may exist, overall, the two formulations appeared to burn in a markedly similar manner, by the same stress-induced combustion mechanism. This might reasonably be expected, based on the similarity of their composition, means of fabrication, and results from prior closed bomb combustion testing.

Figure 42, shows a single exposure x-ray image taken of a sample of TC-51, a member of the Hycar slate. Earlier testing of this sample, both vented closed bomb and ciné x-ray work, showed evidence of sample deconsolidation during combustion. As the image in Figure 42 shows, the remaining fragment of propellant (dark area) is shown to be burning in the free stream and apparently is about to exit the confinement tube. In any event, a loss of confinement is evident, allowing the propellant to burn with a larger exposed surface area than the original cigarette-burn mode.

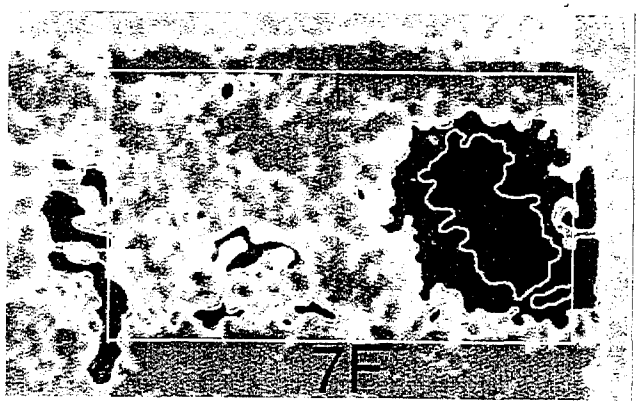

Figure 42. X-ray video image for a sample of TC-51.

The corresponding data for Figure 42 appear in Figure 43. From this figure, it can be seen that the image was obtained during the region where a very fast pressure rise is occurring, as might be expected from the image. Because combustion of the TC-51 sample occurred at a much slower rate than any of the PEG samples, strain gages were not utilized for this experiment. Instead, the camera gate was triggered by the chamber pressure rise. While it is clear from Figure 42 that the TC-51 propellant sample is burning freely in the open gas stream, it is not clear whether the loss of sample confinement resulted from sample deconsolidation brought on by convective combustion or by hot spot ignition at the base (left-hand portion) of the propellant sample which generated high internal pressures and expelled the sample from the confinement tube.

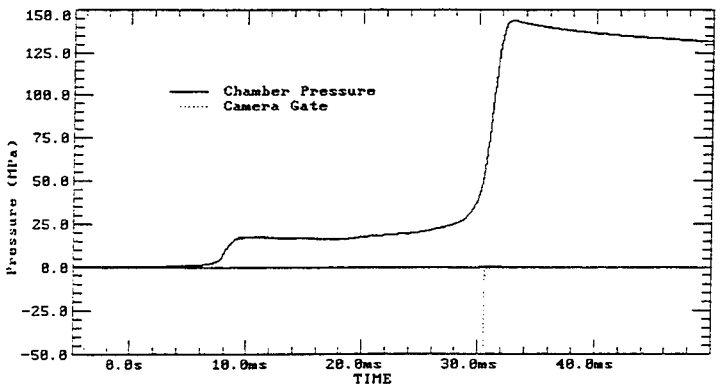

Figure 43. Data for x-ray image shown in Figure 42 for TC-51.

Two additional tests were conducted with the TC-16 formulation, a member of the Kraton slate. During one of these tests using a 95% TMD sample, a single x-ray exposure which showed no obvious change in the density of the propellant sample was obtained. This image was obtained 126 μs after the onset of strain at the first strain gage location. The chamber pressure for this test did not begin rising until 200 μs after the onset of strain at the first gage. While a stress-related mechanism may be at work, possibly resulting in hot-spot ignition very early in the closed bomb test, no evidence of in-depth burning is apparent at a point in time when members of the PEG slate were completely consumed. Therefore, based on this evidence, the combustion mechanism for this propellant sample is believed to be somewhat different from that for the fast-burning members of the PEG slate.

The other test, performed with a 100% TMD sample of TC-16, appeared to show a large-scale deconsolidation of the propellant sample, similar to that observed with the sample of TC-51 shown in Figure 42. This test was conducted with the ciné x-ray video camera system which was operated at a framing rate of 1,000 frames/second. Therefore, multiple images of the sample were produced at 1-ms intervals. Three of these images are presented here in Figures 44–46.

The video frame just preceding that in Figure 44 showed no significant difference from the pretest image. Combustion at the initially exposed surface appears to be followed quickly by combustion over a large internal region of the sample. As indicated in Figure 44, within 1 ms, the combustion event had progressed to the point where a piece of the propellant sample occupied approximately half of the confinement tube, with obvious combustion to the right where ignition occurred, but also with a large combustion region located toward the rear (left) of the propellant sample. In this region, some propellant is still visible (dark areas); however, a significant portion of the sample seems to have been consumed.

Figure 44. Ciné x-ray image of TC-16, 100% TMD sample 69 ms after pressurization.

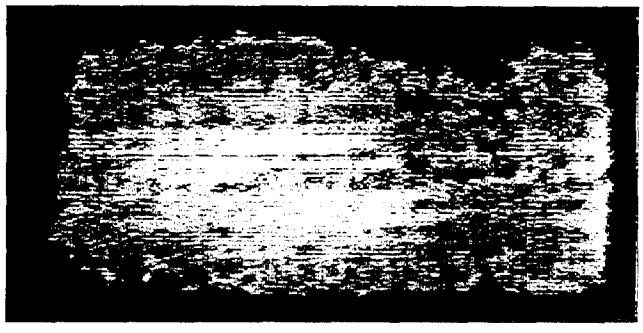

Figure 45. Ciné x-ray image of TC-16, 100% TMD sample 70 ms after pressurization.

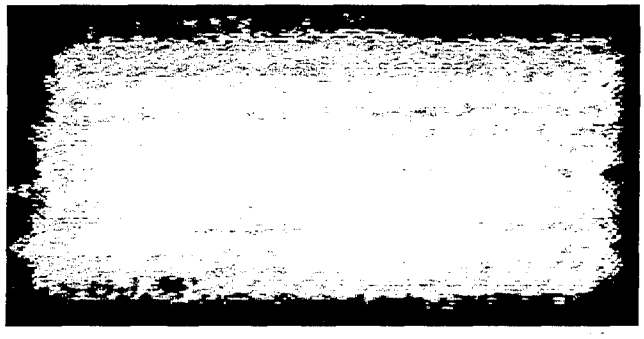

Figure 46. Ciné x-ray image of TC-16, 100% TMD sample 71 ms after pressurization.

In the next image, taken 1 ms later and shown in Figure 45, the unburned propellant is noticeably smaller in size, with a much larger combusted region at the base of the propellant sample. It appears, from this image, that the sample is burning from both ends, and possibly on portions of the outer circumference. Although impossible to confirm, the propellant fragment may also be moving out of the confinement tube, in a left to right direction.

In the final image in this series, shown in Figure 46, the confinement tube is shown to be completely vacant. In this image, the propellant sample is either totally consumed, or whatever fragments remained have moved out into the bomb volume, located at the right of the image shown.

The pressure data for this test are shown in Figure 47. The labels A, B, and C correspond to the points in time at which Figures 44, 45, and 46, respectively, were obtained. As the figure shows, the three images were obtained in the region of the pressure history where a sharp discontinuous pressure rise occurs. Therefore, as theorized earlier in this report, and at earlier times by other investigators, it appears that when a closed bomb pressure history exhibits a sharp increase in its slope, corresponding to an increase in burn rate, this can be attributed to a sudden increase in the propellant surface area available for combustion. This statement does not distinguish between the possible modes by which this surface area is increased, either propellant deconsolidation or hot spot ignition within the sample (i.e., combustion-generated surface area). In any event, the experimental data are fairly conclusive regarding the observed surface area increase, however it is generated.

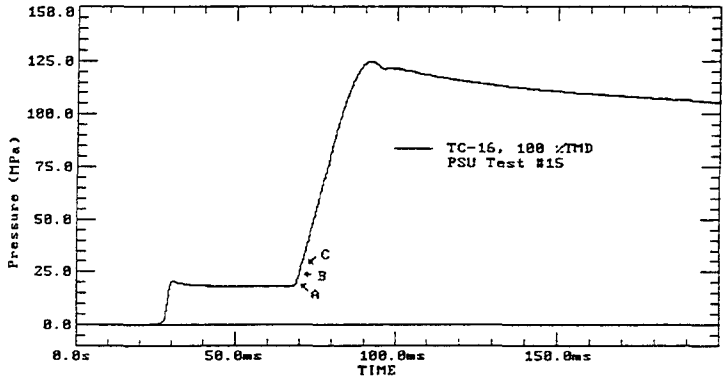

Figure 47. Pressure data for ciné x-ray images in Figures 44–46.

5. HYPOTHESES OF VHBR COMBUSTION MECHANISMS

As a result of the experimental results obtained and observations made during the present and previous programs, the authors of this report have formulated hypotheses concerning prospective mechanisms which explain or otherwise correlate the observed VHBR propellant combustion phenomena. These hypotheses are consistent with the many and varied observations cited in the literature, given previously in section 2, and in the results obtained during the current program, given in section 4.

Currently, it is believed that the combustion of VHBR propellant formulations may be described by one of the following three mechanisms:

(1) Enhanced laminar combustion mechanism

(2) Augmented surface area combustion mechanism

(3) Stress induced combustion mechanism.

In some instances, more than one of the aforementioned mechanisms may be at work for a given sample, such as when transitions from laminar to augmented surface area combustion occur.

5.1 Enhanced Laminar Combustion Mechanism. VHBR propellants, the basic composition of which consists of highly loaded energetic solids in a binder matrix, are classified as heterogeneous propellant formulations. As such, when these propellants burn laminarly, the presence of small energetic particulates is expected to create a surface that is rough and uneven. Combustion of these exposed energetic particles is much faster than at surrounding regions containing mostly binder. Indeed, inert binders absorb energy in a melting/ablation process that tends to depress the overall combustion rate.

It is well-documented that boron hydrides have an effect on the kinetics of nitramine combustion. It is likely that this effect is responsible for accelerating the combustion rate of laminar-burning VHBR propellant formulations. Combustion of nitramines, the primary energetic constituent in VHBR propellant formulations, involves melting of the solid particles as well as pyrolysis and other reaction kinetics. The rates of these reactions are relatively slow at low pressures but increase dramatically until normal laminar combustion is achieved at pressures above about 10 MPa (1,500 psi). It is recognized that ignition and combustion of nitramines is catalyzed by certain boron hydride compounds, in what appears to be surface

reactions. The catalysis mechanism is one that appears to replace an endotherm with a highly exothermic surface reaction at the nitramine melting temperature, which greatly accelerates the ignition and combustion process, especially at low pressures.

Within propellant samples, evidence accumulated to date supports the contention that the presence of a boron hydride species (H498) does act to accelerate the combustion rate of VHBR propellants containing this species. This is best documented by the progressive increases in combustion rate observed for the members of the Hycar slate of propellants (specifically TC-47A, 48A, and 49A in Figure 4) with small increases in the boron hydride content. This is significant in that the increases in burn rate were observed despite the fact that increased boron hydride content actually *decreased* the energy of the propellants somewhat, as shown in Table 8. However, as indicated in Figure 4 for these Hycar formulations, the magnitude of the observed burn rate enhancement is relatively small, and, in the context of the range of burn rates associated with VHBR propellant combustion, might best be described as a second-order effect. However, it is conceivable that, for propellants produced with more optimal energetic particle sizes, this type of laminar burn rate enhancement might lead to somewhat more significant burn rate increases if the burn zone can be thickened.

During combustion of VHBR propellants that exhibit the enhanced laminar combustion mechanism, flame is believed to propagate around the surface of nitramine granules and to spread to adjacent exposed granules so that the combustion zone slowly propagates to the interior of the propellant sample. The rate of in-depth propagation is a function of the proximity and availability of nitramine and boron hydride granules. At low pressures, the combustion zone is thick, but the thickness decreases with increasing pressure as the nitramine burn rate increases. If a nitramine particle is completely encapsulated in binder, then there is no free path to allow the flame to propagate in-depth. Porosity, weak binder adhesion, and burn-through of nitramine particulates all provide a free path for flame to propagate to adjacent nitramine particulate sites in a form of porous or convective combustion.

5.2 Augmented Surface Area Combustion Mechanism. Strong new evidence was obtained during the present program which supports the long-held view that the transitional combustion behavior, from relatively low-rate enhanced laminar combustion to some much higher rate combustion mechanism, observed for certain VHBR propellant formulations is a result of substantial increases in the surface area available for combustion. This increase in surface area may be a result of propellant deconsolidation following convective or porous combustion or compressive ignition at the base or at some location within

the propellant sample. For propellants that burn by this mechanism, it is felt that compressive ignition occurs by friction along crumb boundaries within the sample producing "hot spots," followed by deconsolidation of the sample into relatively large fragments which burn quickly.

When a transition to a higher combustion rate is observed, it usually follows normal ignition in which the sample appears to burn laminarly before experiencing a transition to higher rate combustion. However, in the case of the Kraton propellant slate, virtually instantaneous ignition is sometimes observed in which high rate combustion of the VHBR sample occurs without any noticeable pressure rise attributable to the booster charge. The latter is suggestive of the compressive ignition mechanism proposed for members of the PEG slate and discussed in section 5.3. However, the relative lack of violence associated with these Kraton formulations, when compared to the PEG formulations, suggests that a different mechanism is at work.

The new evidence spoken of previously was provided by the x-ray data obtained at the Penn State laboratory of Dr. Kenneth Kuo. Based on earlier observations, it was speculated that in the case of TC-16 (100% TMD) of the Kraton slate, the transition from low-rate enhanced laminar combustion to the higher rate mechanism may have resulted from compressive ignition somewhere within or near the base of the propellant sample. An occurrence of this type would be expected to expel and partially deconsolidate the remaining propellant into the free stream, and cause it to burn at a suddenly faster rate due to the increased available surface area. This is consistent with the combustion phenomenon observed using the ciné x-ray experimental technique.

Some type of propellant deconsolidation was also observed for TC-51, a member of the Hycar propellant slate. Again the ciné x-ray data show evidence of a small piece of propellant burning freely (unconfined). The framing rate of the video camera was not satisfactory to enable the event sequences to be resolved. However, the nature of this propellant sample suggests at least the possibility that convective or porous combustion might contribute to the observed phenomenon. Porous combustion might enable the flame to spread preferentially through pores or micro-channels within the sample, enhanced by the presence of the boron hydride. This could lead to pressure gradients within the sample, causing failure and deconsolidation of the propellant matrix. Alternatively, the relatively weak matrix might itself fail due to the applied stress from the gas pressure resulting from the combined combustion products of the booster and sample. This stress could fracture the relatively weak propellant matrix of the remaining

sample, producing a region by which the flame might rapidly infiltrate the sample, again enhanced by the presence of the boron hydride.

For the higher burn rate members of the Kraton slate, many of which appear to ignite by compressive means, the ultimate burn rate attained is lower than for the members of the PEG slate and the violence of the reaction is also a great deal less. The Kraton propellant slate was produced with internal "crumb" boundaries. Consequently, for these propellants, it is felt that compressive ignition occurs by friction along these crumb boundaries within the sample producing "hot spots," followed by deconsolidation of the sample into relatively large fragments which burn quickly. If crumb geometry may be considered to be the governing form function following deconsolidation, the resulting combustion of these crumbs would then be expected to proceed at a global rate higher than the expected laminar cigarette rate due to the increased surface area available for combustion, but at a lower rate than that expected for the PEG slate, which is ignited throughout most, if not all, of its volume.

For combustion to occur as quickly as it does for these propellants, it is felt that ignition must occur by other than normal thermal means. With the Kraton propellants, only slight deformation of the steel confinement sleeve was observed; however, the sleeves were literally blown apart by the combustion of PEG samples. The increased violence of PEG sample combustion in itself is suggestive of a different combustion mechanism. Consequently, for the high rate combustion of the Kraton propellants to be so mild, it is felt that a much smaller quantity or burning surface area of propellant must be involved in the combustion than with the PEG slate, which burns via the stress-induced mechanism discussed in the next section.

Although not entirely clear, it is possible that a function of the boron hydride species in this mechanism might be to increase the sensitivity of the sample, making it more susceptible to ignition by friction during deconsolidation or compressive failure. In addition, a catalytic effect, causing the flame to propagate rapidly along the crack surface is also likely. If cracking is especially severe as in the case of compressive failure, or if a high degree of deconsolidation has occurred, the exposed surface area will increase dramatically allowing for increased mobility of the reactants. Opportunities for catalyzed combustion sites are seen to increase by many orders of magnitude, leading to excessive combustion rates. Under strong retention and confinement, internal pressure levels are expected to reach the levels necessary to expel the remaining propellant fragments, possibly fracturing crumbs, and thereby further increasing the surface area available for combustion.

5.3 Stress-Induced Combustion Mechanism. Neither of the two combustion mechanisms presented earlier in this chapter can satisfactorily account for the magnitude of the combustion rates observed for true VHBR (very high rate) combustion behavior. True VHBR combustion behavior is characterized by extremely fast burn rates and violent combustion, typically destroying the steel sleeve confining the sample. This type of combustion has been observed for some members of the PEG slate with relatively small quantities of boron hydride added; although, in these instances (TC-44 and TC-45), another burn-rate-enhancing additive (Pt/C) was also present in small amounts. While the presence of this other burn rate modifier inarguably complicates the situation, it is currently believed that the important factors responsible for producing the observed high rate combustion behavior are related to the mechanical properties and impact sensitivity of these propellant formulations.

As a result of the extremely fast rates of combustion characteristic of true VHBR behavior, combined with the fact that it has been shown earlier in this report that, at least in one instance, the entire propellant sample was consumed before the pressure level in the bomb had reached a significant level, the question arises as to the use of bomb chamber pressure as a measure for determining burn rate. In other words, at these high rates, gas dynamic effects could contribute significantly to delaying the rate of pressure rise within the bomb chamber. Therefore, any burn rate based on this pressure trace would not accurately depict the magnitude of the actual combustion rate. What might represent the characteristic burn rates of these true VHBR propellants more accurately might be the measured propagation rates of the in-depth combustion reaction, which was on the order of 1,300 m/s.

The evolution of the stress-induced combustion mechanism, which has been hypothesized to explain true VHBR combustion behavior, began with the observation that most of the members of the PEG propellant slate showed evidence of compressive ignition. These same formulations also exhibited signs of what can be called "true VHBR behavior," illustrated by extremely rapid and violent combustion causing severe damage to the steel confinement sleeve. Compressive ignition is manifested by the virtually instantaneous ignition of propellant samples, before the pressure generated by combustion of the booster charge is even sensed by the pressure transducer located in the closed bomb chamber.

Since these very fast-burning PEG-based formulations were very homogeneous in appearance yet seemed to be more susceptible to compressive ignition than either of the other propellant slates, for these formulations an alternate type of compressive ignition mechanism was theorized. These formulations appear to be ignited from compression much the way samples are ignited during impact sensitivity testing.

In other words, the energy from the impact heats the sample and the force from the impact acts to disrupt the sample on a microscopic scale, causing friction on the surface of the energetic particulates.

In addition, it seemed plausible to expect that these same formulations might also burn by a similar compressive mechanism, in which ignition of the sample is propagated in-depth on the strength of a compressive stress wave. Although this compressive wave is apparently initiated by the pressure pulse from the initiator or initial combustion of the booster charge, it probably does not reach the strength necessary to ignite the sample in-depth until suitable thrust is generated by combustion at the exposed surface of the cylindrical sample. In some instances, transition to rapid burning occurs after the booster charge was partially or even fully burned. This may suggest that the delay in transition to a high rate mode of combustion for these propellants may be due to possible differences in either the mechanical strength, sample resiliency (related to the compressive modulus), or impact sensitivity. It is recognized that the impact sensitivity of a given propellant probably depends on some complex function of the sample strength and compressive modulus, along with its chemical formulation. For samples that exhibit sufficient impact sensitivity, the compressive stress waves propagating through the sample, generated by vigorous combustion at the free surface, might then produce ignition of the sample in-depth. This combustion mechanism is remarkably similar to the mechanism governing the DDT mechanism, and, as stated in the body of the text, there are a large number of general similarities observed between VHBR propellant combustion and DDT/PDC experimentation.

The PEG family of VHBR propellants which burned at these very high combustion rates also exhibited very stiff and inelastic mechanical properties. In addition, the samples tested tended to fail via brittle modes during drop weight testing. In fact, certain unconfined samples of PEG slate formulations were pulverized during this testing in a manner indicative of catastrophic failure. These observations appear consistent with a stress-related combustion mechanism, in which the propagation of stress waves into a confined sample is responsible for ignition of the sample, possibly as a result of friction between small fractured surfaces or energetic solid particles.

Ciné x-ray data for certain of the fast-burning samples indicate that the sample is burning in-depth shortly following the passage of the compressive stress wave as measured by the miniature strain gages. This miniature strain gage experimental technique was developed during the current program to measure the in-depth propagation rate of the compressive stress waves over the length of the sample. Further data

shows evidence that another of these samples was completely consumed at a time just prior to the onset of rapid pressurization of the closed bomb chamber.

Although the effect of the boron hydride species on the combustion mechanism cannot be absolutely stated from the available evidence, it may have the effect of increasing the sensitivity of the propellant sample to external stimuli, such as impact. This may result by allowing ignition to occur more readily once the stress wave has disrupted the sample. In addition, this species might also be expected to accelerate the localized combustion rates once ignition does occur, possibly accelerating the already high combustion rates.

Some might argue that these measured stresses constitute a "chicken or the egg" type of circumstance in which the measured stress waves are a result rather than the cause of the rapid propagation of in-depth combustion. However, an assumption of this type necessitates the need to postulate the existence of some novel chemical reaction kinetics capable of accounting for the extremely rapid propagation rates of the reaction front, as measured with the aid of the strain gages. Conversely, the stress-induced mechanism of the DDT phenomenon has been theorized and documented for many years. Moreover, the many similarities between the experimental conditions necessary to achieve DDT and VHBR combustion, as well as the similar stress wave characteristics, lend credence to the argument. Finally, the extremely fast propagation rates of the reaction zone, as measured via strain gages, are consistent with expected speed of sound and possibly even detonation velocities reported in the literature. Therefore, it is believed that the evidence supports the existence of DDT phenomena in what has been referred to as true VHBR combustion behavior.

6. CONCLUSIONS AND RECOMMENDATIONS

6.1 Summary of Progress. During the present program, a large step was taken in the understanding and rationalization of the wide variety of observed combustion behaviors associated with VHBR propellant formulations. Toward this end, some new and unique experimental approaches were developed. Data from this and other experimental work have been compiled into hypotheses of the mechanisms at work for combustion of VHBR propellants. This hypothesis, although not yet proven, is plausible and consistent with the observed combustion characteristics of this complex propellant family.

In addition to the experimental work, an extensive literature survey was undertaken, reaching into such areas as previous VHBR propellant research, nitramine decomposition studies, and DDT studies. This work enabled the groundwork for the combustion hypotheses to be laid and serves as a comprehensive starting point for anyone wishing to extend this interesting area of research.

6.2 Summary of Proposed Combustion Mechanisms. Summarizing the combustion hypotheses developed during this program, it is apparent that virtually all high rate combustion involves mechanical degradation of the sample, whether in the form of fracture, compressive ignition, or stress-induced in-depth ignition. When the mechanical properties of the propellant are resilient enough that the applied stresses from combustion gases do little more than compress the sample, flame propagation occurs by the relatively slow enhanced laminar combustion mechanism. Ample evidence exists to suggest that the presence of a boron hydride species can enhance the nitramine combustion rate, by creating a strong exotherm at the nitramine melting temperature. This can then enhance the laminar combustion rate and promote porous or convective combustion if the binder is weak or if sufficient porosity exists. However, this primarily chemical mechanism is not sufficient to explain what the authors have termed "true VHBR" burn rates.

When the mechanical properties of the propellant are suitable, a sort of intermediate combustion mechanism dominates. This mechanism, termed augmented surface area combustion by the authors, involves sample deconsolidation, either by porous or convective combustion or by fracture, allowing rapid flame propagation in-depth along the fault. For the Kraton propellants studied, it appears as if this mechanism could occur immediately, igniting the sample upon compression by the booster combustion gases, or later, following a period of enhanced laminar combustion before a transition to the augmented surface area combustion mechanism. Internal pressure buildup augmented by confinement may then result in further deconsolidation and expulsion of large propellant fragments into the gas stream, producing rapid increases in combustion rate due to the even greater increase in surface area available for combustion.

Finally, what has been termed true VHBR behavior by the authors, observed for the PEG propellant slate during this program, appears to be derived from a stress-induced combustion mechanism, in which the sample is ignited in-depth and throughout the majority of the sample volume by a strong compressive stress wave. Again, it appears that this mechanism is highly dependant on the existence of the proper propellant mechanical properties. That is, samples must be stiff, and suffer catastrophic brittle-mode failure when compressed in a manner such as with the DWMPT technique described in this report. Also, it is reasonable to expect these samples to be more sensitive to impact. Although no definitive

reproducibility testing was conducted for the PEG slate during this program, the appearance of true VHBR combustion was consistent in each test that was conducted.

6.3 Recommendations for Future Work. At the time of this writing, the future of VHBR propellant research is unclear. However, if further research is dedicated to the study of these interesting propellant formulations, it would be useful to expand upon some of the research areas touched on by the present work to help validate or disprove the proposed combustion hypotheses. It is, therefore, suggested that diagnostic testing be continued to expand areas where existing data might be insufficient. The type of diagnostic testing recommended includes the combination of strain gage and ciné x-ray techniques developed and used successfully during the present program to study members of the VHBR family which exhibited true VHBR behavior.

In addition, what might be the most important area that should be explored further relates to the nature and range of propellant mechanical properties necessary to produce true VHBR combustion behavior. This could include further compressive modulus and yield stress studies, compressive failure studies, and detailed quantitative study of all relevant sensitivity testing (including friction and impact). This should be combined with a study of the effect of boron hydride composition on combustion behavior. It would be interesting to determine whether a propellant formulation can be produced which has no boron hydride content but yet exhibits true VHBR behavior. Determination of these factors would eventually enable propellant designers to be capable of developing new propellant formulations tailored to specific applications and having the appropriate combustion rate characteristics.

For example, certain burn rate requirements are expected to exist for traveling charge applications. Likewise, if high-density monolithic charge increments are to be designed, moderate and controlled burn rate behavior is required. Therefore, the propellant designed for this application must burn reliably. In addition, the ability of HIVELITE to accelerate ignition of propellant formulations highly loaded with RDX, without negatively affecting the resultant burn rate, might be of interest for those studying the ignition of LOVA propellant formulations. LOVA propellants resist ignition by thermal means, and as a result are traditionally hard to ignite in gun chambers. It is possible that the addition of a burn rate modifier, such as boron hydride, might assist ignition. However, the effect of the addition of this species on such things as propellant insensitivity, reduction in total energy and propellant cost, must be considered. Conversely, it may be possible to add the boron hydride particles to the LOVA igniter material. In this

way, it may be possible to take advantage of catalytic surface reactions during ignition without modifying the burn rate of the propellant or changing its sensitivity.

Finally, with respect to the PEG slate of propellants, which was representative of propellant types exhibiting true VHBR behavior, the apparent high sensitivity to mechanical compression and subsequent violent combustion raises the question of whether such propellants are safe and suitable for inclusion in gun systems especially in larger masses. If, as the authors theorize, DDT is a factor in some VHBR combustion behavior, then scaling to larger systems with longer run-up distances may not be possible. Before such questions are answered, exhaustive safety testing apart from and in addition to the types mentioned previously must be conducted.

INTENTIONALLY LEFT BLANK.

7. REFERENCES

[1] Fisher, E., and W. Hollar. "Very High Burning Rate (VHBR) Propellant Combustion and Formulation Research." Report No. BO6-01-87, Veritay Technology, Inc., East Amherst, NY, January 1988.

[2] Fisher, E., and J. Barnes. "Very High Burning Rate (VHBR) Propellant Combustion and Formulations Research." Report No. NY4-88-1, Veritay Technology, Inc., East Amherst, NY, October 1988.

[3] Juhasz, A. A. "Workshop Report: Boron Hydrides in Very High Burning Rate (VHBR) Applications." BRL-TR-2854, U.S. Army Ballistic Research Laboratory, Aberdeen Proving Ground, MD, October 1987.

[4] Fifer, R. A. "Workshop Report: Combustion of Very High Burning Rate (VHBR) Propellants." ARBRL-TR-02441, U.S. Army Ballistic Research Laboratory, Aberdeen Proving Ground, MD, 1982.

[5] Barnes, J. T., E. B. Fisher, W. Hollar, K. White, and A. Juhasz. "Characterization of the Combustion Behavior of Hycar-Based VHBR Propellants." Proceedings of the 25th JANNAF Combustion Meeting, CPIA Publication 498, p. II-289, October 1988.

[6] Juhasz, A. A., S. T. Peters, R. E. Hanson, and L. K. Asaoka. "Development of VHBR Propellant Formulations With Improved Safety Characteristics." Proceedings of the 21st JANNAF Combustion Meeting, CPIA Publication 412, October 1984.

[7] Moniz, J. C., and S. T. Peters. "Traveling Charge Propellant Formulation and Processing Studies." IHTR 1234 (Final Report), 6 November 1989.

[8] Fifer, R. "Workshop Report: Combustion of Very High Burning Rate (VHBR) Propellants." Proceedings of the 18th JANNAF Combustion Meeting, CPIA Publication 347, October 1981.

[9] Juhasz, A. A., and I. W. May. "Advanced Propellants for Hypervelocity Gun Applications." Proceedings of the 6th International Symposium on Ballistics, pp. 21–31, October 1981.

[10] May, I. W., F. R. Lynn, A. A. Juhasz, E. Fisher, and P. S. Gough. "Thrust Characterization of Very High Burning Rate Propellants." Proceedings of the 18th JANNAF Combustion Meeting, CPIA Publication 347, October 1981.

[11] Juhasz, A., I. May, W. Aungst, and F. Lynn. "Combustion Studies of Very High Burning Rate (VHBR) Propellants." ARBRL-MR-03152, U.S. Army Ballistic Research Laboratory, Aberdeen Proving Ground, MD, February 1982. (AD A113 029).

[12] Freedman, E. "The Thermodynamics of VHBR Propellants." Proceedings of the 18th JANNAF Combustion Meeting, CPIA Publication 347, October 1981.

[13] Fisher, E. B. "Closed Bomb Tests of Hivelite-Based VHBR Propellants." ARBRL-CR-00449, U.S. Army Ballistic Research Laboratory, Aberdeen Proving Ground, MD, March 1981. (AD B057 344L).

[14] Fisher, E. B., and C. C. Morphy. "Closed Bomb Combustion of Hivelite-Based Very High Burn Rate (VHBR) Propellant." BRL-CR-542, U.S. Army Ballistic Research Laboratory, Aberdeen Proving Ground, MD, April 1985.

[15] Fisher, E. "One-Dimensional Closed-Bomb Tests of Very High Burn Rate (VHBR) Propellants." DAAK11-80-C-0062, Calspan Report No. 6744-D-1, U.S. Army Ballistic Research Laboratory, Aberdeen Proving Ground, MD, June 1982.

[16] Leveritt, C. S. "Ultra-High Burning Rate Propellants for Traveling Charge Gun." ARBRL-CR-00447, U.S. Army Ballistic Research Laboratory, Aberdeen Proving Ground, MD, February 1981.

[17] White, K. J., D. G. McCoy, J. O. Doali, W. P. Aungst, R. E. Bowman, and A. A. Juhasz. "Closed Chamber Burning Characteristics of New VHBR Formulations." BRL-MR-3471, U.S. Army Ballistic Research Laboratory, Aberdeen Proving Ground, MD, October 1985.

[18] White, K., R. Tompkins, and A. A. Juhasz. "Combustion Diagnostic Studies of VHBR Propellants." JANNAF/ARO Workshop on Boron Hydrides in Very High Burn Rate (VHBR) Applications, 1986.

[19] Trimble, J., R. Frey, A. Bines, and K. White. "X-Ray Studies of the Combustion of Some VHBR Propellants." CPIA Publication 412, October 1984.

[20] Juhasz, A. A., S. T. Peters, R. E. Hanson, and L. K. Asaoka. "Development of VHBR Formulations with Improved Safety Characteristics." Proceedings of the 21st JANNAF Combustion Meeting, CPIA Publication 412, October 1984.

[21] Helmy, A. "Thermal Decomposition of Propellant Oxidizers with B10H10 Salts." JANNAF/ARO Workshop on Boron Hydrides in Very High Burn Rate (VHBR) Applications, 1986.

[22] Duff, P. J. "Studies of the Effect of Hivelite and Other Boron Compounds on Nitramine Decomposition by Pyrolysis GC-FTIR." CPIA Publication 432, 1985.

[23] Liebman, S. A., A. P. Snyder, J. H. Kramer, D. J. Reulter, M. A. Schroeder, R. A. and Fifer. "Time Resolved Analytical Pyrolysis Studies of Nitramine Decomposition with a Triple Quadrupole Mass Spectrometer System." Journal of Analytical and Applied Pyrolysis, vol. 12, p. 83, 1987.

[24] Fifer, R. A., S. A. Liebman, P. J. Duff, K. D. Fickie, and M. A. Schroeder. "Thermal Degradation Mechanisms of Nitramine Propellants." Proceedings of the 22nd JANNAF Combustion Meeting, 1985.

[25] Tompkins, R. E., K. J. White, W. F. Oberle, and A. A. Juhasz. "Traveling Charge Concept - Combustion and Interior Ballistics Studies." Proceedings of the 23rd JANNAF Combustion Meeting, 1986.

[26] Juhasz, A. A. Personal Communication. U.S. Army Research Laboratory, Aberdeen Proving Ground, MD, 1987.

[27] Gough, P. "A Model of the Traveling Charge." ARBRL-CR-00432, USA ARRADCOM, U.S. Army Ballistic Research Laboratory, Aberdeen Proving Ground, MD, July 1980. (AD B053 309L).

[28] Baer, P. "Simulation of Closed Chamber Burning of Very-High Burning Rate Propellant." Proceedings of the 18th JANNAF Combustion Meeting, CPIA Publication 347, October 1981.

[29] Kooker, D., and R. Anderson. "A Mechanism for the Burning Rate of High Density, Porous, Energetic Materials." Proceedings of the 18th JANNAF Combustion Meeting, CPIA Publication 347, October 1981.

[30] Schroeder, M. A. "Borohydride Catalysis of Nitramine Thermal Decomposition and Combustion: Literature Review and Wrapup Discussion of Possible Chemical Mechanisms." Proceedings of the 25th JANNAF Combustion Meeting, CPIA Publication 498, October 1988.

[31] Kooker, D. E., and R. D. Anderson. "Closed Bomb Combustion Simulation of Hivelite Solid Propellant." Proceedings of the 20th JANNAF Combustion Meeting, Monterrey, CA, 1983.

[32] Kooker, D. E. "Modeling of Compaction Wave Behavior In Confined Granular Energetic Material." BRL-TR-3138, U.S. Army Ballistic Research Laboratory, Aberdeen Proving Ground, MD, August 1990.

[33] Bernecker, R. R., H. W. Sandusky, and A. R. Clairmont. "Deflagration-to-Detonation Transition Studies of Porous Explosive Charges in Plastic Tubes." Seventh Symposium (International) on Detonation, Naval Surface Warfare Center, MP 82-334, June 1981.

[34] Bernecker, R. R. "The Deflagration-to-Detonation Transition for High Energy Propellants - A Review." AIAA Journal, vol. 24, no. 1, 1986.

[35] Sandusky, H. W., and B. C. Glancy. Communication to D. E. Kooker. Naval Surface Warfare Center, White Oak Laboratory, January 1990.

[36] Bernecker, R. R. "DDT Studies of a Spherical, Double-Base Ball Propellant." 1987 JANNAF Propulsion Systems Hazards Subcommittee Meeting, CPIA Publication 464, p. I-1, April 1987.

[37] Campbell, A. W. "Deflagration-to-Detonation Transition in Granular HMX." 1980 JANNAF Propulsion Systems Hazards Subcommittee Meeting, CPIA Publication 330, p. I-105, October 1980.

[38] Sandusky, H. W., B. C. Glancy, R. L. Campbell, A. D. Krall, W. L. Elban, and P. J. Coyne, Jr. "Compaction and Compressive Reaction Studies for a Spherical, Double-Base Ball Propellant." Proceedings of the 25th JANNAF Combustion Meeting, CPIA Publication 498, p. I-83, October 1988.

[39] Frey, R., and K. White. Personal Communication. Personal communication between R. Frey and K. White, relayed to J. Barnes, U.S. Army Research Laboratory, Aberdeen Proving Ground, MD, October 1990.

[40] Oberle, W. F., A. A. Juhasz, and T. Griffie. "A Simplified Computer Code For Reduction To Burning Rates of Closed Bomb Pressure-Time Data (MINICB)." BRL-TR-2841, U.S. Army Ballistic Research Laboratory, Aberdeen Proving Ground, MD, August 1987.

[41] Asaoka, L. K. "Synergistic Catalysis of Nitramine Propellants." Proceedings of the 21st JANNAF Combustion Meeting, Chemical Propulsion Information Agency, October 1984.

[42] Kooker, D. E. "A Reactive Shock Wave Model for Compaction Waves in Granular Energetic Material." Proceedings of the 1987 JANNAF Propulsion Systems Hazards Meeting, CPIA Publication 464, p. I-39, March 1987.

[43] Kooker, D. E. "Predictions for the Piston-Driven-Compaction Experiment Based on a Transient Shock Wave Model." Proceedings of the 1989 JANNAF Propulsion Systems Hazards Meeting, CPIA Publication 509, p. I-47, February 1989.

[44] Kooker, D. E. "A Numerical Study of Compaction Waves in Class D HMX." Proceedings of the 1986 JANNAF Propulsion Systems Hazards Meeting, CPIA Publication 446, p. I-213, March 1986.

[45] Kooker, D. E. "Collision of Reactive Compaction/Shock Waves in Granular Energetic Material." Proceedings of the 1988 JANNAF Propulsion Systems Hazards Meeting, CPIA Publication 477, p. I-17, March 1988.

[46] Sandusky, H. W. "Compressive Ignition and Burning in Porous Beds of Energetic Materials." Proceedings of the 1983 JANNAF Propulsion Systems Hazards Meeting, CPIA Publication 381, p. I-249, September 1983.

[47] Costantino, M. "Volumes and Sound Speeds of Two Gun Propellants at High Pressure." Propellants, Explosives, Pyrotechnics, vol. 9, pp. 22–29, 1984.

BIBLIOGRAPHY

Additional Related References: BH/RDX/HMX Decomposition

Behrens, R. "RDX Thermal Decomposition by Simultaneous Thermogravimetry, Modulated-Molecular-Beam Mass Spectrometry." Sandia Combustion Facility, 1986 Annual Report, p. 5, 1986.

Fifer, R. A., S. A. Liebman, and M. A. Schroeder. "The Role of Borohydrides in Nitramine Catalysis." Proceedings of the 17th International Annual Conference of ICT - Analysis of Propellants and Explosives, p. 24-1, June 1986.

Fifer, R., and I. Stobie. "Combustion Thermodynamics of Some Boron-Nitrogen-Hydrogen Compounds." Proceedings of the 20th JANNAF Combustion Meeting, CPIA Publication 383, p. I-611, October 1983.

Liebman, S. A., A. P. Snyder, J. H. Kremer, D. J. Reutter, M. A. Schroeder, and R. A. Fifer. "Time-Resolved Analytical Pyrolysis Studies of Nitramine Decomposition with a Triple Quadrupole Mass Spectrometer System." Journal of Analytical and Applied Pyrolysis, vol. 12, p. 83, Elsevier Science Publishers, 1987.

Schroeder, M. A. "Critical Analysis of Nitramine Decomposition Results: Some Comments on Chemical Mechanisms." Proceedings of the 16th JANNAF Combustion Meeting, CPIA Publication 308, p. II-17, September 1979.

Schroeder, M. A. "Critical Analysis of Nitramine Decomposition Data: Activation Energies and Frequency Factors for HMX and RDX Decomposition." Proceedings of the 17th JANNAF Combustion Meeting, CPIA Publication 329, p. II-493, September 1980.

Schroeder, M. A. "Critical Analysis of Nitramine Decomposition Data Product Distributions from HMX and RDX Decomposition." Proceedings of the 18th JANNAF Combustion Meeting, CPIA Publication 347, p. II-395, October 1981.

Schroeder, M. A. "Critical Analysis of Nitramine Decomposition Data: Some Preliminary Comments on Auto-acceleration and Auto-inhibition in HMX and RDX Decomposition." Proceedings of the 19th JANNAF Combustion Meeting, CPIA Publication 366, p. I-321, October 1982.

Schroeder, M. A. "Critical Analysis of Nitramine Decomposition Data Preliminary Comments on Autoacceleration and Autoinhibition in HMX and RDX Decomposition." ARBRL-MR-03370, U.S. Army Ballistic Research Laboratory, Aberdeen Proving Ground, MD, August 1984.

Schroeder, M. A. "Critical Analysis of Nitramine Decomposition Data: Update, Some Comments on Pressure and Temperature Effects, and Wrap-Up Discussion of Chemical Mechanisms." Proceedings of the 21st JANNAF Combustion Meeting, CPIA Publication 412, p. II-595, October 1984.

Schroeder, M. A. "Critical Analysis of Nitramine Decomposition Data: Product Distributions from HMX and RDX Decomposition." Final Report, BRL-TR-2659, June 1985.

Schroeder, M. A. "Critical Analysis of Nitramine Decomposition Data: Activation Energies and Frequency Factors for HMX and RDX Decomposition." BRL-TR-2673, U.S. Army Ballistic Research Laboratory, Aberdeen Proving Ground, MD, September 1985.

Schroeder, M. A. "Thermal Decomposition of RDX and RDX-Borohydride Mixtures." Proceedings of the 23rd JANNAF Combustion Meeting, CPIA Publication 457, pp. II--43, October 1986.

Schroeder, M. A. "Thermal Decomposition of Catalyzed and Uncatalyzed HMX Propellant Formulations." Proceedings of the 24th JANNAF Combustion Meeting, CPIA Publication 476, p. III-103, October 1987.

Schroeder, M. A. "Borohydride Catalysis of Nitramine Thermal Decomposition and Combustion: Literature Review and Wrap-up Discussion of Possible Chemical Mechanisms." Proceedings of the 25th JANNAF Combustion Meeting, October 1988.

Snyder, A. P., J. H. Kremer, S. A. Liebman, M. A. Schroeder, and R. A. Fifer. "Characterization of Cyclotrimethylenetrinitramine (RDX) by N,H Isotope Analyses with Pyrolysis-Atmospheric Pressure Ionization Tandem Mass Spectrometry." Organic Mass Spectrometry, vol. 24, p. 15, 1989.

Additional Related References: DDT/PDC Experiments and Modelling

Boggs, T. L., C. F. Price, D. E. Zurn, R. L. Derr, and E. J. Dibble. "Temperature Sensitivity of Deflagration Rates of Cyclotetramethylenetetranitramine (HMX)." Proceedings of the 13th JANNAF Combustion Meeting, CPIA Publication 281, p. I-45, December 1976.

Campbell, R. L., W. L. Elban, and P. J. Coyne, Jr. "Side-Wall Pressure Measurements in Quasi-Static Compaction of Porous Beds of HMX Powders and ABL 2523 Casting Powder." Proceedings of the 1988 JANNAF Propulsion Systems Hazards Subcommittee Meeting, CPIA Publication 477, p. I-1, March 1988.

Cole, J. E., and R. A. Fifer. "Burn Rate Behavior of High Density Binderless HMX." Proceedings of the 16th JANNAF Combustion Meeting, CPIA Publication 308, p. II-1, December 1979.

Costantino, M., and D. Ornellas. "The Experimental High Pressure Equation of State of a Very Fast Burning Gun Propellant." Proceedings of the 21st JANNAF Combustion Meeting, CPIA Publication 412, p. II-383, October 1984.

Derr, R. L., T. L. Boggs, D. E. Zurn, and E. J. Dibble. "The Combustion Characteristics of HMX." Proceedings of the 11th JANNAF Combustion Meeting, CPIA Publication 261, p. I-231, December 1974.

Fifer, R. A., and J. A. Cole. "Burning Rate for Steel-Cased, Pressed Binderless HMX." Proceedings of the 17th JANNAF Combustion Meeting, CPIA Publication 329, p. II-413, November 1980.

Jacobs, S. J., and H. W. Sandusky. "Modeling of Porous Bed Compaction With Deformed Spheres in a Regular Lattice." Proceedings of the 1986 Propulsion Systems Hazards Subcommittee Meeting, CPIA Publication 446, p. I-149, March 1986.

Kooker, D. E. "A Workshop Summary of 'Model Predictions of the Piston-Driven-Compaction Experiment." BRL-TR-3029, U.S. Army Ballistic Research Laboratory, Aberdeen Proving Ground, MD, August 1989.

Kuo, K. K., B. B. Moore, and V. Yang. "Measurement and Correlation of Intragranular Stress and Particle-Wall Friction in Granular Propellant Beds." Proceedings of the 16th JANNAF Combustion Meeting, CPIA Publication 308, p. I-559, December 1979.

McAfee, J. M., and A. W. Campbell. "An Experimental Study of the Deflagration-to-Detonation Transition in Heavily Confined HMX." Proceedings of the 1986 Propulsion Systems Hazards Subcommittee Meeting, CPIA Publication 446, p. I-163, March 1986.

Nicolaides, S., J. Pinto, and D. A. Wiegand. "Mechanical Properties, Mechanical Grain Failure and Changes in the Burning Performance of Gun Propellant." Proceedings of the 1980 JANNAF Propulsion Meeting, CPIA Publication 315, p. I-399, March 1980.

Nicolaides, S., D. A. Wiegand, and J. Pinto. "The Mechanical Behavior of Gun Propellant Grains and Its Role in Interior Ballistics." Proceedings of the JANNAF Structures and Mechanical Behavior Subcommittee, 16th Meeting,, CPIA Publication 311, p. I-145, March 1980.

Wires, R. A., J. P. Pfau, and J. J. Rocchio. "The Effect of High Rates of Applied Force and Temperature on the Mechanical Properties of Gun Propellants." Proceedings of the 1979 JANNAF Propulsion Meeting, CPIA Publication 300, p. III-25, July 1979.

Additional Related References: VHBR/Traveling Charge

Avrami, L., R. Velicky, D. Anderson, and D. Downs. "A Comparative Study of Very High Burning Rate Materials - Hivelite Compositions 300511 and 300435." ARLCD-TR-82015, U.S. Army Armament Research and Development Command, August 1982.

Baer, P. S. "Simulation of Closed Chamber Burning of Very-High Burning Rate Propellant." BRL-TR-2919, U.S. Army Ballistic Research Laboratory, Aberdeen Proving Ground, MD, July 1988.

Bernstein, C. N., and W. J. Casey. "Hivelite Cord/Black Powder 105mm Artillery Primers." ARLCD-CR-80002, U.S. Army Ballistic Research Laboratory, Aberdeen Proving Ground, MD, December 1980.

Bernstein, C. N., and R. D. Meyers. "Hivelite-Treated Combustible Containers for 60-MM Mortar Propellant Increments." ARLCD-CR-81046, U.S. Army Armament Research and Development Command, August 1981.

Fifer, R. A., and W. F. McBratney. "Catalysis of Nitramine Propellants by Metal Borohydrides." ARBRL-MR-03300, U.S. Army Ballistic Research Laboratory, Aberdeen Proving Ground, MD, July 1983.

Kaste, P. J. "Studies of the Effect of Hivelite and Other Boron Compounds on Nitramine Decomposition by Pyrolysis GC-FTIR." BRL-TR-2973, U.S. Army Ballistic Research Laboratory, Aberdeen Proving Ground, MD, December 1988.

Oberle, W. F., G. P. Wren, F. W. Robbins, K. J. White, R. E. Tompkins, and A. A. Juhasz. "Parameters for Optimizing a Traveling Charge Gun System." BRL-TR-2910, U.S. Army Ballistic Research Laboratory, Aberdeen Proving Ground, MD, May 1988.

Paul Gough Associates, Inc. "A Two-Phase Model of the Interior Ballistics of Hybrid Solid-Propellant Traveling Charges." BRL-CR-565, U.S. Army Ballistic Research Laboratory, Aberdeen Proving Ground, MD, March 1987.

Price, E. W., R. K. Sigman, and R. R. Panyam. "Combustion Mechanisms of Solid Propellants." Annual Report, Georgia Institute of Technology, September 1981.

Robbins, F. W., and F. R. Lynn. "Analytic Solutions to the Closed Bomb." BRL-TR-2892, U.S. Army Ballistic Research Laboratory, Aberdeen Proving Ground, MD, March 1988.

Salizzoni, R. M., W. H. Hsieh, A. Peretz, and K. K. Kuo. "Regression Behavior and Temperature Sensitivity of Very High Burning Rate Propellants." Proceedings of the 27th JANNAF Combustion Subcommittee, CPIA Publication 557, p. I-531, November 1990.

Tompkins, R. E., K. J. White, and W. F. Oberle. "Combustion Diagnostics and Ballistic Results of Proposed Traveling Charge Propellant." BRL-TR-2902, U.S. Army Ballistic Research Laboratory, Aberdeen Proving Ground, MD, April 1988.

Tompkins, R. E., K. J. White, W. F. Oberle, and A. A. Juhasz. "Traveling Charge Gun Firings Using Very Burning Rate Propellants." BRL-TR-2970, U.S. Army Ballistic Research Laboratory, Aberdeen Proving Ground, MD, December 1988.

Yee, R. Y., and E. C. Martin. "Effects of Surface Interactions and Mechanical Properties of Plastic Bonded Explosives on Explosive Sensitivity. Part 2: Model Formulation." NWC TP 6619, Naval Weapons Center, Edwards Air Force Base, CA, March 1985.

NO. OF COPIES	ORGANIZATION
2	ADMINISTRATOR ATTN DTIC DDA DEFENSE TECHNICAL INFO CTR CAMERON STATION ALEXANDRIA VA 22304-6145
1	DIRECTOR ATTN AMSRL OP SD TA US ARMY RESEARCH LAB 2800 POWDER MILL RD ADELPHI MD 20783-1145
3	DIRECTOR ATTN AMSRL OP SD TL US ARMY RESEARCH LAB 2800 POWDER MILL RD ADELPHI MD 20783-1145
1	DIRECTOR ATTN AMSRL OP SD TP US ARMY RESEARCH LAB 2800 POWDER MILL RD ADELPHI MD 20783-1145
	ABERDEEN PROVING GROUND
5	DIR USARL ATTN AMSRL OP AP L (305)

NO. OF COPIES	ORGANIZATION
1	OSD SDIO IST ATTN DR LEN CAVENY WASHINGTON DC 20301-7000
3	COMMANDER ATTN SMCAR AEE B S MOI D DOWNS D CHIU US ARMY ARDEC PCTNY ARSNL NJ 07806-5000
1	COMMANDER ATTN SMCAR AEE J LANNON US ARMY ARDEC PCTNY ARSNL NJ 07806-5000
2	COMMANDER ATTN TECH LIB D MANN PO BOX 12211 US ARMY RESEARCH LABORATORY RSCH TRI PK NC 27709
1	NAWCWPN DIV ATTN BILL WILSON 474220D C02353 CHINA LAKE CA 93555
2	NAWCWPN DIV ATTN TIM PARR TOM BOGGS 474320D C02392 CHINA LAKE CA 93555
1	COMMANDER ATTN MICHAEL E SITZMANN CODE 9110 NAVAL SURFACE WARFARE CENTER INDIAN HEAD MD 20640-5035
1	NAWX WPNS DIV ATTN LARRY MERWIN CODE 474230D CHINA LAKE CA 93555
1	NAVAL RESEARCH LABS ATTN RICHARD GILARDI LSM 6030 WASHINGTON DC 20375

NO. OF COPIES	ORGANIZATION
1	NAVAL RESEARCH LABS ATTN TOM RUSSELL CODE 6110 WASHINGTON DC 20375
1	ONR ATTN DICK MILLER MECHANICS & ENERGY CONVERSION DIV 800 N QUINCY ST ARLINGTON VA 22217-5610
1	COMMANDER ATTN STEVE MITCHELL BLDG 20 CODE TDE NAVAL SURFACE WARFARE CENTER INDIAN HEAD MD 20640-5035
1	COMMANDER ATTN A G STERN BLDG 600 CODE 9110 NAVAL SURFACE WARFARE CENTER INDIAN HEAD MD 20640-5035
1	COMMANDER ATTN W M KOPPES BLDG 600 CODE 9110 NAVAL SURFACE WARFARE CENTER INDIAN HEAD MD 20640-5035
1	COMMANDER ATTN STEVE COLLIGNON BLDG 556 CODE 90H NAVAL SURFACE WARFARE CENTER INDIAN HEAD MD 20640
1	COMMANDER ATTN YVONNE TRAN BLDG 863 CODE 9410F NAVAL SURFACE WARFARE CENTER INDIAN HEAD MD 20640
1	COMMANDER ATTN JACQUELINE ROSE PO DRAWER 160 NAVAL SURFACE WARFARE CENTER YORKTOWN VA 23691-0160
2	COMMANDER ATTN 610 C SMITH 6110C S PETERS NAVAL SURFACE WARFARE CENTER INDIAN HEAD MD 20640-5035

NO. OF COPIES	ORGANIZATION
1	NATIONAL GROUND INTELLIGENCE CENTER ATTN CHRIS BELTER IANG RMT 220 SEVENTH ST NE CHARLOTTESVILLE VA 22902-5396
1	LAWRENCE LIVERMORE NATIONAL LAB ATTN PHILLIP F PAGORLA PO BOX 808 I282 LIVERMORE CA 94550
1	DEPT OF CHEMISTRY ATTN PETER POLITZER UNIVERSITY OF NEW ORLEANS NEW ORLEANS LA 70148
1	GEORGIA INSTITUTE OF TECHNOLOGY ATTN EDWARD PRICE 778 ATLANTIC DR ATLANTA GA 30332
1	PRINCETON COMBUSTION RSCH LAB ATTN N MESSINA 11 DEERPARK DR BLDG IV STE 119
1	CA INST OF TECH ATTN L D STRAND MS125 224 4800 OAK GROVE DR JET PROPULSION LAB PASADENA CA 91109
1	SRI INTERNATIONAL ATTN JEFFREY C BOTTARO P3318 333 RAVENSWOOD AVE MENLO PARK CA 94025
1	SRI INTERNATIONAL ATTN ROBERT SCHMITT PS281 333 RAVENSWOOD AVE MENLO PARK CA 94025
1	THIOKOL CORP ATTN DAVID MCGRATH MS G 25 PO BOX 241 ELKTON MD 21922-0241
1	SAIC ATTN WOODWARD WAESCHE 1710 GOODRIDGE DR MS 2 6 6 MCLEAN VA 22102

NO. OF COPIES	ORGANIZATION
1	AEROJET ATTN JAY GLAD BOX 13222 SACRAMENTO CA 95813
1	AEROJET ATTN GERRY MANSER BOX 13222 SACRAMENTO CA 95813
1	THIOKOL CORP ATTN CAROL HINSHAW PO BOX 707 MS 244 BRIGHAM CITY UT 84302-0707
1	FLUOROCHEM INC ATTN KURT BAUM 6805 AYON AVE AZUSA CA 91702
1	OLIN ORDNANCE ATTN V MCDONALD LIBRARY PO BOX 222 ST MARKS FL 32355
1	PAUL GOUGH ASSOCIATES INC ATTN P S GOUGH 1048 SOUTH STREET PORTSMOUTH NH 03801-5423
1	ELI FREEDMAN & ASSOCIATES ATTN E FREEDMAN 2411 DIANA RD BALTIMORE MD 21209
10	VERITAY TECHNOLOGY INC 4845 MILLERSPORT HWY PO BOX 305 EAST AMHERST NY 14051-0305
1	GEO CENTERS ATTN DAVE PARITOSH 762 RT 15 SOUTH LAKE HOPATCONG NJ 07849
1	THIOKOL CORP ELKTON DIV ATTN JIM HARTWELL PO BOX 241 BLDG 846 55 THIOKOL RD ELKTON MD 21922-0241

NO. OF
COPIES ORGANIZATION

1 ALLIANT TECH SYSTEMS INC
ATTN W J WORRELL
RTE 114 PO BOX 1
RADFORD VA 24141-0100

1 OLIN ORDNANCE
ATTN J BUZZET
10101 9TH ST NORTH
ST PETERSBURG FL 33716

1 GENERAL ELECTRIC CO
ATTN DR J MANDZY
MAIL DROP 43 220
100 PLASTICS AVE
PITTSFIELD MA 01201

1 UT CSD
ATTN JOHN GULMONT
PO BOX 49028
SAN JOSE CA 95161-9028

ABERDEEN PROVING GROUND

2 CDR USACSTA
ATTN S WALTON
G RICE

24 DIR USARL
ATTN AMSRL-WT-P, A HORST
AMSRL-WT-PA,
W OBERLE
A JUHASZ 2 CPS
C LEVERITT 2 CPS
I STOBIE
K WHITE 4 CPS
D KOOKER
AMSRL-WT-PB, E SCHMIDT
AMSRL-WT-PD, B BURNS
AMSRL-WT-T, W MORRISON
AMSRL-WT-WG, P KASTE
AMSRL-WT-PC,
D BEYER
R PESCE-RODRIGUEZ
R FIFER
M SCHROEDER
J HEIMERL
T KOTLAR
AMSRL-WT-PD,
R LIEB
M LEADORE

USER EVALUATION SHEET/CHANGE OF ADDRESS

This Laboratory undertakes a continuing effort to improve the quality of the reports it publishes. Your comments/answers to the items/questions below will aid us in our efforts.

1. ARL Report Number ARL-CR-242 Date of Report September 1995

2. Date Report Received _____

3. Does this report satisfy a need? (Comment on purpose, related project, or other area of interest for which the report will be used.) _____

4. Specifically, how is the report being used? (Information source, design data, procedure, source of ideas, etc.) _____

5. Has the information in this report led to any quantitative savings as far as man-hours or dollars saved, operating costs avoided, or efficiencies achieved, etc? If so, please elaborate. _____

6. General Comments. What do you think should be changed to improve future reports? (Indicate changes to organization, technical content, format, etc.) _____

CURRENT ADDRESS

_____
Organization

_____
Name

_____
Street or P.O. Box No.

_____
City, State, Zip Code

7. If indicating a Change of Address or Address Correction, please provide the Current or Correct address above and the Old or Incorrect address below.

OLD ADDRESS

_____
Organization

_____
Name

_____
Street or P.O. Box No.

_____
City, State, Zip Code

(Remove this sheet, fold as indicated, tape closed, and mail.)
(DO NOT STAPLE)